centro appunti
www.centroappunti.it
Corso Luigi Einaudi, 55/B - Torino

Appunti universitari
Tesi di laurea
Cartoleria e cancelleria
Stampa file e fotocopie
Print on demand
Rilegature

NUMERO: 1446A - ANNO: 2015

A P P U N T I

STUDENTE: Raviglione

MATERIA: Sovrastrutture (Inglese). Prof. Santagata

Il presente lavoro nasce dall'impegno dell'autore ed è distribuito in accordo con il Centro Appunti.
Tutti i diritti sono riservati. È vietata qualsiasi riproduzione, copia totale o parziale, dei contenuti inseriti nel presente volume, ivi inclusa la memorizzazione, rielaborazione, diffusione o distribuzione dei contenuti stessi mediante qualunque supporto magnetico o cartaceo, piattaforma tecnologica o rete telematica, senza previa autorizzazione scritta dell'autore.

ATTENZIONE: QUESTI APPUNTI SONO FATTI DA STUDENTI E NON SONO STATI VISIONATI DAL DOCENTE.
IL NOME DEL PROFESSORE, SERVE SOLO PER IDENTIFICARE IL CORSO.

© Proprietà riservata dell'autore - Digitalizzazione e distribuzione a cura del CENTRO APPUNTI - Corso Luigi Einaudi, 55 - Torino / Pagina 3 di 286

SOVRASTRUTTURE

(Pavement and track)

Prof. Santagata

© Proprietà riservata dell'autore - Digitalizzazione e distribuzione a cura del CENTRO APPUNTI - Corso Luigi Einaudi, 55 - Torino / Pagina 3 di 286

© Proprietà riservata dell'autore - Digitalizzazione e distribuzione a cura del CENTRO APPUNTI - Corso Luigi Einaudi, 55 - Torino / Pagina 5 di 286

Adequate parameters

- Mechanistic approach : material characterization and in service experimental evaluation

Required for:

- structural design;
- condition assessment of in service P&T's;
- allowable loads;
- maintenance planning;
- research and development of improved P&T materials and structures.

© Proprietà riservata dell'autore - Digitalizzazione e distribuzione a cura del CENTRO APPUNTI - Corso Luigi Einaudi, 55 - Torino / Pagina 5 di 286

© Proprietà riservata dell'autore - Digitalizzazione e distribuzione a cura del CENTRO APPUNTI - Corso Luigi Einaudi, 55 - Torino / Pagina 7 di 286

- Binder course : large aggregate than those which constitute the surface course, and less bitumen. Functions:
  - load distribution.
- Base Course : composed by granular mixture or dense-graded bituminous mixture. It is also possible to use stabilized mixtures with a component (bitumen, lime ...) which increase shear stiffness and resistence. Function:
  - load distribution.
- Subbase course : composed by unbound granular mixture
  Functions: - load distribution
  - filter
- Track coat : treatment needed between two layers of bituminous mixture → light application of bitumen. Function:
  - create a continuous structure with no discontinuity
- prime coat : ensure bond between a bituminous and a granular layer. It is thicker than track coat.
- Subgrade : it has to support the pavement. This support should be uniform to avoid localized stresses. The top of this layer has to be compacted.

Rigid pavements

They are made with cement concrete and granular materials

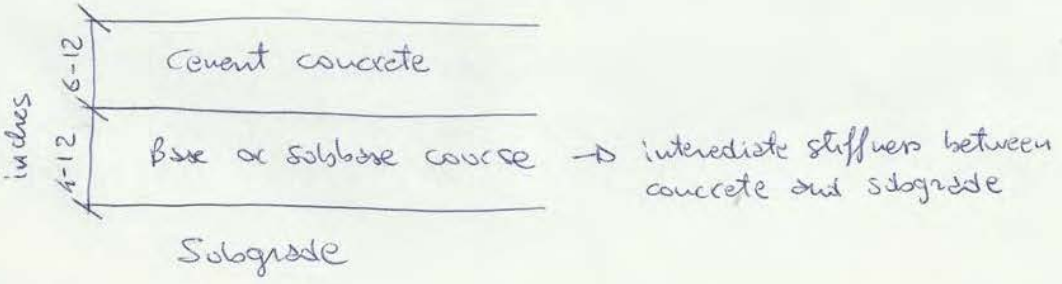

© Proprietà riservata dell'autore - Digitalizzazione e distribuzione a cura del CENTRO APPUNTI - Corso Luigi Einaudi, 55 - Torino / Pagina 7 di 286

© Proprietà riservata dell'autore - Digitalizzazione e distribuzione a cura del CENTRO APPUNTI - Corso Luigi Einaudi, 55 - Torino / Pagina 9 di 286

Alternative

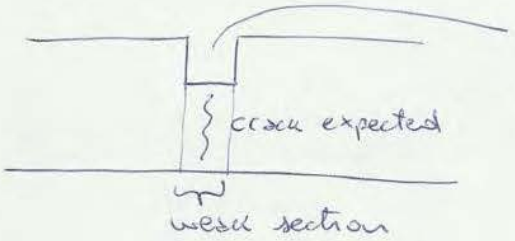

long slabs : relative movement greater

- jointed reinforced concrete pavements
  Steel reinforcement to increase spacing → 30 ÷ 100 ft
  Dowel are always required (very long slabs) the amount of steel is designed to hold cracks
- continuous reinforced concrete pavements
  Distribution of thin transverse cracks in the entire slab. Steel designed to control spacing and width of cracks and maximum stress on steel.
- pretensed concrete pavements
  Reduction of tensile stresses → it allows to decrease layer thickness

Semi-rigid pavements

Flexible pavement plus extra base layer made by cement (in general) stabilized material to provide a stiff support.
The cement stabilized sub-base provides a stiff support while the bituminous mixtures provide a flexible and smooth surfacing and so, there are flexible pavements with an extra resistance given by the cement stabilized base.

Composite pavements (very expensive)
Cement concrete plus bituminous mixtures → Cracks don't reflect on bituminous layer.

© Proprietà riservata dell'autore - Digitalizzazione e distribuzione a cura del CENTRO APPUNTI - Corso Luigi Einaudi, 55 - Torino / Pagina 9 di 286

© Proprietà riservata dell'autore - Digitalizzazione e distribuzione a cura del CENTRO APPUNTI - Corso Luigi Einaudi, 55 - Torino / Pagina 11 di 286

Fonctions: - load distribution
- damping of most of the train vibration (voids which reduce propagation of vibration)
- fast drainage of rainwater

- Subballast: additional layer which is typically made of gravel sand, recently bituminous mixture or cement stabilized material. Functions: - load distribution
- protect the subgrade from the penetration of big stone from ballast (physical barrier)
- fast drainage of water
- damping effect: dissipation of part of the energy

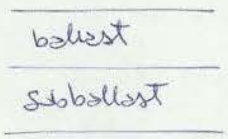

- Subgrade: soil which support uniformly the railway tracks it is around 2 meters the depth of disturbances from train passage.

© Proprietà riservata dell'autore - Digitalizzazione e distribuzione a cura del CENTRO APPUNTI - Corso Luigi Einaudi, 55 - Torino / Pagina 11 di 286

© Proprietà riservata dell'autore - Digitalizzazione e distribuzione a cura del CENTRO APPUNTI - Corso Luigi Einaudi, 55 - Torino / Pagina 13 di 286

Since vehicles are moving along the road, the load is going to change on our pavements; that's because pavements are not perfectly flat. That causes accelerations to respond masses inside the vehicles (dynamic effect).

Loading speed (or frequency) will affect all those speed-dependent materials (bituminous ones).

Vehicles are masses composed by moving parts: we should consider the real interaction between the entire vehicle and the pavement and not only the vehicle one.

So - frequency: would be matching with vehicles speed;
- stress;
- temperature: we have air temperature from meteorological data, but inside pavements there will be temperature profiles changing by time. There are however models converting air temperature into pavement Temperature.

We can divide the problem into different scheme:
- first is due to stress/load action;
- second is due to ΔT.

We also have to consider that:
- materials weak in time because of damage effects;
- Soil change properties in time in terms of lift

Rigid

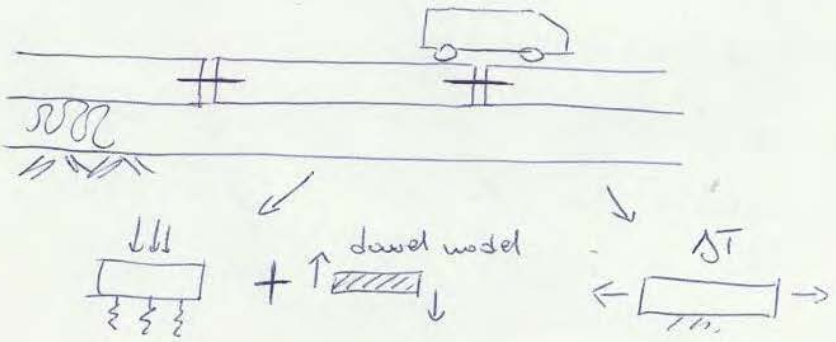

© Proprietà riservata dell'autore - Digitalizzazione e distribuzione a cura del CENTRO APPUNTI - Corso Luigi Einaudi, 55 - Torino / Pagina 13 di 286

© Proprietà riservata dell'autore - Digitalizzazione e distribuzione a cura del CENTRO APPUNTI - Corso Luigi Einaudi, 55 - Torino / Pagina 15 di 286

- Loading not only vertical but also horizontal (such as in waves), longitudinally and transversally (different models for each of them);
- Sleeping model;
- Ballast model: we have rectangular patches and it's not a continuous material (study the problem physics).

© Proprietà riservata dell'autore - Digitalizzazione e distribuzione a cura del CENTRO APPUNTI - Corso Luigi Einaudi, 55 - Torino / Pagina 15 di 286

© Proprietà riservata dell'autore - Digitalizzazione e distribuzione a cura del CENTRO APPUNTI - Corso Luigi Einaudi, 55 - Torino / Pagina 17 di 286

The basic assumption to be satisfied are:

- each layer is homogeneous, isotropic and linearly elastic with an elastic modulus E and a poisson ratio ν;
- the material is weightless and infinite in area extent;
- each layer has a finite thickness h, except the lowest layer is infinite in thickness;
- a uniform pressure q is applied on the surface over a circular area of radius a;
- continuity conditions are satisfied at the layer interface as indicate the same vertical stress, shear stress, vertical displacement and radial displacement.

By contrast multi-layer elastic theory has some limitations:

- pavement isn't indefinite in width. This problem can be neglected if the load is applied at more than 0,6 m from the edge;
- pavement's layers are not constant in thickness but variations of layer thickness are always expected. We can divide each layer in areas with constant thickness;
- loading area isn't circular and so shear stresses always exist;
- pavement's layer are not perfectly bound to each other but we have an intermediate condition (neither bound or unbound);
- materials are not elastic but they have an elastic, plastic, viscous and visco-elastic behaviour. It is not linear and depends of stresses;
- materials are not homogeneous and in fact granular materials are particulate in nature;
- in granular materials, particles orientation affects structural response and this means that pavement's material aren't isotropic.

© Proprietà riservata dell'autore - Digitalizzazione e distribuzione a cura del CENTRO APPUNTI - Corso Luigi Einaudi, 55 - Torino / Pagina 17 di 286

© Proprietà riservata dell'autore - Digitalizzazione e distribuzione a cura del CENTRO APPUNTI - Corso Luigi Einaudi, 55 - Torino / Pagina 19 di 286

- rigid plate

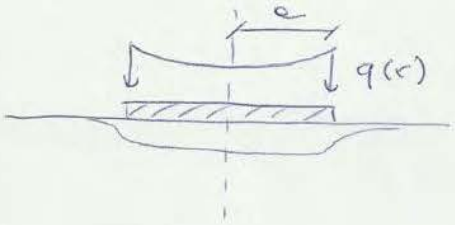

Ullitz formulation (1987)

$$q(r) = \frac{q\,a}{\varepsilon (a^2 - r^2)^{0,5}}$$ pressure distribution

Boussinesq's solution for this particular distribution

$$w_\phi = \frac{\pi (1-\nu^2) q\,a}{2E}$$

The displacement for the same radius and pressure is slightly smaller than the one which occurs in case of flexible plate.

- BURMISTER'S THEORY

Burmister studied a two layers system in which each layer is homogeneous, isotropic, linearly elastic with an elastic modulus and Poisson ratio, and has an uniform thickness and infinite extension in horizontal direction, resting on a semi-infinite elastic half-space.

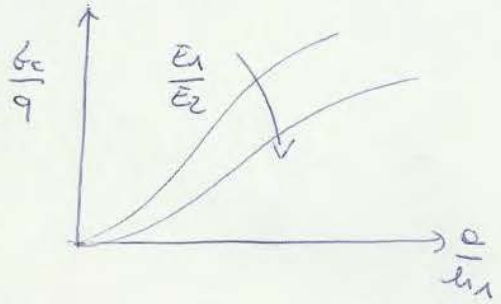

Vertical stress decreases considerably if the modulus ratio $\frac{E_1}{E_2}$ increases.

σ_c = maximum compressive tension admitted at the interface

$\frac{E_1}{E_2}$ high : the material on top is very stiff → < slope of the curve : I need very high variation of the thickness to have variation on the distribution of stresses.

© Proprietà riservata dell'autore - Digitalizzazione e distribuzione a cura del CENTRO APPUNTI - Corso Luigi Einaudi, 55 - Torino / Pagina 19 di 286

© Proprietà riservata dell'autore - Digitalizzazione e distribuzione a cura del CENTRO APPUNTI - Corso Luigi Einaudi, 55 - Torino / Pagina 21 di 286

$$\varepsilon_{z1} = \frac{\sigma_{z1}}{E_1} - \nu\frac{\sigma_{t1}}{E_1} - \nu\frac{\sigma_{r1}}{E_1} = \frac{\sigma_{z1}-\sigma_{r1}}{E_1}$$

$$\varepsilon_{z2} = \frac{\sigma_{z2}}{E_2} - \nu\frac{\sigma_{t2}}{E_2} - \nu\frac{\sigma_{r2}}{E_2} = \frac{\sigma_{z2}-\sigma_{r2}}{E_2}$$

$$\varepsilon_{r1} = \frac{\sigma_{r1}}{E_1} - \nu\frac{\sigma_{z1}}{E_1} - \nu\frac{\sigma_{t1}}{E_1} = \frac{\sigma_{r1}-\sigma_{z1}}{2E_1}$$

$$\varepsilon_{r2} = \frac{\sigma_{r2}}{E_2} - \nu\frac{\sigma_{z2}}{E_2} - \nu\frac{\sigma_{t2}}{E_2} = \frac{\sigma_{r2}-\sigma_{z2}}{2E_2}$$

At the interfaces: $\varepsilon_{r1} = \varepsilon_{r1}^{*} \rightarrow \frac{\sigma_{r1}-\sigma_{z1}}{2E_1} = \frac{\sigma_{r1}^{*}-\sigma_{z1}}{2E_2}$

- ODEMARK'S THEORY

This theory is also called "Method of Equivalent thickness" and it allow to transform a multi-layer system in which layers have different modulus and Poisson ratio into an equivalent homogeneous half-space in which each-layer has the same modulus and Poisson ratio but different thickness.
In this case it is possible to use Boussinesq equations to calculate stresses, strains and deflections.

Hypothesis: $\begin{cases} \frac{E_i}{E_{i+1}} \geq 2 \\ h_{ei} \geq a \end{cases}$

E = elastic modulus
h_{ei} = equivalent thickness
a = radius of the loading area

Odemark assumed that for each layer:

$\frac{E}{1-\nu^2} = \text{const}$ It means that each layer has a constant stiffness.

© Proprietà riservata dell'autore - Digitalizzazione e distribuzione a cura del CENTRO APPUNTI - Corso Luigi Einaudi, 55 - Torino / Pagina 21 di 286

TABLE 2.1
Boussinesq's equations for a point load

Normal Stresses
$\sigma_z = 3P/(2\pi R^2) * \cos^3\theta$
$\sigma_r = P/(2\pi R^2) * [3\cos\theta \sin^2\theta - (1-2\mu)/(1+\cos\theta)]$
$\sigma_t = P/(2\pi R^2) * (1-2\mu)[-\cos\theta + 1/(1+\cos\theta)]$
$\sigma_1 = 3P/(2\pi R^2) * \cos\theta$
$\sigma_v = 1/3(\sigma_1 + \sigma_2 + \sigma_3) = P/(3\pi R^2) * (1+\mu)\cos\theta$
Shear Stresses
$\tau_{rz} = 3P/(2\pi R^2) * \cos^2\theta \sin\theta$
$\tau_{rt} = \tau_{tz} = 0$
Normal Strains
$\varepsilon_z = (1+\mu)P/(2\pi R^2 E) * (3\cos^3\theta - 2\mu\cos\theta)$
$\varepsilon_r = (1+\mu)P/(2\pi R^2 E) * [-3\cos^3\theta + (3-2\mu)\cos\theta - (1-2\mu)/(1+\cos\theta)]$
$\varepsilon_t = (1+\mu)P/(2\pi R^2 E) * [-\cos\theta + (1-2\mu)/(1+\cos\theta)]$
$\varepsilon_v = \varepsilon_z + \varepsilon_r + \varepsilon_t = (1+\mu)P/(\pi R^2 E) * (1-2\mu)\cos\theta$
Displacements
$d_z = (1+\mu)P/(2\pi RE) * [2(1-\mu) + \cos^2\theta]$
$d_r = (1+\mu)P/(2\pi RE) * [\cos\theta \sin\theta - (1-2\mu)\sin\theta/(1+\cos\theta)]$
$d_t = 0$

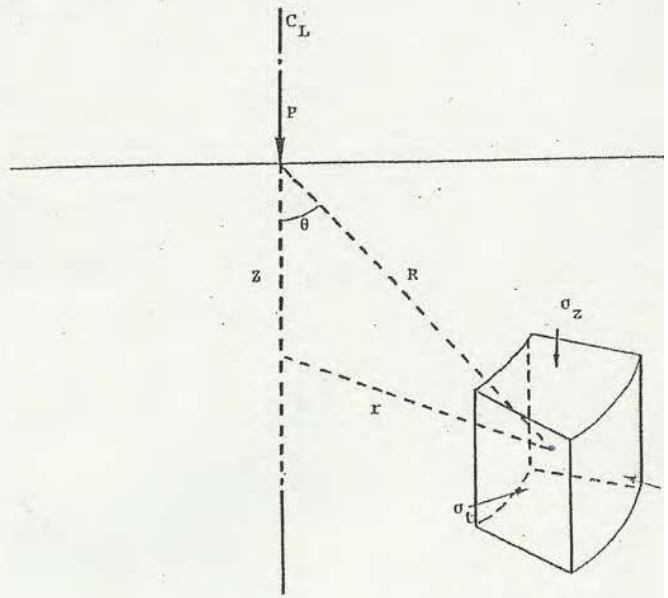

Fig. 2.2. Notation in polar coordinates used with Boussi equations

At the center line of the load the equations for ve stress, strain and displacement reduce to:

$$\sigma_z = 3 * P/(2\pi)/z^2 \quad (2.4)$$

$$\varepsilon_z = (1 + \mu) * (3 - 2 * \mu) * P/(2\pi)/z^2/E \quad (2.5)$$

$$d_z = (1 + \mu) * (3 - 2 * \mu) * P/(2\pi)/z/E \quad (2.6)$$

© Proprietà riservata dell'autore - Digitalizzazione e distribuzione a cura del CENTRO APPUNTI - Corso Luigi Einaudi, 55 - Torino / Pagina 23 di 286
© Proprietà riservata dell'autore - Digitalizzazione e distribuzione a cura del CENTRO APPUNTI - Corso Luigi Einaudi, 55 - Torino / Pagina 23 di 286

© Proprietà riservata dell'autore - Digitalizzazione e distribuzione a cura del CENTRO APPUNTI - Corso Luigi Einaudi, 55 - Torino / Pagina 25 di 286

Graphic representation of the resolution of the equation before

d=0 → centre line

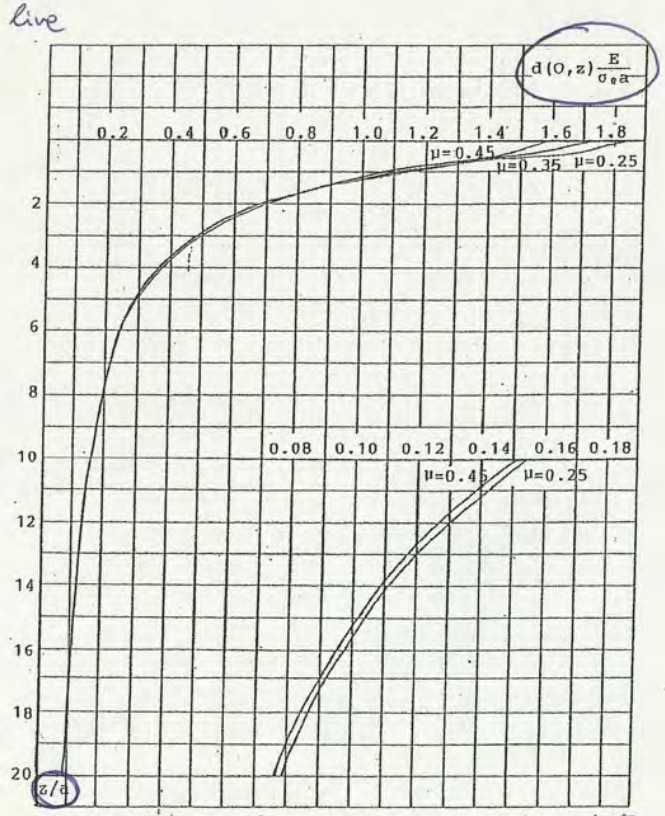

You can use in all of case (you can change the elastic modul you obtain the same graph)

Fig. 2.3, Deflection as a function of relative depth. Centerline of a uniformly distributed circular load.

Not diverticon representation

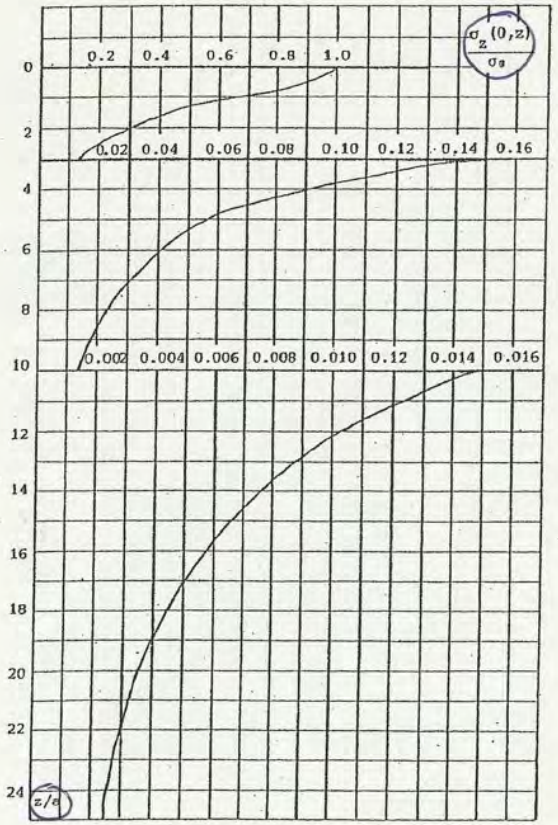

Fig. 2.4. Vertical normal stress as a function of relative depth. Center line of a uniformly distributed circular load.

different curve corrispond to a different Poisson ratio

© Proprietà riservata dell'autore - Digitalizzazione e distribuzione a cura del CENTRO APPUNTI - Corso Luigi Einaudi, 55 - Torino / Pagina 25 di 286

© Proprietà riservata dell'autore - Digitalizzazione e distribuzione a cura del CENTRO APPUNTI - Corso Luigi Einaudi, 55 - Torino / Pagina 27 di 286

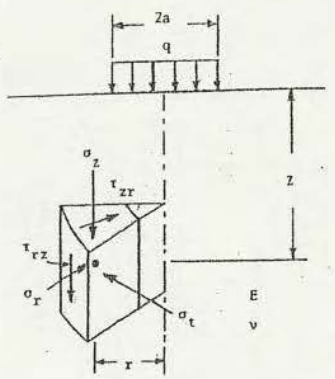

Figure 2.1 Component of stresses under axisymmetric loading.

different curve represent different value from the center line (r/a)
Vertical stress not depend of Poisson ratio

All strains can be obtained by using Hooke's law

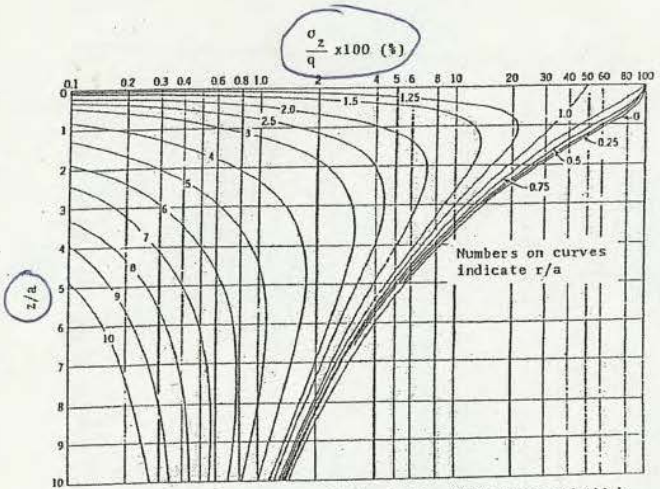

Figure 2.2 Vertical stresses due to circular loading. (After Foster and Ahlvin (1954).) Not dimensional representation

© Proprietà riservata dell'autore - Digitalizzazione e distribuzione a cura del CENTRO APPUNTI - Corso Luigi Einaudi, 55 - Torino / Pagina 27 di 286

© Proprietà riservata dell'autore - Digitalizzazione e distribuzione a cura del CENTRO APPUNTI - Corso Luigi Einaudi, 55 - Torino / Pagina 29 di 286

TABLE 2.1. Summary of One-Layer Elastic Equations[a] (after Ahlvin and Ulery)

Parameter	General Case	Special Case ($\mu = 0.5$)
Vertical stress	$\sigma_z = p[A + B]$	(same)
Radial horizontal stress	$\sigma_r = p[2\mu A + C + (1 - 2\mu)F]$	$\sigma_r = p[A + C]$
Tangential horizontal stress	$\sigma_t = p[2\mu A - D + (1 - 2\mu)E]$	$\sigma_t = p[A - D]$
Vertical radial shear stress	$\tau_{rz} = \tau_{zr} = pG$	(same)
Vertical strain	$\epsilon_z = \frac{p(1+\mu)}{E_1}[(1 - 2\mu)A + B]$	$\epsilon_z = \frac{1.5p}{E_1}B$
Radial horizontal strain	$\epsilon_r = \frac{p(1+\mu)}{E_1}[(1 - 2\mu)F + C]$	$\epsilon_r = \frac{1.5p}{E_1}C$
Tangential horizontal strain	$\epsilon_t = \frac{p(1+\mu)}{E_1}[(1 - 2\mu)E - D)]$	$\epsilon_t = -\frac{1.5p}{E_1}D$
Vertical deflection	$\Delta_z = \frac{p(1+\mu)a}{E_1}\left[\frac{z}{a}A + (1 - \mu)H\right]$	$\Delta_z = \frac{1.5pa}{E_1}\left(\frac{z}{a}A + \frac{H}{2}\right)$
Bulk stress	$\theta = \sigma_z + \sigma_r + \sigma_t$	
Bulk strain	$\epsilon_\theta = \epsilon_z + \epsilon_r + \epsilon_t$	
Vertical tangential shear stress	$\tau_{rt} = \tau_{tr} = 0 \therefore [\sigma_\lambda(\epsilon_t)$ is principal stress (strain)$]$	
Principal stresses	$\sigma_{1,2,3} = \frac{(\sigma_z + \sigma_r) \pm \sqrt{(\sigma_z - \sigma_r)^2 + (2\tau_{rz})^2}}{2}$	
Maximum shear stress	$\tau_{max} = \frac{\sigma_1 - \sigma_3}{2}$	

[a] See Table 2.2 for values of the functions A, B, C, D, E, F, G, and H. $(+)$ values compressive.

TABLE 2.2. One-Layer Elastic Function Values (after Ahlvin and Ulery)

Depth in (z) Radii	Function A																				
	Offset (r) in Radii																				
	0	0.2	0.4	0.6	0.8	1	1.2	1.5	2	3	4	5	6	8	10	12	14
0	1.0	1.0	1.0	1.0	1.0	.5	0	0	0	0	0	0	0	0	0	0	0
0.1	.90050	.89748	.88679	.86126	.78797	.49015	.09645	.02787	.00856	.00211	.00084	.00042					
0.2	.80588	.79824	.77884	.73483	.63014	.38269	.15483	.05251	.01680	.00419	.00167	.00083	.00048	.00020			
0.3	.71265	.70518	.68316	.62690	.52081	.34373	.17964	.07199	.02440	.00622	.00250						
0.4	.62861	.62015	.59241	.53767	.44329	.31048	.18709	.08593	.03118								
0.5	.55279	.54403	.51622	.46448	.38390	.28156	.18556	.09499	.03701	.01013	.00407	.00209	.00118	.00033	.00023	.00014	.00009
0.6	.48550	.47691	.45078	.40427	.33676	.25588	.17952	.10010									
0.7	.42554	.41874	.39491	.35428	.29833	.21727	.17124	.10228	.04558								
0.8	.37531	.36832	.34729	.31243	.26381	.21297	.16206	.10236									
0.9	.33104	.32492	.30669	.27707	.23832	.19488	.15253	.10094									
1	.29289	.28763	.27005	.24697	.21468	.17868	.14329	.09849	.05185	.01742	.00761	.00393	.00226	.00097	.00050	.00029	.00018
1.2	.23178	.22795	.21662	.19890	.17626	.13101	.12370	.09192	.05260	.01935	.00871	.00459	.00269	.00115			
1.5	.16795	.16552	.15877	.14804	.13436	.11892	.10296	.08048	.05116	.02142	.01013	.00548	.00325	.00141	.00073	.00043	.00027
2	.10557	.10453	.10140	.09647	.09011	.08269	.07471	.06275	.04496	.02221	.01160	.00659	.00399	.00180	.00094	.00056	.00036
2.5	.07152	.07098	.06947	.06698	.06373	.05974	.05355	.04880	.03787	.02143	.01221	.00732	.00463	.00242	.00115	.00068	.00043
3	.05132	.05101	.05022	.04886	.04707	.04487	.04241	.03839	.03150	.01980	.01220	.00770	.00505	.00262	.00132	.00079	.00051
4	.02986	.02976	.02907	.02832	.02802	.02749	.02651	.02490	.02193	.01592	.01109	.00768	.00536	.00282	.00160	.00099	.00065
5	.01942	.01938				.01573			.01749	.01249	.00949	.00708	.00527	.00298	.00179	.00113	.00075
6	.01361					.01307			.01168	.00983	.00795	.00628	.00492	.00299	.00188	.00124	.00084
7	.01005					.00976			.00894	.00784	.00661	.00548	.00445	.00291	.00193	.00130	.00091
8	.00772					.00735			.00703	.00633	.00554	.00472	.00398	.00276	.00189	.00134	.00094
9	.00612					.00600			.00566	.00520	.00466	.00409	.00353	.00256	.00184	.00133	.00096
10									.00463	.00438	.00397	.00352	.00326	.00241			

© Proprietà riservata dell'autore - Digitalizzazione e distribuzione a cura del CENTRO APPUNTI - Corso Luigi Einaudi, 55 - Torino / Pagina 29 di 286

© Proprietà riservata dell'autore - Digitalizzazione e distribuzione a cura del CENTRO APPUNTI - Corso Luigi Einaudi, 55 - Torino / Pagina 31 di 286

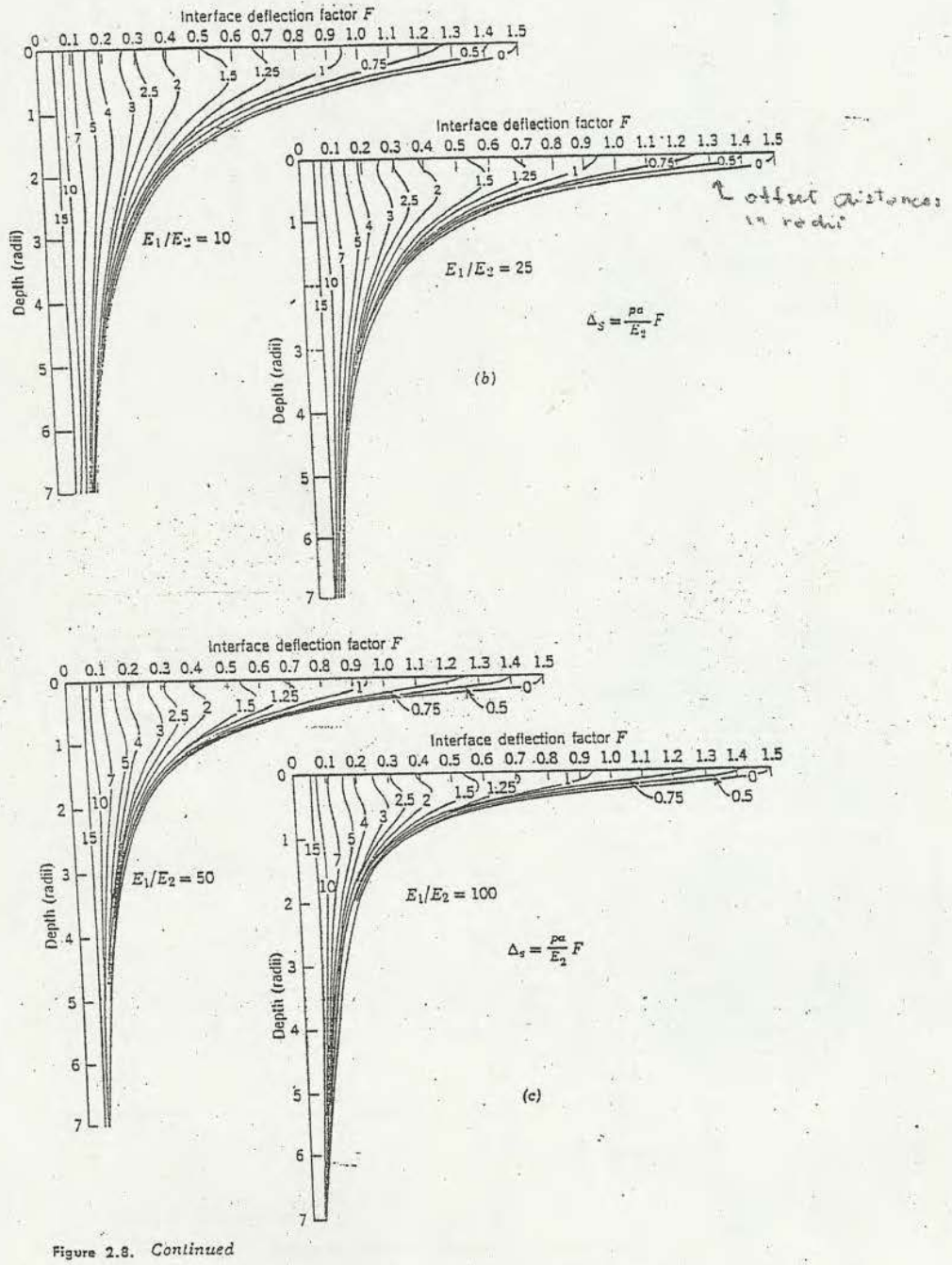

Figure 2.8. *Continued*

© Proprietà riservata dell'autore - Digitalizzazione e distribuzione a cura del CENTRO APPUNTI - Corso Luigi Einaudi, 55 - Torino / Pagina 31 di 286

© Proprietà riservata dell'autore - Digitalizzazione e distribuzione a cura del CENTRO APPUNTI - Corso Luigi Einaudi, 55 - Torino / Pagina 33 di 286

TABLE 2.3. Three-Layer Stress Factors (after Jones)

	$H = 0.125$ $k_1 = 0.2$			$H = 0.125$ $k_1 = 2.0$			$H = 0.125$ $k_1 = 20.0$			$H = 0.125$ $k_1 = 200.0$		
a_1	$(ZZ1-RR1)$	$(ZZ2-RR2)$	$(ZZ2-RR3)$	$(ZZ1-RR1)$	$(ZZ2-RR2)$	$(ZZ2-RR3)$	$(ZZ1-RR1)$	$(ZZ2-RR2)$	$(ZZ2-RR3)$	$(ZZ1-RR1)$	$(ZZ2-RR2)$	$(ZZ2-RR3)$
			$k_2 = 0.2$			$k_2 = 0.2$			$k_2 = 0.2$			$k_2 = 0.2$
0.1	0.12438	0.00332	0.01859	0.71614	0.00350	0.01750	1.80805	0.00322	0.01611	2.87564	0.00201	0.01005
0.2	0.13546	0.01278	0.06391	1.01561	0.01348	0.06741	3.75440	0.01249	0.06244	7.44285	0.00788	0.03940
0.4	0.10428	0.04480	0.22160	0.83924	0.04669	0.23346	6.11847	0.04421	0.22105	15.41021	0.02913	0.14566
0.8	0.09011	0.10975	0.54877	0.63961	0.11484	0.57418	3.38600	0.11468	0.57342	9.70261	0.08714	0.43568
1.6	0.08777	0.13755	0.68777	0.65723	0.13756	0.68630	1.81603	0.13687	0.68436	7.02380	0.13705	0.68524
3.2	0.04120	0.10147	0.50736	0.38165	0.09467	0.47335	1.75101	0.07578	0.37890	2.38439	0.06594	0.32971
			$k_2 = 2.0$			$k_2 = 2.0$			$k_2 = 2.0$			$k_2 = 2.0$
0.1	0.12285	0.01693	0.00846	0.70622	0.01716	0.00858	1.81178	0.01642	0.00771	3.02259	0.00959	0.00485
0.2	0.12916	0.06558	0.03279	0.97966	0.06847	0.03324	3.76886	0.06008	0.03002	5.02453	0.03812	0.01906
0.4	0.08115	0.23257	0.11629	0.70970	0.23531	0.11766	5.16717	0.21640	0.10820	17.54176	0.14286	0.07143
0.8	0.01823	0.62863	0.31432	0.22319	0.63003	0.31501	3.42531	0.60493	0.30247	27.27701	0.45208	0.22604
1.6	−0.04136	0.98754	0.49377	−0.19982	0.97707	0.48853	1.16211	0.97145	0.48573	23.38638	0.90861	0.45430
3.2	−0.03804	0.82102	0.41051	−0.28916	0.84030	0.42015	−0.08894	0.88358	0.44179	11.87014	0.91469	0.45735
			$k_2 = 20.0$			$k_2 = 20.0$			$k_2 = 20.0$			$k_2 = 20.0$
0.1	0.12032	0.03657	0.00183	0.69332	0.03467	0.00173	1.80664	0.02985	0.00149	3.17763	0.01980	0.00099
0.2	0.11787	0.14336	0.00717	0.92086	0.13541	0.00677	3.74573	0.11697	0.00585	8.66097	0.07827	0.00391
0.4	0.03474	0.52691	0.02635	0.46583	0.49323	0.02476	5.05489	0.43263	0.02163	20.12259	0.20887	0.01494
0.8	−0.14872	1.61727	0.08086	−0.66536	1.49612	0.07481	2.92533	1.33735	0.06687	36.29943	1.01694	0.05085
1.6	−0.50533	3.58944	0.17947	−2.82859	3.28512	0.16426	−1.27093	2.99215	0.14961	49.40857	2.64313	0.13216
3.2	−0.80990	5.15409	0.25770	−5.27006	5.05952	0.25298	−7.35384	5.06489	0.25324	57.84369	4.80895	0.24495
			$k_2 = 200.0$			$k_2 = 200.0$			$k_2 = 200.0$			$k_2 = 200.0$
0.1	0.11720	0.05413	0.00027	0.67488	0.04848	0.00024	1.78941	0.04010	0.00020	3.26987	0.02809	0.00014
0.2	0.10495	0.21314	0.00170	0.85397	0.19043	0.00095	3.68097	0.15781	0.00079	9.02869	0.11136	0.00056
0.4	−0.01709	0.80400	0.00402	0.21155	0.71221	0.00356	4.80711	0.59391	0.00297	21.56482	0.43035	0.00215
0.8	−0.34427	2.67934	0.01340	−1.55954	2.32652	0.01163	1.90825	1.98709	0.00979	41.89573	1.53070	0.00765
1.6	−1.21139	7.35078	0.03680	−6.47707	6.26538	0.03133	−6.28803	5.25110	0.02626	60.63127	4.56707	0.02284
3.2	−2.89282	16.22830	0.08114	−16.67376	14.25621	0.07128	−21.52546	12.45068	0.06225	120.95231	11.42045	0.05710

TABLE 2.3. (continued)

	$H = 0.25$ $k_1 = 0.2$			$H = 0.25$ $k_1 = 2.0$			$H = 0.25$ $k_1 = 20.0$			$H = 0.25$ $k_1 = 200.0$		
a_1	$(ZZ1-RR1)$	$(ZZ2-RR2)$	$(ZZ2-RR3)$	$(ZZ1-RR1)$	$(ZZ2-RR2)$	$(ZZ2-RR3)$	$(ZZ1-RR1)$	$(ZZ2-RR3)$	$(ZZ2-RR3)$	$(ZZ1-RR1)$	$(ZZ2-RR2)$	$(ZZ2-RR3)$
			$k_2 = 0.2$			$k_2 = 0.2$			$k_2 = 0.2$			$k_2 = 0.2$
0.1	0.05696	0.00274	0.01370	0.28658	0.00277	0.01384	0.61450	0.00202	0.01011	0.85644	0.00000	00.0431
0.2	0.12628	0.01060	0.05302	0.72176	0.01076	0.05377	1.76675	0.00793	0.03964	2.71354	0.00357	0.01784
0.4	0.14219	0.03744	0.18722	1.03476	0.03842	0.19211	3.59650	0.02931	0.14653	6.83021	0.01365	0.06824
0.8	0.12300	0.09539	0.49196	0.88833	0.10337	0.51687	4.56845	0.08771	0.43854	13.19664	0.04524	0.23118
1.6	0.10534	0.13917	0.69586	0.66438	0.14102	0.70510	2.31165	0.14039	0.70194	13.79134	0.10591	0.52955
3.2	0.05063	0.11114	0.55589	0.41539	0.09804	0.49020	1.24415	0.07587	0.37934	2.72901	0.08608	0.43037
			$k_2 = 2.0$			$k_2 = 2.0$			$k_2 = 2.0$			$k_2 = 2.0$
0.1	0.05477	0.01409	0.00704	0.28362	0.01353	0.00677	0.63215	0.00962	0.00481	0.96553	0.00407	0.00203
0.2	0.12136	0.05484	0.02742	0.70225	0.05278	0.02639	1.83786	0.03781	0.01891	3.10763	0.01611	0.00805
0.4	0.12390	0.19780	0.09890	0.96634	0.19178	0.09589	3.56770	0.14159	0.07079	5.37852	0.06221	0.03110
0.8	0.06482	0.56039	0.28019	0.66885	0.55211	0.27605	5.50796	0.44710	0.22355	18.95534	0.21880	0.10930
1.6	−0.00319	0.96216	0.48108	0.17331	0.95080	0.47540	4.24281	0.90115	0.45058	31.18909	0.58553	0.29277
3.2	−0.02218	0.87221	0.43610	−0.08691	0.89390	0.44695	1.97494	0.93254	0.46627	28.98500	0.89191	0.44595
			$k_2 = 20.0$			$k_2 = 20.0$			$k_2 = 20.0$			$k_2 = 20.0$
0.1	0.05192	0.03116	0.00156	0.27580	0.02728	0.00136	0.65003	0.01930	0.00096	1.08738	0.00861	0.00043
0.2	0.11209	0.12227	0.00611	0.67115	0.10710	0.00536	1.90693	0.07623	0.00381	3.59448	0.03421	0.00171
0.4	0.08632	0.45504	0.02275	0.84462	0.39919	0.01996	4.13976	0.29072	0.01454	10.30223	0.13365	0.00668
0.8	−0.07351	1.44285	0.07214	0.21951	1.26565	0.06328	5.48948	0.98565	0.04928	26.41442	0.49135	0.02457
1.6	−0.40234	3.37001	0.16850	−1.22411	2.94866	0.14743	5.95639	2.55231	0.12762	57.46409	1.53833	0.07692
3.2	−0.71901	5.10060	0.25503	−3.04320	4.89878	0.24494	6.05854	4.76234	0.23812	99.29034	3.60964	0.18048
			$k_2 = 200.0$			$k_2 = 200.0$			$k_2 = 200.0$			$k_2 = 200.0$
0.1	0.04956	0.04704	0.00024	0.26776	0.03814	0.00019	0.55732	0.02711	0.00014	1.19099	0.01311	0.00007
0.2	0.10066	0.18557	0.00093	0.63873	0.15040	0.00075	1.93764	0.10741	0.00054	4.00968	0.05223	0.00026
0.4	0.04248	0.70524	0.00353	0.71620	0.57046	0.00285	4.26004	0.41459	0.00207	11.96405	0.20551	0.00103
0.8	−0.24071	2.40585	0.01203	−0.28250	1.92636	0.00963	5.94871	1.46947	0.00735	32.97364	0.77584	0.00388
1.6	−1.00743	6.82481	0.03412	−3.09856	5.35936	0.02680	5.55770	4.36521	0.02183	82.77997	2.63962	0.01320
3.2	−2.54264	15.46031	0.07730	−9.18214	12.64315	0.06322	10.63614	10.93570	0.05468	189.37439	7.60287	0.03801

© Proprietà riservata dell'autore - Digitalizzazione e distribuzione a cura del CENTRO APPUNTI - Corso Luigi Einaudi, 55 - Torino / Pagina 33 di 286

© Proprietà riservata dell'autore - Digitalizzazione e distribuzione a cura del CENTRO APPUNTI - Corso Luigi Einaudi, 55 - Torino / Pagina 35 di 286

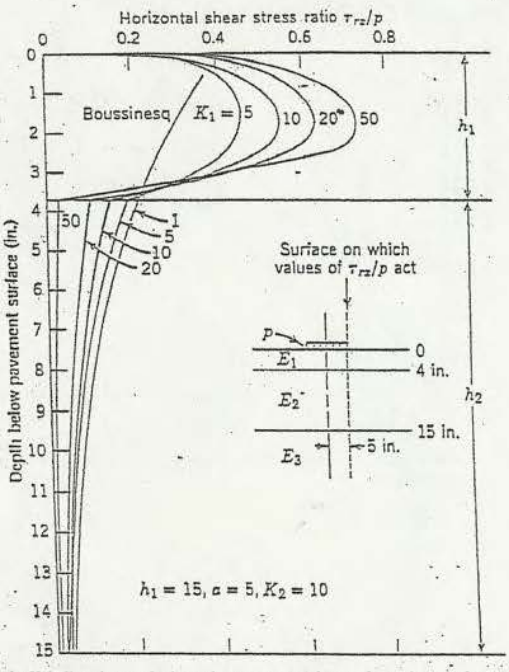

Figure 2.12. Typical distribution of shearing stresses in a three-layered system. (From Nielson.)

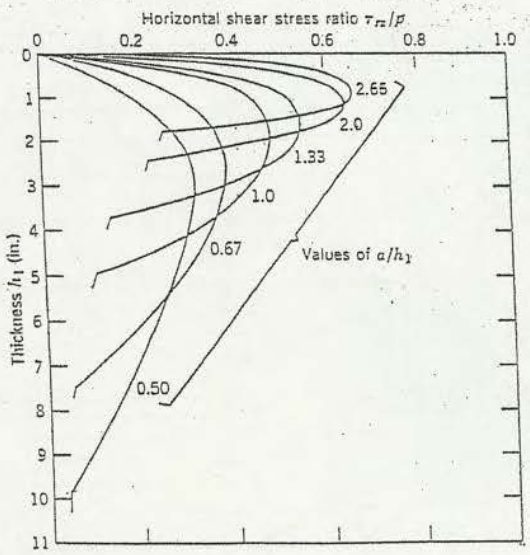

Figure 2.13. Influence of a/h on the depth and magnitude of (τ_{rz}/p) for $a = 5$ inches and $K_1 = K_2 = 20$. (From Nielson.)

© Proprietà riservata dell'autore - Digitalizzazione e distribuzione a cura del CENTRO APPUNTI - Corso Luigi Einaudi, 55 - Torino / Pagina 35 di 286

© Proprietà riservata dell'autore - Digitalizzazione e distribuzione a cura del CENTRO APPUNTI - Corso Luigi Einaudi, 55 - Torino / Pagina 37 di 286

effect of contact pressure

effect are equal

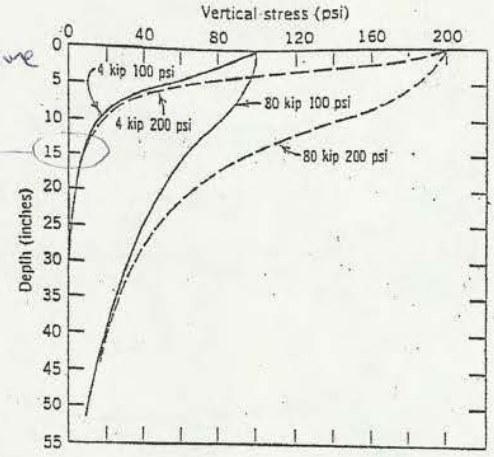

Figure 2.15. Variation of vertical stress with depth, Boussinesq problem.

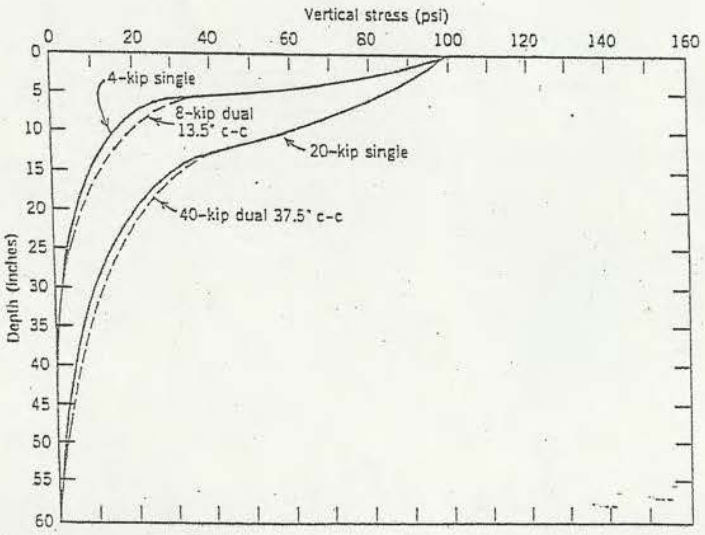

Figure 2.16. Effect of number of wheels on vertical stress. Boussinesq problem. Notes (1) All tires have 100 psi inflation. (2) Depth at which interaction of dual wheels is significant is about equal to one-half the clear distance between tires. (3) Depth at which dual tires will act as a single tire is about two times the c-c spacing of the tires.

© Proprietà riservata dell'autore - Digitalizzazione e distribuzione a cura del CENTRO APPUNTI - Corso Luigi Einaudi, 55 - Torino / Pagina 37 di 286

© Proprietà riservata dell'autore - Digitalizzazione e distribuzione a cura del CENTRO APPUNTI - Corso Luigi Einaudi, 55 - Torino / Pagina 39 di 286

GOLDBECK'S FORMULA (1929)

Load applied at the corner of a slab (vertical load)

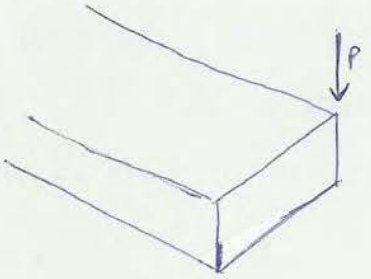

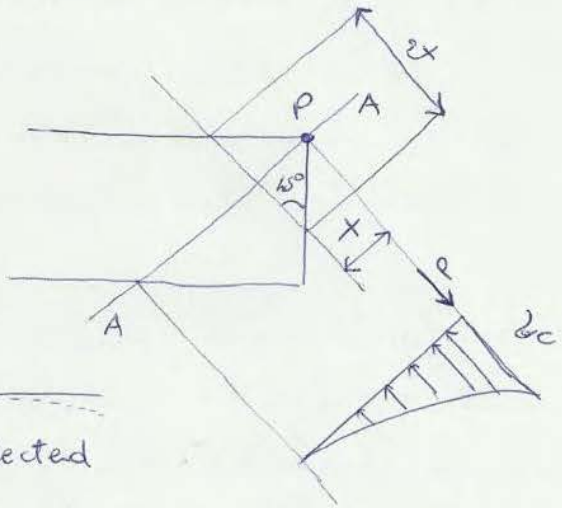

model : cantilever beam

subgrade support neglected

Stress in the slab is symmetrical respect diagonal A-A.

The deflection of the corner depends upon the :

- intensity of the force;
- stiffness;
- response of the supporting layer.

This last one is a function of x (distance from the loading point) but Goldbeck neglects these reaction for a conservative point of view → deflection Gold > real deflection.

Considering a cross section equal to x, the bending moment is $P \cdot x$ while the width is $2x$.

The tensile stress on the top of the slab is:

$$\sigma_c = \frac{P \cdot x}{\frac{1}{12} 2x h^3} \frac{h}{2} = \frac{3P}{h^2}$$

it indicates that the stress is indipendent from x.

© Proprietà riservata dell'autore - Digitalizzazione e distribuzione a cura del CENTRO APPUNTI - Corso Luigi Einaudi, 55 - Torino / Pagina 39 di 286

© Proprietà riservata dell'autore - Digitalizzazione e distribuzione a cura del CENTRO APPUNTI - Corso Luigi Einaudi, 55 - Torino / Pagina 41 di 286

$$L = \sqrt{\frac{P}{0,5227\,q}}$$

Area of the equivalent circle is:

$$\pi a^2 = 2 \cdot 0,5227 L^2 + (S_d - 0,6L)L = 0,445 L^2 + S_d L$$

so $$a = \sqrt{\frac{0,351\,P}{q\pi} + \frac{S_d}{\pi}\left(\frac{P}{0,5227\,q}\right)^{1/2}}$$

In fact if we use a loading area equal to the sum of the two wheel loading areas, we will obtain higher stresses and deflections. This is why we consider a larger loading area composed by contact areas + the area between the tires.

Westergaard considers four load configuration:

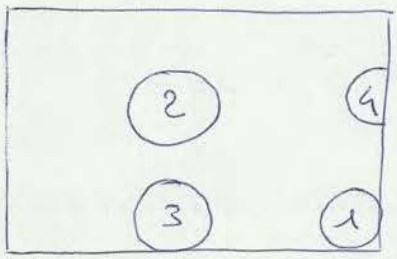

1- corner loading
2- interior loading
3- edge loading (circular area)
4- edge loading (semi-circular area)

1- corner loading

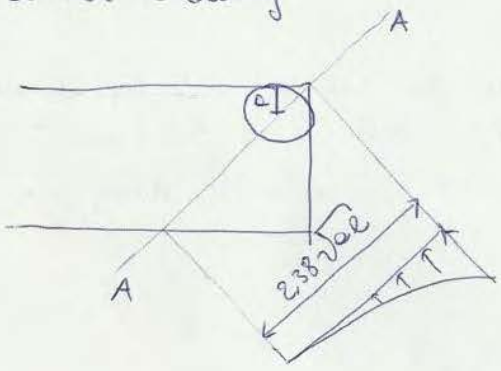

in this point there is the minim contribute from the continuity of the slab so we expect to have the higher stresses.
Reactive forces are not neglected.

$$\sigma_c = \frac{3P}{h^2}\left[1 - \left(\frac{a\sqrt{2}}{\ell}\right)^{0,6}\right]$$

a = radius of the circular joint

© Proprietà riservata dell'autore - Digitalizzazione e distribuzione a cura del CENTRO APPUNTI - Corso Luigi Einaudi, 55 - Torino / Pagina 41 di 286

© Proprietà riservata dell'autore - Digitalizzazione e distribuzione a cura del CENTRO APPUNTI - Corso Luigi Einaudi, 55 - Torino / Pagina 43 di 286

h- edge loading (semicircle area)

$$\delta_i = \frac{3(1+\nu)P}{\pi(3+\nu)h^2}\left[\ln\left(\frac{Eh^3}{100\,k a^4}\right) + 3{,}84 - \frac{4\nu}{3} + \frac{(1+2\nu)a}{2\ell}\right]$$

$$\Delta_i = \frac{\sqrt{2+1{,}2\nu P}}{\sqrt{Eh^3 k}}$$

Westergaard's theory has some limitations:

- Slabs aren't isolated because they are jointed togheter through dowels and ties bars;
- Slab support doesn't behave as a winkler foundation and it is only a semplify behaviour;
- Single wheel load isn't realistic but we expect multiple loading.

PICKETT and RAY'S INFLUENCE CHARTS (1951)

These charts are developed in order to consider the case of multiple loads in any configuration.

They consider Westergaard's theory assuming $\nu = 0{,}15$ and a liquid foundation (winkler).

The charts give the value of the moment and of the deflection in a specific point and in a specific direction.

There are two available cases:

- interior loading;
- edge loading.

The charts are different but the procedure to use and the expressions of M_A and Δ_i are the same

© Proprietà riservata dell'autore - Digitalizzazione e distribuzione a cura del CENTRO APPUNTI - Corso Luigi Einaudi, 55 - Torino / Pagina 43 di 286

© Proprietà riservata dell'autore - Digitalizzazione e distribuzione a cura del CENTRO APPUNTI - Corso Luigi Einaudi, 55 - Torino / Pagina 45 di 286

TEMPERATURE VARIATIONS in RIGID PAVEMENTS

State of stress induced in slabs by temperature variations.

During the day temperature on the top of the pavement is greater than the temperature to the bottom → Downward curling
During the night is exactly the opposite → Upward curling

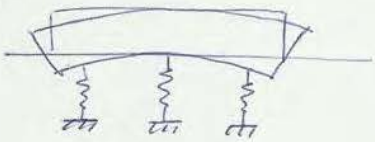

Day - downward curling

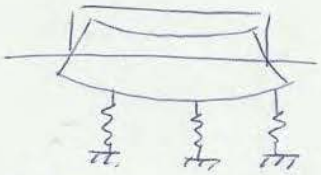

Night - Upward curling

During the day, the weight of slab counter-balances the curvature due to thermal variations. If the movement are allowed, the stresses don't appear in the pavement but, in the real case slab are connected themselves and so the movements aren't allowed and this bring to stresses.

Adopting a winkler foundation it is possible to explain what happens considering the soil reaction. In the first case ($T_{top} > T_{bottom}$) we have springs which push up the pavement

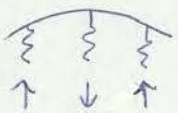

while in the second case ($T_{top} < T_{bottom}$) there are compressed spring

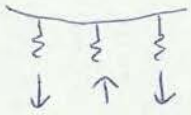

Westergaard gives an analytical solution for this problem:

$$\varepsilon_x = \frac{\sigma_x}{E} - \nu\frac{\sigma_y}{E}$$

$$\varepsilon_y = \frac{\sigma_y}{E} - \nu\frac{\sigma_x}{E}$$

} Hooke's law : state of stress σ_x, σ_y which introduces a state of strain

© Proprietà riservata dell'autore - Digitalizzazione e distribuzione a cura del CENTRO APPUNTI - Corso Luigi Einaudi, 55 - Torino / Pagina 45 di 286

© Proprietà riservata dell'autore - Digitalizzazione e distribuzione a cura del CENTRO APPUNTI - Corso Luigi Einaudi, 55 - Torino / Pagina 47 di 286

Stresses in x direction is equal to stress due to bending in x direction plus due to bending in y direction.

$$\sigma_x = \frac{E\alpha\Delta T}{2(1-\nu^2)} \qquad \text{bending in x direction}$$

$$\sigma_x = \nu\left(\frac{E\alpha\Delta T}{2(1-\nu^2)}\right) \qquad \text{bending in y direction}$$

The total stress is the sum of these two compoents:

$$\sigma_{x\,tot} = \frac{E\alpha\Delta T}{2(1-\nu)}$$

At the same thing we can obtain $\sigma_{y\,tot}$ in the other direction:

$$\sigma_{y\,tot} = \frac{E\alpha\Delta T}{2(1-\nu)}$$

These are the cases of infinite plate where every direction is identical to the others → There aren't effects of the lenght and the width of the slabs.

The slab has a finite lenght and width in reality. So we start from the expression of σ_x and σ_y for the infinite slab and we introduce correction factors which refers to the contribute of bending in x direction and in the y direction.

Obtaining different dimension X and Y.

Streses at the center of the slab are:

$$\sigma_x = \frac{C_x E\alpha\Delta T}{2(1-\nu^2)} + C_y\nu\frac{E\alpha\Delta T}{2(1-\nu^2)}$$

$$\sigma_y = C_y\frac{E\alpha\Delta T}{2(1-\nu^2)} + C_x\nu\frac{E\alpha\Delta T}{2(1-\nu^2)}$$

© Proprietà riservata dell'autore - Digitalizzazione e distribuzione a cura del CENTRO APPUNTI - Corso Luigi Einaudi, 55 - Torino / Pagina 47 di 286

© Proprietà riservata dell'autore - Digitalizzazione e distribuzione a cura del CENTRO APPUNTI - Corso Luigi Einaudi, 55 - Torino / Pagina 49 di 286

to the critical length, beyond which, the upward deflection remains constant.

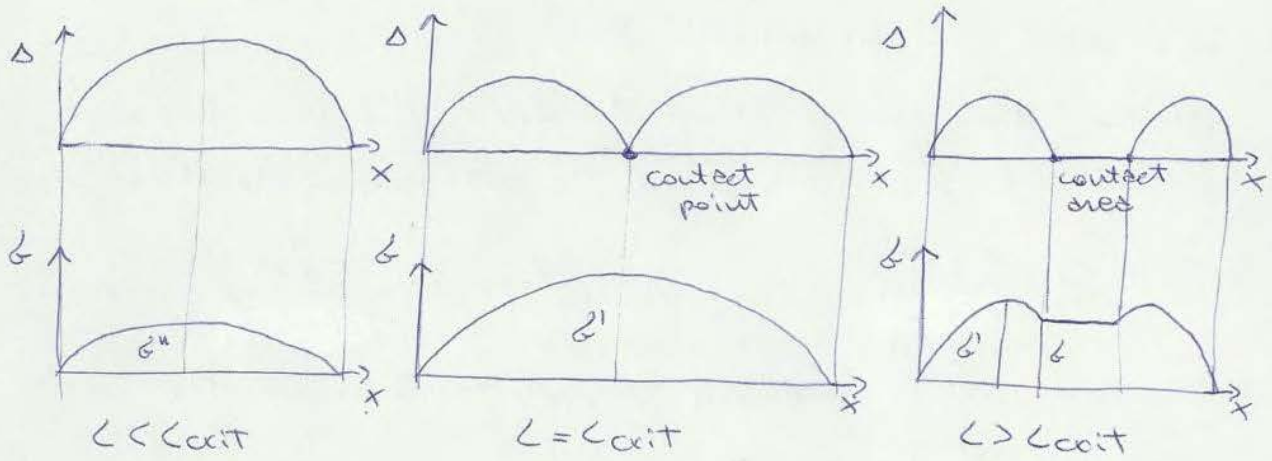

where: $\delta = \frac{E \alpha_T \Delta T}{2(1-\nu^2)}$

$\delta' = 1{,}2 \cdot \delta$

$\delta'' = \left(\frac{L}{0{,}91 L_{crit}}\right)^2 \cdot \delta$

Determination of L_{crit}:

model used:

- slab supported at his end
- loaded by its own weight

In the case of:

- rectangular plate → $L_{crit} = 20h\sqrt{2\Delta T E}$
- square plate → $L_{crit} = 22{,}8\,h\sqrt{2\Delta T E}$

The real length L is $L - 40$ cm because the support isn't a point.

© Proprietà riservata dell'autore - Digitalizzazione e distribuzione a cura del CENTRO APPUNTI - Corso Luigi Einaudi, 55 - Torino / Pagina 49 di 286

© Proprietà riservata dell'autore - Digitalizzazione e distribuzione a cura del CENTRO APPUNTI - Corso Luigi Einaudi, 55 - Torino / Pagina 51 di 286

theory in order to calculate joints opening.

$$\Delta L = CL(\varepsilon + \alpha \Delta T)$$

where: ΔL = joint opening;

C = adjustment factor (= 0,65 stabilized base
= 0,80 granular base);

L = slab lenght;

ε = drying shrinkage coefficient;

α = coefficient of thermal expansion;

ΔT = temperature range which is the difference between the local temperature and lowest monthly average temperature.

Now we need to study the effects of temperature variations on the jointing elements: dowel bars, tie bars, steel reinforcements.

- distributed steel: controls the width of crack opening (temperature cracking) no structural function;
- dowel bars: transfer loads; they have to be heavy and closely spaced to provide sufficient resistence. They must be smooth → they have to respond shear stresses;
- tie bars: tie two slabs together to ensure load transfere. Smaller than dowel bars, spaced with greater interval

STRESSES in DOWEL BARS

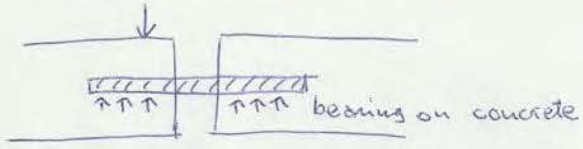

Shear response to vertical action:
- Timoshenko's approach
- Friberg's developments
- numerical analysis (FEM)

To use these methods we must make some simplifying assumptions:

- dowel are perfectly aligned and free to move in longitudinal direction

© Proprietà riservata dell'autore - Digitalizzazione e distribuzione a cura del CENTRO APPUNTI - Corso Luigi Einaudi, 55 - Torino / Pagina 51 di 286

© Proprietà riservata dell'autore - Digitalizzazione e distribuzione a cura del CENTRO APPUNTI - Corso Luigi Einaudi, 55 - Torino / Pagina 53 di 286

- FRUBERG'S ANACYSIS (1960)

He considers a symmetrical distribution of reacting forces due to a load P_t applied on the slabs, near the joint.

Solution of elastic line y:

$$M = -EI\frac{d^2y}{dx^2} = -\frac{e^{-\beta x}}{\beta}\cdot\left[P_t \sin\beta x - \beta\Pi_0\cdot(\sin\beta x + \cos\beta x)\right]$$

$$T = \frac{dM}{dx} = -e^{-\beta x}\left[(2\beta\Pi_0 - P_t)\sin\beta x + P_t\cos\beta x\right]$$

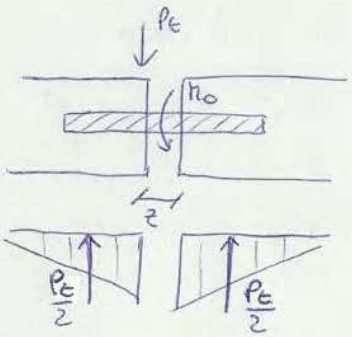

z = joint opening

$\Pi_0 = \frac{P_t - z}{2}$ → not the entire load is transferred to the following bar

There can be two situations:

- dowel group 100% efficient. In this case there are the same deflections and the same reactive forces ($P_t/2$) and the trasmitted shear force is equal to $P_t/2$.

$$Y_\phi = \frac{P_t}{4\beta^3 EI}\cdot(2+\beta z) \qquad P_t = \text{load on one dowel}$$

Bearing stress proportional to deformation

$$\sigma_\phi = K\cdot Y_\phi = \frac{k P_t}{4\beta^3 EI}(2+\beta z)$$

σ_ϕ should be compared with the allowable bearing stress

$$f_b = \frac{4-b}{3} f'_c \qquad f'_c = \text{ultimate compressive strenght of concrete}$$

The higher stress on concrete occurs at the face of the joint.

© Proprietà riservata dell'autore - Digitalizzazione e distribuzione a cura del CENTRO APPUNTI - Corso Luigi Einaudi, 55 - Torino / Pagina 53 di 286

© Proprietà riservata dell'autore - Digitalizzazione e distribuzione a cura del CENTRO APPUNTI - Corso Luigi Einaudi, 55 - Torino / Pagina 55 di 286

- interior load

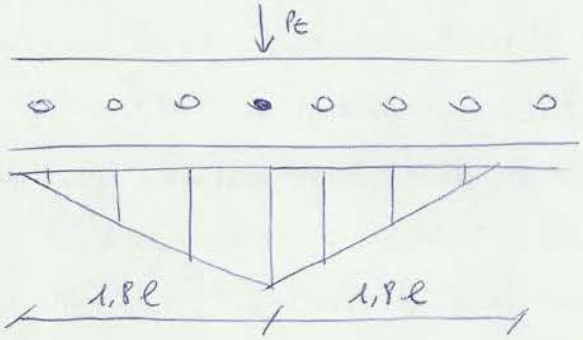

If there are two or more loads, we have to superpose the effects.

- HEINRICH'S AT AL (1989)

They done a numerical analysis. They found that the linear distribution is not true.

The load carried by the most critical dowel is greater than the one calculated by Friberg.

The maximum moment occurs at 1,0 ℓ.

There are no temperature effect on dowels because they are free to move.

STRESSES IN TIE BARS

Employing the tie bars, we can use bigger slabs.

The tie bars effect of tying two slabs together depends upon the shear stresses occuring between concrete and steel. In the crack we can consider that all the load is supported by the tie bars and we can done an average shear stress in the tie bars.

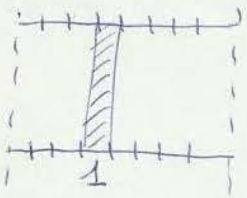

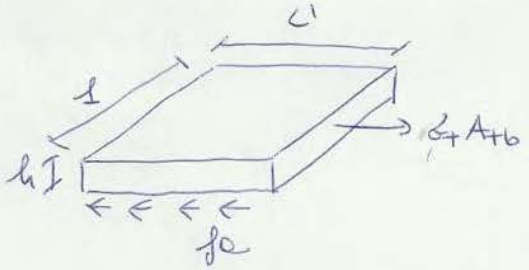

© Proprietà riservata dell'autore - Digitalizzazione e distribuzione a cura del CENTRO APPUNTI - Corso Luigi Einaudi, 55 - Torino / Pagina 55 di 286

© Proprietà riservata dell'autore - Digitalizzazione e distribuzione a cura del CENTRO APPUNTI - Corso Luigi Einaudi, 55 - Torino / Pagina 57 di 286

Their function is to keep the concrete together after cracking (also thermal cracking) and maintain load transfer through interlock.

Considering a unit width slab with crack in the middle, for the equilibrium across the crack:

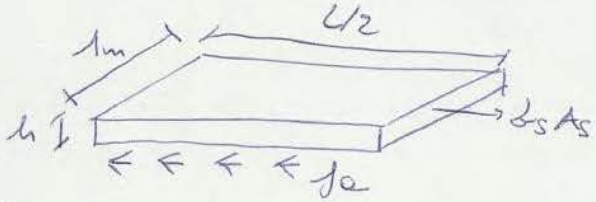

$$\gamma \cdot h \cdot \frac{L}{2} f_a = \sigma_s A_s$$

$$\sigma_s = \frac{\gamma h \cdot L \cdot f_a}{2 A_s}$$

* calculation should be done also for the other direction.

In design imposing a certain stress on steel we can design the amount of steel.

σ_s can be reduced by increasing the cross section of the steel, or by reducing the slab lenght L.

The last one is the more pratical solution.

Prefabbricated wire: if there is a big difference between L_x and L_y → it is needed less steel in transverse direction.

It is more convenient to design a different amount of steel in the two directions. Closely spaced and small bars (better distribution) are more effective than lager bars with greater intervals.

© Proprietà riservata dell'autore - Digitalizzazione e distribuzione a cura del CENTRO APPUNTI - Corso Luigi Einaudi, 55 - Torino / Pagina 57 di 286

© Proprietà riservata dell'autore - Digitalizzazione e distribuzione a cura del CENTRO APPUNTI - Corso Luigi Einaudi, 55 - Torino / Pagina 59 di 286

RESPONCE UNDER VERTICAL LOADING

RAILS

Assumptions used :
- quasi-static vertical load
- rails are considered as a beam subjected to bending (small strain and small displacements)
- elastic support body of all the elements (ballast, sub-ballast, subgrade)

Winkler considered continuously supported rails of infinite lenght and a reactive pressure proportional to deflection. Few years later, Timoshenko showed that Winkler's theory was still valid for a non continuous support like ballast.

Zimmermann gives an analytical solution for this problem.

$$P(y) = -u \cdot y_\phi$$

u is modulus of track stiffness (elasticity). For a high value of u rail is well supported (small deflection).

u depends on :
- number of ties
- geometry of ties
- ballast thickness
- ballast material
- subgrade
- type of rail

Bending moment is maximum under the load and it is equal to 0 when there is a change in curvature.

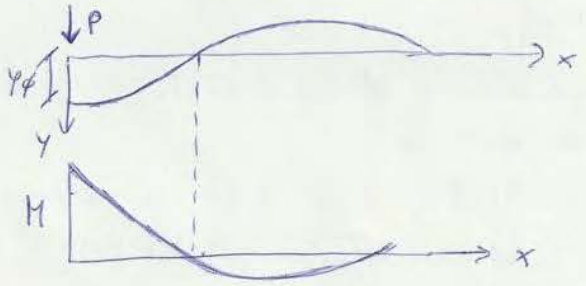

© Proprietà riservata dell'autore - Digitalizzazione e distribuzione a cura del CENTRO APPUNTI - Corso Luigi Einaudi, 55 - Torino / Pagina 59 di 286

© Proprietà riservata dell'autore - Digitalizzazione e distribuzione a cura del CENTRO APPUNTI - Corso Luigi Einaudi, 55 - Torino / Pagina 61 di 286

$$-\frac{EI\,d^2y}{dx^2} = P\left(\frac{EI}{64u}\right)^{0,25} e^{-\lambda x}(\cos\lambda x - \sin\lambda x)$$ is the bending moment in vertical plane

$$EI\,\frac{d^3y}{dx^3} = -\frac{P}{2}\,e^{-\lambda x}\cos\lambda x$$ is the shear

$$EI\,\frac{d^4y}{dx^4} = P\left(\frac{u}{64EI}\right)^{0,25} e^{-\lambda x}(\cos\lambda x + \sin\lambda x)$$ is the unit pressure equal to $p = -yu$

Notice that there is a change in the sinusoidal sign.

From the previous equations we can calculate the maximum values, which occur under the load, where there is the maximum curvature.

$$y_{max}\,(x=0) = \frac{P}{(64EIu^3)^{0,25}} \qquad M_{max} = P\left(\frac{EI}{64u}\right)^{0,25}$$

$$T_{max} = -\frac{P}{2} \qquad p_{max} = P\left(\frac{u}{64EI}\right)^{0,25}$$

Talbot considers two characteristic point:

- First where, for the first time, $M=0$ assign x_1;
- Second where, for the first time, $y=0$ assign x_2.

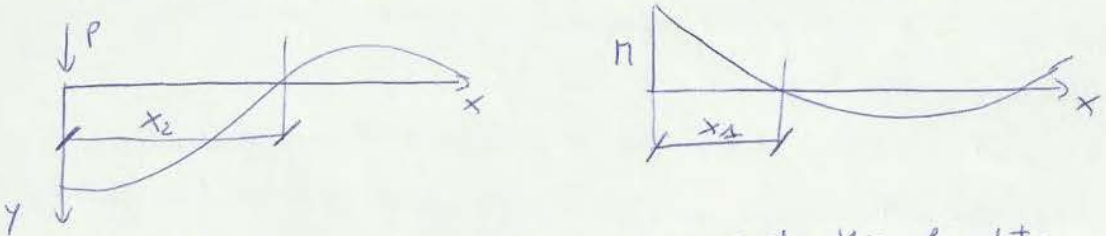

Using Zimmermann's equation to evaluate this lenght:

$$M=0 : \cos\lambda x - \sin\lambda x = 0 \rightarrow \lambda x = \frac{\pi}{4} \rightarrow x = \frac{1}{\lambda}\frac{\pi}{4}$$

$$y=0 : \cos\lambda x + \sin\lambda x = 0 \rightarrow \lambda x = \frac{3\pi}{4} \rightarrow x = \frac{3\pi}{4\lambda}$$

© Proprietà riservata dell'autore - Digitalizzazione e distribuzione a cura del CENTRO APPUNTI - Corso Luigi Einaudi, 55 - Torino / Pagina 61 di 286

© Proprietà riservata dell'autore - Digitalizzazione e distribuzione a cura del CENTRO APPUNTI - Corso Luigi Einaudi, 55 - Torino / Pagina 63 di 286

In this case we obtain more flatter and rectangular displacements even if they are bigger. The curvature is lower than the single load case and so the bending moment at the centre line is lower.

Seating load: load transferred from the rail to a generic sleeper. The applied load on a sleeper, called P, will not be entirely transferred by the rail also to the next sleepers. So we call Q the load transferred from the rail to the sleeper below the loading point. Therefore Q depends on the stiffness on the entire system while the number of sleepers involved in supporting the load P, depends on the stiffness of the entire system and on the spacing S between the sleepers.

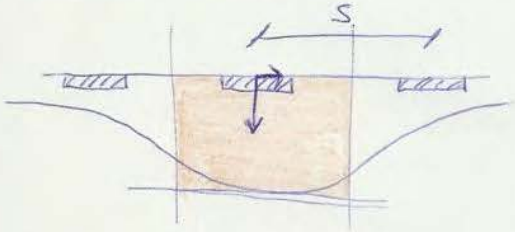

Using Zimmermann:

$$P = -\mu y$$

$$P = \int_{-\infty}^{+\infty} p(x)\,dx$$

The idea is that a single sleeper has to absorb the pressure in an influence area with a lenght equal to S:

$$Q = \int_{-S/2}^{S/2} p(x)\,dx$$

If we approximate the curve with a rectangle (conservative approach) and remember Talbot's equation:

$$Q = p_{max} \cdot S = 0{,}391 \frac{P}{\pi_1} S$$

$p_{max} \cdot S$: rectangle area

© Proprietà riservata dell'autore - Digitalizzazione e distribuzione a cura del CENTRO APPUNTI - Corso Luigi Einaudi, 55 - Torino / Pagina 63 di 286

Using Bernoulli hypothesis:

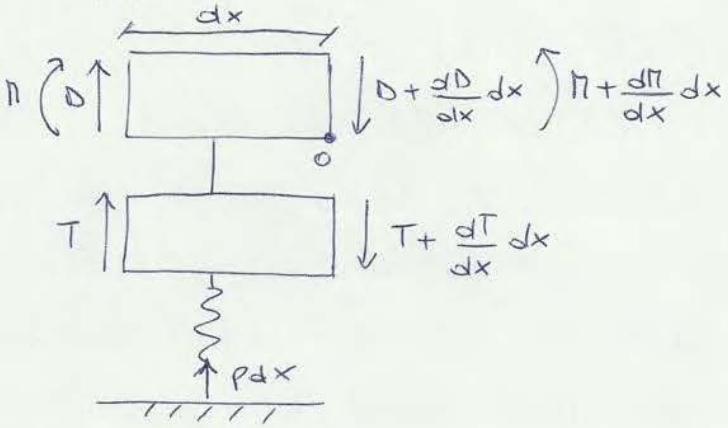

For the equilibrium:

$$\uparrow) \quad D - D - \frac{dD}{dx}dx + T - T - \frac{dT}{dx}dx + p\,dx = 0$$

$$O\downarrow \quad D\,dx + T\,dx + p\,dx\,\frac{dx}{2} + M - M - \frac{dM}{dx}dx = 0$$

Using also these equations:

$$T = GA\,\frac{dy}{dx} \quad ; \quad p = -\mu y \quad ; \quad M = -EI\,\frac{d^2y}{dx^2}$$

Solving the system we obtain:

$$EI\,\frac{d^4y}{dx^4} - GA\,\frac{d^2y}{dx^2} + \mu y = 0$$

If we put $GA = 0$ → some equation before studied.

The elastic line is:

$$y(x) = \frac{P}{8EI\,ab\,\lambda^2}\,e^{-bx}(a\cos ax + b\sin bx)$$

lower displacements than in the case of Winkler theory.

where:

$$a = \frac{1}{2}\sqrt{4\lambda^2 - \gamma} \quad ; \quad b = \frac{1}{2}\sqrt{4\lambda^2 + \gamma} \quad ; \quad \gamma = \frac{GA}{EI} \quad ; \quad \lambda = \sqrt[4]{\frac{\mu}{4EI}}$$

a, b depend on relative shear behaviour

γ is the relative stiffness between shear stresses and bending moment

λ is the damping factor

© Proprietà riservata dell'autore - Digitalizzazione e distribuzione a cura del CENTRO APPUNTI - Corso Luigi Einaudi, 55 - Torino / Pagina 67 di 286

- We are not considering dynamic effects which can come from a lot of factors like moving elements, imperfection, transversal moving, variation of acceleration.
The dynamic effect are taken into account by increasing the static load by a factor.
Therefore, introducing a dynamic amplification factor DAF

$P_{dynamic} = DAF \cdot P_{static}$

To be conservative $DAF = 1,5$ → 50% increase

For Talbot is a function of speed:

$$P_{dyn} = DAF \cdot P_{st} = \left[1 + 0,01 (V - 5) f_i\right] P_{st}$$

where V is expressed in mph (if $V < 5$, $DAF = 1$ and this means that slow speeds don't cause dynamic effects)
f_i is an impact factor which takes into account the variation of the contact area, which influences the dynamic effect, due to wheel diameters:

$$f_i = \frac{A_{33}}{A_D}$$

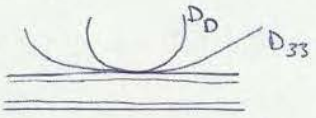

A_{33} is the contact area of the standard wheel (diameter 33 in)
A_D is a contact area of non standard wheel
Reducing A_D f_i increases because the roughness of the surface affects the dynamic effect are more for a wheel with a small diameter.
Some years later, AREA (american railways engineering association) makes a semplification of this theory:
They assume that the dynamic effect must be taken into

/3

© Proprietà riservata dell'autore - Digitalizzazione e distribuzione a cura del CENTRO APPUNTI - Corso Luigi Einaudi, 55 - Torino / Pagina 67 di 286

© Proprietà riservata dell'autore - Digitalizzazione e distribuzione a cura del CENTRO APPUNTI - Corso Luigi Einaudi, 55 - Torino / Pagina 69 di 286

$$DAF = \begin{cases} 1 + t\varphi & \text{for } V < 60 \text{ km/h} \\ 1 + t\varphi\left[1 + \frac{V-60}{140}\right] & \text{for } 60 < V < 200 \text{ km/h} \end{cases}$$

t is a probabilistic factor which depends on the degree of confidence we expect to have in the estimation of the dynamic effects.

According to the normal distribution:

$$\epsilon = \begin{cases} 1 \rightarrow 68,3\,\% \text{ confidence} \\ 2 \rightarrow 95,4\,\% \text{ confidence} \\ 3 \rightarrow 99,7\,\% \text{ confidence} \end{cases}$$

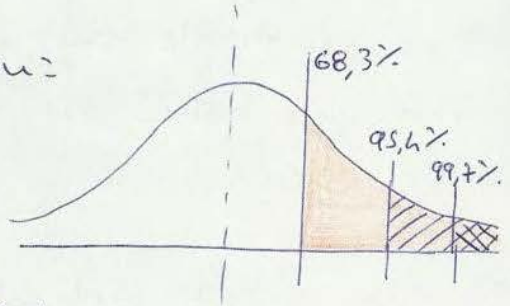

φ describes the state of maintenance:

$$\varphi = \begin{cases} 0,1 & \text{very good condition} \\ 0,2 & \text{standard condition} \\ 0,3 & \text{bad condition} \end{cases}$$

© Proprietà riservata dell'autore - Digitalizzazione e distribuzione a cura del CENTRO APPUNTI - Corso Luigi Einaudi, 55 - Torino / Pagina 69 di 286

© Proprietà riservata dell'autore - Digitalizzazione e distribuzione a cura del CENTRO APPUNTI - Corso Luigi Einaudi, 55 - Torino / Pagina 71 di 286

In this way he approximated the semi-elliptical distribution to a rectangular distribution.

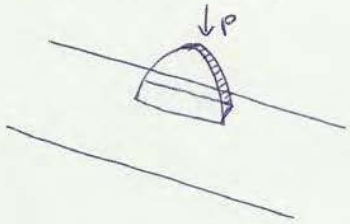

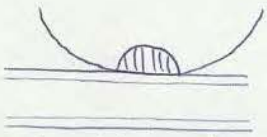

longitudinal direction

transverse direction

Using the mean value of $\bar{E}$:

$$\sigma_{mean} = \sqrt{\frac{\pi \bar{E}}{6\sqrt{2}(1-\nu^2)} \frac{P}{r\,b}} = 1374 \sqrt{\frac{P}{r}}$$

r = wheel curvature

The second equation derives from the first one, substituting the standard values of $\bar{E}$, ν and b.

With this equation we can calculate the stress on the top of the rail, but we need to know also the stress inside the rail.

Inside the rail we have a stress, like the one we have in a homogeneous half-space and so we can use Boussinesq theory. In fact the loading area is like a point and so we can consider the rail area as an half-space.

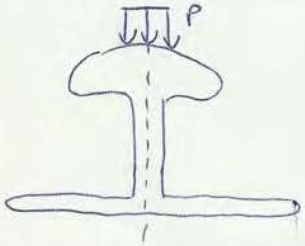

the maximum shear isn't on the top but it is a bit under, around 6 mm.

$\tau_{max} \cong 0{,}3 \cdot \sigma_{mean}$

Very often rail fail due to contact area because are not considered. We should use failure criteria like Tresca or Von Mises.

© Proprietà riservata dell'autore - Digitalizzazione e distribuzione a cura del CENTRO APPUNTI - Corso Luigi Einaudi, 55 - Torino / Pagina 71 di 286

© Proprietà riservata dell'autore - Digitalizzazione e distribuzione a cura del CENTRO APPUNTI - Corso Luigi Einaudi, 55 - Torino / Pagina 73 di 286

To prevent this problem expecially the center bound track it is possible to use a twin block tie.

APPROXIMATE METHODS :

we are going to see four different methods which derive from the different combination of two different factors: rigid body / elastic beam – full support / end support.

RIGID BODY – FULL SUPPORT

In this case we have a symmetrical load on a Winkler support and we can assume as Q the highest value between Q_1 and Q_2.

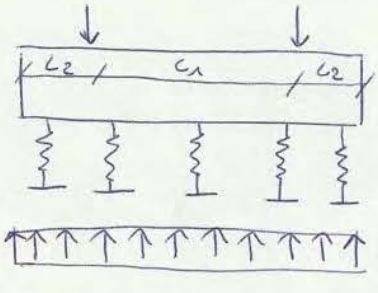

$$\ell = \ell_1 + 2\ell_2$$

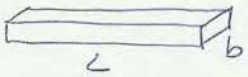

b is the width of contact area between ties and ballast.

Equilibrium : $2Q = p_b \cdot b \cdot \ell \rightarrow p_b = \frac{2Q}{b\ell} \left[\frac{N}{m^2}\right]$

load per unit area

$$p'_b = \frac{2Q}{\ell} \left[\frac{N}{m}\right]$$

$$M_{rail} = p'_b \frac{\ell_2^2}{2} = \frac{2Q}{\ell} \frac{\ell_2^2}{2} = \frac{Q\ell_2^2}{\ell} = \frac{Q}{\ell}\left(\frac{\ell}{2} - \frac{\ell_1}{2}\right)^2 = \frac{Q}{4}\frac{(\ell-\ell_1)^2}{\ell}$$

$$M_{centre} = p'_b \cdot \frac{\ell}{2} \cdot \frac{\ell}{4} - Q\frac{\ell_1}{2} = \frac{2Q}{\ell}\frac{\ell}{2}\frac{\ell}{4} - Q\frac{\ell_1}{2} = \frac{Q}{4}(\ell - 2\ell_1)$$

$$\sigma_{max} = \frac{M}{I} c = \frac{M}{\frac{bh^3}{12}} \frac{h}{2} = \frac{6M}{bh^2}$$

To verify the tie, you need to put the highest value between M_{rail}, M_{centre}

37

© Proprietà riservata dell'autore - Digitalizzazione e distribuzione a cura del CENTRO APPUNTI - Corso Luigi Einaudi, 55 - Torino / Pagina 73 di 286

© Proprietà riservata dell'autore - Digitalizzazione e distribuzione a cura del CENTRO APPUNTI - Corso Luigi Einaudi, 55 - Torino / Pagina 75 di 286

ELASTIC BEAM - FULL SUPPORT

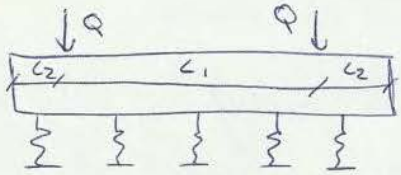

we need to introduce costitutive models:

$$M = -EI \frac{d^2y}{dx^2} \quad ; \quad p' = -uy$$

the elastic line: $\frac{d^4y}{dx^4} + 4\alpha^4 y = 0$ (differential equation)

where $\alpha = \sqrt[4]{\frac{kb}{4E_t I_t}}$

b = width of the tie
E_t = elasticity modulus of tie
I_t = inertia moment of tie
K = equivalent of u (but u include the contribute of ties K no!).

$$y = e^{\alpha x}(c_1 \operatorname{sen}\alpha x + c_2 \cos\alpha x) + e^{-\alpha x}(c_3 \operatorname{sen}\alpha x + c_4 \cos\alpha x)$$

from $y(x) \rightarrow M(x)$.

ELASTIC BEAM - END SUPPORT

like in the second case → spring under the rail

constitutive equations → differential equations → solution $y(x)$

$y(x)$ is different respect the case with full support

From $y(x) \rightarrow M(x)$.

This last two method should be resolved numerically.

/38

© Proprietà riservata dell'autore - Digitalizzazione e distribuzione a cura del CENTRO APPUNTI - Corso Luigi Einaudi, 55 - Torino / Pagina 75 di 286

© Proprietà riservata dell'autore - Digitalizzazione e distribuzione a cura del CENTRO APPUNTI - Corso Luigi Einaudi, 55 - Torino / Pagina 77 di 286

To calculate bending moment we can put the axis in correspondence of the load and then we have to consider the two forces:

$$M_{rail} = \frac{Q_{max}}{2b\ell_2} \cdot b\ell_2 \cdot \frac{\ell_2}{2} - \frac{Q_{max}}{2be} \cdot be \cdot \frac{e}{2} = \frac{Q_{max}}{4}(\ell_2 - e)$$

In fact we have a symmetrical load configuration and so also the bending moment is symmetrical. This is why we have considered only the forces on one side.

In order to obtain the same results obtained in field observations it was introduced a correction factor equal to 1,6 and so the first equation is:

$$M_{rail} = 1,6 \frac{Q_{max}}{4}(\ell_2 - e)$$

M_{centre} is difficult to evaluate because it is very variable.

It is proposed a relation: $M_{centre} = 1,2\, M_{rail} \frac{(EI)_{centre}}{(EI)_{rail}}$

Even with the sleepers there can be problems due to contact stresses in the contact area between the rail and the sleepers

$$\sigma_{rail-tie} = \frac{Q + Q_0}{A_{rail-tie}}$$

where: Q_0 is the pretensed force due to fastenings.

The allowable contact stress depends on the tie material, for example we can allow a higher stress for concrete and a lower stress for wood.

© Proprietà riservata dell'autore - Digitalizzazione e distribuzione a cura del CENTRO APPUNTI - Corso Luigi Einaudi, 55 - Torino / Pagina 77 di 286

© Proprietà riservata dell'autore - Digitalizzazione e distribuzione a cura del CENTRO APPUNTI - Corso Luigi Einaudi, 55 - Torino / Pagina 79 di 286

For a design problem, we can assume a $P_{sub\ max}$ and then, with this equation, we can calculate h, which is the minimum allowable ballast thickness, or to which is the width of the tie.

Another kind of approach considers the effects of multiple ties on the surface:

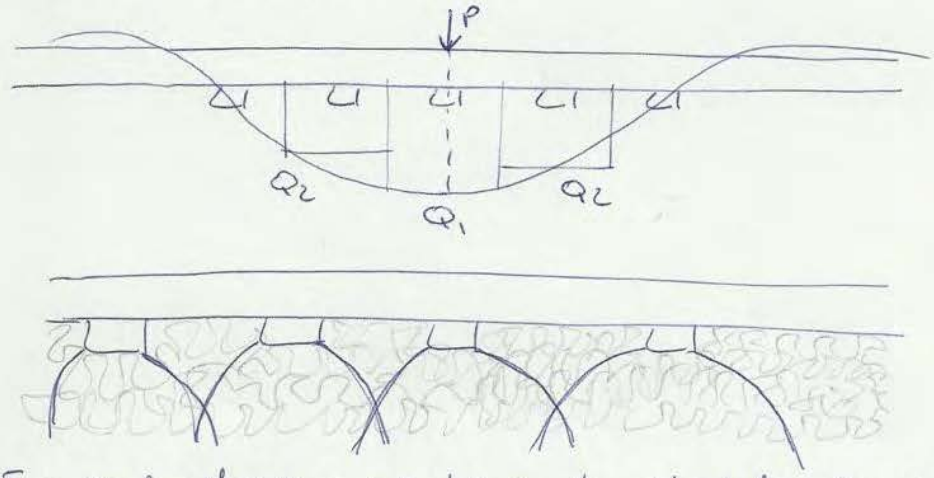

For each sleeper, we have to calculate Q_i and then we can convert Q_i in the pressure transferred to the ballast which depend on the type of support (end or full), finding $P_{ball,1}$; $P_{ball,2}$.

Know $P_{ball,i}$ we have to consider that each tie generates a bubble which influences the other ones.

Therefore, we have to take into account even the adjacent sleepers. In order to solve this problem we can use:

- the infinite strip theory;
- multilayer elastic solution with load on a circular area (rectangular area to a circular);
- Odemark's approach (half-homogeneus half-space)

© Proprietà riservata dell'autore - Digitalizzazione e distribuzione a cura del CENTRO APPUNTI - Corso Luigi Einaudi, 55 - Torino / Pagina 79 di 286

© Proprietà riservata dell'autore - Digitalizzazione e distribuzione a cura del CENTRO APPUNTI - Corso Luigi Einaudi, 55 - Torino / Pagina 81 di 286

The equivalent layer and the bending layer have the same bending stiffness.

Going down through ballast layer, the pressure becomes more uniform and at a distance equal to the spacing between sleepers we can consider to have a uniform distribution of pressure.

This is way, at a certain depth, we can substitute ballast with subballast.

- Last kind of approach is Talbot's one.

He said that pressure have a bell-shade distribution and that moving through ballast in depth, the bells become wider and flatter.

Talbot derived an equation trying to fit together the solution obtained:

$$p(x) = \frac{K p_b}{\sqrt{\pi}} e^{-k^2 x^2} \qquad p_{sub} = \frac{16{,}8\, p_b}{h^{1{,}25}}$$

where h is the thickness of the ballast layer, measured in inches.

© Proprietà riservata dell'autore - Digitalizzazione e distribuzione a cura del CENTRO APPUNTI - Corso Luigi Einaudi, 55 - Torino / Pagina 81 di 286

© Proprietà riservata dell'autore - Digitalizzazione e distribuzione a cura del CENTRO APPUNTI - Corso Luigi Einaudi, 55 - Torino / Pagina 83 di 286

In additional restrain is offered by fastenings → the rail cannot freely rotate.

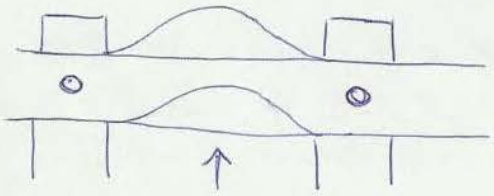

Finally we can also add a normal load which remains constant along the rail and which is due to the temperature variations.

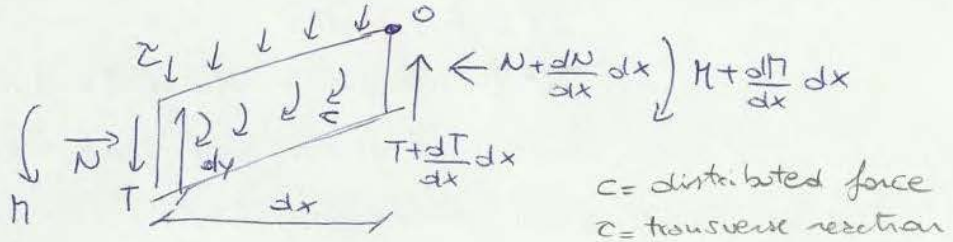

c = distributed force
c = transverse reaction

Equilibrium:

$$\uparrow) \quad -T_0 - c\,dx + T_0 + \frac{dT_0}{dx}dx = 0 \quad \rightarrow dT_0 = c\,dx$$

$$\circlearrowright \quad -M_0 - N_0\,dy - T_0\,dx + c\,dx + M_0 + \frac{dM_0}{dx}dx = 0$$

$$\rightarrow dM_0 = N_0\,dy + T_0\,dx - c\,dx$$

Deriving second equation:

$$\frac{dM}{dx} = N_0\frac{dy}{dx} + T_0 - c$$

Another time:

$$\frac{dM}{dx^2} = N_0\frac{d^2y}{dx^2} + \underbrace{\frac{dT_0}{dx}}_{c} - \frac{dc}{dx}$$

Substituting $M = -EI\frac{d^2y}{dx^2}$

$$EI\frac{d^4y}{dx^4} + N_0\frac{d^2y}{dx^2} + c - \frac{dc}{dx} = 0$$

There are some problem using this formulation → it is difficult to evaluate c and c.

42

© Proprietà riservata dell'autore - Digitalizzazione e distribuzione a cura del CENTRO APPUNTI - Corso Luigi Einaudi, 55 - Torino / Pagina 83 di 286

© Proprietà riservata dell'autore - Digitalizzazione e distribuzione a cura del CENTRO APPUNTI - Corso Luigi Einaudi, 55 - Torino / Pagina 85 di 286

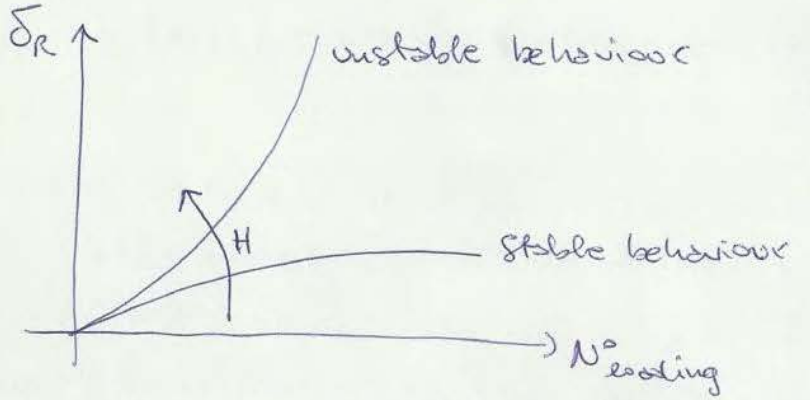

δ_R = horizontal displacement residual

The transaction from stable to unstable behaviour occours for a certain value of H which is called H_L.

$H < H_L$ stable behaviour where the non reversible displacents decrease in time (we want this situation).

$H > H_L$ unstable behaviour where the material becomes less stiff and so the non reversible displacent increase.

$H_{cr}^{static} \sim H_L^{dynamic}$ by experiments.

Biermann (German railway): $H_L = \alpha\left(1+\frac{P}{3}\right)$ $\alpha = 0{,}95 \div 1{,}43$

Hansen: $H_L = 1+\frac{P}{3}$

For design purpose, we can add a security coefficient equal to 0,85 in order to be more conservative: $H_L = 0{,}85\left(1+\frac{P}{3}\right)$

© Proprietà riservata dell'autore - Digitalizzazione e distribuzione a cura del CENTRO APPUNTI - Corso Luigi Einaudi, 55 - Torino / Pagina 85 di 286

© Proprietà riservata dell'autore - Digitalizzazione e distribuzione a cura del CENTRO APPUNTI - Corso Luigi Einaudi, 55 - Torino / Pagina 87 di 286

$N_x = r_e \cdot x$

In this case we are considering a plastic response of the support, infact we have a constant distribution of r_e. r_e is the response due to one rail for unit lenght (some times it is given the responce of two rails so we have to use $r_e/2$).

We can also choose an elastic response of the support. The normal force N increase linearly till a maximum value $N_{max} = \alpha \Delta T E_c A_c$. Beyond the point where $N = N_{max}$ the rail isn't moving because the central part of the rail is subjected to a constant load.

Breathing lenght is the lenght where rail moves and there is a zone where it isn't moving.

$$\frac{r_e}{2} L_B = \alpha \Delta T E_c A_R \rightarrow L_B = \frac{2 \alpha \Delta T E_c A_c}{r_e}$$

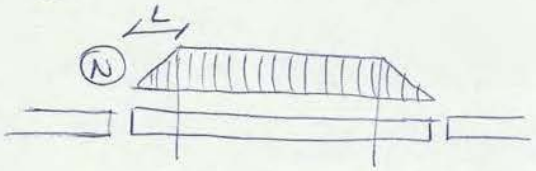

In order to consider other effects different from temperature variations, we have to increase N by 20%.

If we have welded the rails, we have a constant N but you must to evaluate if N is higher than the tensile resistance of the steel or if the welding breaks.

/44

© Proprietà riservata dell'autore - Digitalizzazione e distribuzione a cura del CENTRO APPUNTI - Corso Luigi Einaudi, 55 - Torino / Pagina 87 di 286

© Proprietà riservata dell'autore - Digitalizzazione e distribuzione a cura del CENTRO APPUNTI - Corso Luigi Einaudi, 55 - Torino / Pagina 89 di 286

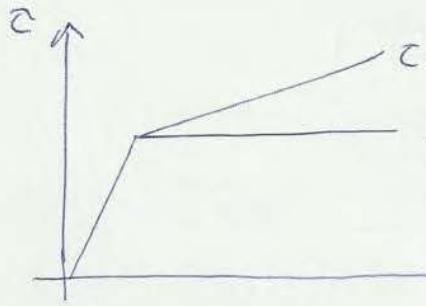

$c = -\beta \cdot z(x)$ (winkler)

$c = cost$ → perfect plastic assumption

$$M = -EI \frac{d^2 z}{dx^2}$$

Energy approach: $W_{tot} = W_{beam} + W_c - W_N \overset{\text{must be}}{=} 0$

where: W_{beam} = energy necessary to bending coil;

W_c = energy for deformation lateral restrain system

W_N = energy for normal forces

Quantify these three terms:

$$W_{beam} = \frac{1}{2}\int_0^L EI \frac{d^2 z}{dx^2} dx$$

moment × curvature

EI = bending stiffness of the system

$$W_c = \frac{1}{2}\int_0^L \beta z z \, dx$$

unit force × displacement

β = coefficient of lateral resistence

$$W_N = \frac{1}{2}\int_0^L N \left(\frac{dz}{dx}\right)^2 dx$$

we obtain: entering with expression of $z(x)$

$$W_{tot} = \frac{z_0^2 L}{4}\left[EI\left(\frac{2\pi}{L}\right)^4 + \beta - N\left(\frac{2\pi}{L}\right)^2\right]$$

Equilibrium

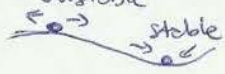

$$\frac{dW_{tot}}{dz_0} = 0 \rightarrow N = \frac{4\pi^2 EI}{L^2} + \frac{\beta L^2}{4\pi^2}$$

We have to see if this is a stable (local minimum) or unstable (local massimum) equilibrium, so we have to calculate the curvature:

© Proprietà riservata dell'autore - Digitalizzazione e distribuzione a cura del CENTRO APPUNTI - Corso Luigi Einaudi, 55 - Torino / Pagina 89 di 286

© Proprietà riservata dell'autore - Digitalizzazione e distribuzione a cura del CENTRO APPUNTI - Corso Luigi Einaudi, 55 - Torino / Pagina 91 di 286

a sort of sinusoidal trend due to imperfections.
When the beam deforms itself under loading it assumes a bigger sinusoidal trend (we have the sum of two sinusoidal functions).

Energy method to this new system:

$$W_{tot} = \frac{L}{4}\left\{ z_0^2 EI \left(\frac{2\pi}{L}\right)^4 + \frac{8 C_0 z_0}{\pi} - N\left[(z_0+f_0)^2 - f_0^2\right]\left(\frac{2\pi}{L}\right)^2 \right\}$$

$f_0 = z_0$ in undeformed condition

Equilibrium:

$$\frac{dW}{dz_0} = 0 \rightarrow \frac{L}{4}\left\{ 2 z_0 EI \left(\frac{16\pi^4}{L^4}\right) + \frac{8 C_0}{\pi} - N\left[2(z_0+f_0)\right]\left(\frac{4\pi^2}{L^2}\right)\right\}$$

$$N = \frac{z_0}{z_0+f_0}\left(\frac{4\pi^2 EI}{L^2} + \frac{z_0 L^2}{\pi^3 z_0}\right)$$

Even in this case we can calculate $\frac{\partial^2 W}{\partial z_0^2}$ to discuss stability.

Critical conditions:

$$\frac{\partial N}{\partial L} = 0 \rightarrow L_{crit}^2 = 2\sqrt{\frac{\pi^5 f_0 EI}{C_0}}$$

$$\rightarrow N_{crit} = 4\sqrt{\frac{C_0 EI}{\pi f_0}}$$

Last critical condition is $\left(\frac{z_0}{f_0}\right) \sim 1$

This method is better than the Eulero's because is more conservative.

© Proprietà riservata dell'autore - Digitalizzazione e distribuzione a cura del CENTRO APPUNTI - Corso Luigi Einaudi, 55 - Torino / Pagina 91 di 286

© Proprietà riservata dell'autore - Digitalizzazione e distribuzione a cura del CENTRO APPUNTI - Corso Luigi Einaudi, 55 - Torino / Pagina 93 di 286

Contents

© Proprietà riservata dell'autore - Digitalizzazione e distribuzione a cura del CENTRO APPUNTI - Corso Luigi Einaudi, 55 - Torino / Pagina 93 di 286

© Proprietà riservata dell'autore - Digitalizzazione e distribuzione a cura del CENTRO APPUNTI - Corso Luigi Einaudi, 55 - Torino / Pagina 95 di 286

1

DISTRESSES FOR PAVEMENTS WITH ASPHALT CONCRETE SURFACES

This section covers asphalt concrete-surfaced pavements (ACP), including ACP overlays on either asphalt concrete (AC) or portland cement concrete (PCC) pavements. Each of the distresses has been grouped into one of the following categories:

A. Cracking
B. Patching and Potholes
C. Surface Deformation
D. Surface Defects
E. Miscellaneous Distresses

Table 1 summarizes the various types of distress and unit of measurement. Some distresses also have defined severity levels.

TABLE 1 Asphalt Concrete-Surfaced Pavement Distress Types

DISTRESS TYPE	UNIT OF MEASURE	DEFINED SEVERITY LEVELS?
A. Cracking / page **3**		
1. Fatigue Cracking	Square Meters	Yes
2. Block Cracking	Square Meters	Yes
3. Edge Cracking	Meters	Yes
4a. Wheel Path Longitudinal Cracking	Meters	Yes
4b. Non-Wheel Path Longitudinal Cracking	Meters	Yes
5. Reflection Cracking at Joints		
Transverse Reflection Cracking	Not Measured	N/A
Longitudinal Reflection Cracking	Not Measured	N/A
6. Transverse Cracking	Number, Meters	Yes
B. Patching and Potholes / page **15**		
7. Patch/Patch Deterioration	Number, Square Meters	Yes
8. Potholes	Number, Square Meters	Yes
C. Surface Deformation / page **21**		
9. Rutting	Millimeters	No
10. Shoving	Number, Square Meters	No
D. Surface Defects / page **25**		
11. Bleeding	Square Meters	No
12. Polished Aggregate	Square Meters	No
13. Raveling	Square Meters	No
E. Miscellaneous Distresses / page **29**		
14. Lane-to-Shoulder Dropoff	Not Measured	N/A
15. Water Bleeding and Pumping	Number, Meters	No

© Proprietà riservata dell'autore - Digitalizzazione e distribuzione a cura del CENTRO APPUNTI - Corso Luigi Einaudi, 55 - Torino / Pagina 95 di 286

© Proprietà riservata dell'autore - Digitalizzazione e distribuzione a cura del CENTRO APPUNTI - Corso Luigi Einaudi, 55 - Torino / Pagina 97 di 286

1

FATIGUE CRACKING

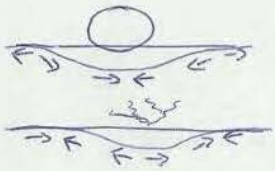

Description

Occurs in areas subjected to repeated traffic loadings (wheel paths). Can be a series of interconnected cracks in early stages of development. Develops into many-sided, sharp-angled pieces, usually less than 0.3 meters (m) on the longest side, characteristically with a chicken wire/alligator pattern, in later stages.

Must have a quantifiable area.

Severity Levels

LOW
An area of cracks with no or only a few connecting cracks; cracks are not spalled or sealed; pumping is not evident.

MODERATE
An area of interconnected cracks forming a complete pattern; cracks may be slightly spalled; cracks may be sealed; pumping is not evident.

HIGH
An area of moderately or severely spalled interconnected cracks forming a complete pattern; pieces may move when subjected to traffic; cracks may be sealed; pumping may be evident.

How to Measure

Record square meters of affected area at each severity level. If different severity levels existing within an area cannot be distinguished, rate the entire area at the highest severity present.

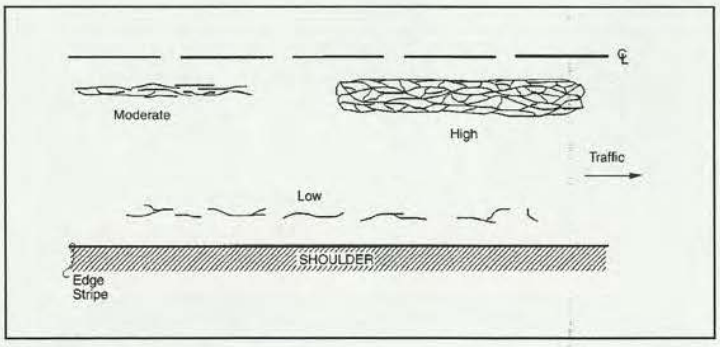

FIGURE 3
Distress Type ACP 1—Fatigue Cracking

We have cyclical loading which bring to cracks which propagate themselves from the bottom to the surface. This is called bottom-up cracking. The critical parameter to consider is the tensile stress at the bottom of bituminous layer.

© Proprietà riservata dell'autore - Digitalizzazione e distribuzione a cura del CENTRO APPUNTI - Corso Luigi Einaudi, 55 - Torino / Pagina 97 di 286

© Proprietà riservata dell'autore - Digitalizzazione e distribuzione a cura del CENTRO APPUNTI - Corso Luigi Einaudi, 55 - Torino / Pagina 99 di 286

2

BLOCK CRACKING

Description

A pattern of cracks that divides the pavement into approximately rectangular pieces. Rectangular blocks range in size from approximately 0.1 m² to 10 m².

In consequence of : - temperature differential
- low level of loading

Severity Levels

LOW
Cracks with a mean width ≤ 6 millimeters (mm); or sealed cracks with sealant material in good condition and with a width that cannot be determined.

MODERATE
Cracks with a mean width > 6 mm and ≤ 19 mm; or any crack with a mean width ≤ 19 mm and adjacent low severity random cracking.

HIGH
Cracks with a mean width > 19 mm; or any crack with a mean width ≤ 19 mm and adjacent moderate to high severity random cracking.

How to Measure

It stands thought the entire width of the pavement area → ≠ from fatigue (along wheel direction).

Record square meters of affected area at each severity level. If fatigue cracking exists within the block cracking area, the area of block cracking is reduced by the area of fatigue cracking.

Note: An occurrence should be at least 15 m long before rating as block cracking.

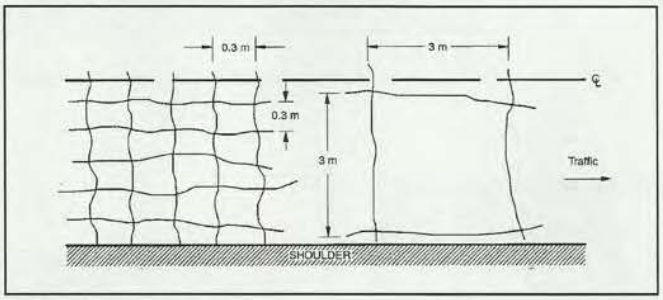

FIGURE 8
Distress Type ACP 2—Block Cracking

FIGURE 9
Distress Type ACP 2—Block Cracking with Fatigue Cracking in the Wheel Paths

FIGURE 10
Distress Type ACP 2—High Severity Block Cracking

© Proprietà riservata dell'autore - Digitalizzazione e distribuzione a cura del CENTRO APPUNTI - Corso Luigi Einaudi, 55 - Torino / Pagina 99 di 286

© Proprietà riservata dell'autore - Digitalizzazione e distribuzione a cura del CENTRO APPUNTI - Corso Luigi Einaudi, 55 - Torino / Pagina 101 di 286

Problem : longitudinal crack can interact with thermal or fatigue fenomena. They can derive from construction problem

4

LONGITUDINAL CRACKING

Description

Cracks predominantly parallel to pavement centerline. Location within the lane (wheel path versus non-wheel path) is significant.

Severity levels

LOW
A crack with a mean width ≤ 6 mm; or a sealed crack with sealant material in good condition and with a width that cannot be determined.

MODERATE
Any crack with a mean width > 6 mm and ≤ 19 mm; or any crack with a mean width ≤ 19 mm and adjacent low severity random cracking.

HIGH
Any crack with a mean width > 19 mm; or any crack with a mean width ≤ 19 mm and adjacent moderate to high severity random cracking.

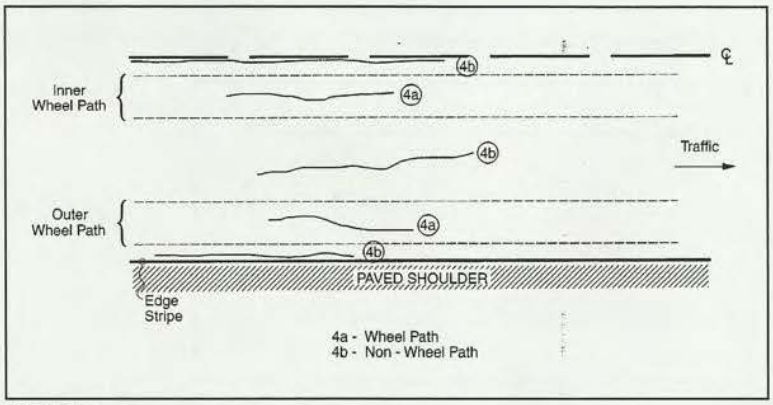

FIGURE 13
Distress Type ACP 4—Longitudinal Cracking

© Proprietà riservata dell'autore - Digitalizzazione e distribuzione a cura del CENTRO APPUNTI - Corso Luigi Einaudi, 55 - Torino / Pagina 101 di 286

© Proprietà riservata dell'autore - Digitalizzazione e distribuzione a cura del CENTRO APPUNTI - Corso Luigi Einaudi, 55 - Torino / Pagina 103 di 286

5

REFLECTION CRACKING AT JOINTS

Description

Cracks in asphalt concrete overlay surfaces that occur over joints in concrete pavements.

Note: The slab dimensions beneath the AC surface must be known to identify reflection cracks at joints.

Severity Levels

LOW
An unsealed crack with a mean width ≤ 6 mm; or a sealed crack with sealant material in good condition and with a width that cannot be determined.

MODERATE
Any crack with a mean width > 6 mm and ≤ 19 mm; or any crack with a mean width ≤ 19 mm and adjacent low severity random cracking.

HIGH
Any crack with a mean width > 19 mm; or any crack with a mean width ≤ 19 mm and adjacent moderate to high severity random cracking.

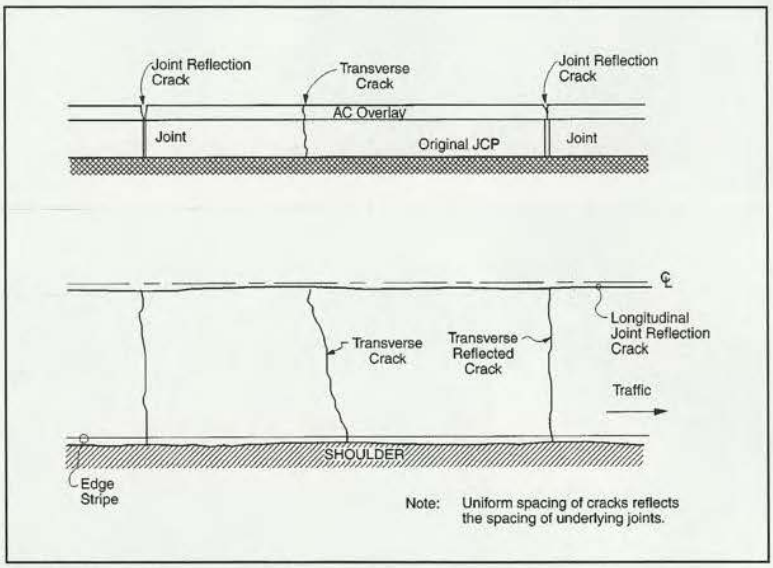

FIGURE 16
Distress Type ACP 5—Reflection Cracking at Joints

© Proprietà riservata dell'autore - Digitalizzazione e distribuzione a cura del CENTRO APPUNTI - Corso Luigi Einaudi, 55 - Torino / Pagina 103 di 286

© Proprietà riservata dell'autore - Digitalizzazione e distribuzione a cura del CENTRO APPUNTI - Corso Luigi Einaudi, 55 - Torino / Pagina 105 di 286

6

TRANSVERSE CRACKING

Description

Cracks that are predominantly perpendicular to pavement centerline.

Ca could be thermal cracking

Severity Levels

LOW
An unsealed crack with a mean width ≤ 6 mm; or a sealed crack with sealant material in good condition and with a width that cannot be determined.

MODERATE
Any crack with a mean width > 6 mm and ≤ 19 mm; or any crack with a mean width ≤ 19 mm and adjacent low severity random cracking.

HIGH
Any crack with a mean width > 19 mm; or any crack with a mean width ≤ 19 mm and adjacent moderate to high severity random cracking.

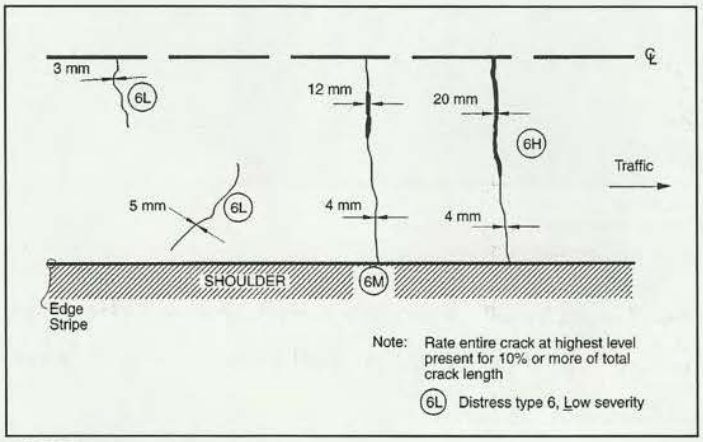

FIGURE 18
Distress Type ACP 6—Transverse Cracking Asphalt Concrete Surfaces

© Proprietà riservata dell'autore - Digitalizzazione e distribuzione a cura del CENTRO APPUNTI - Corso Luigi Einaudi, 55 - Torino / Pagina 105 di 286

© Proprietà riservata dell'autore - Digitalizzazione e distribuzione a cura del CENTRO APPUNTI - Corso Luigi Einaudi, 55 - Torino / Pagina 107 di 286

B

Patching and Potholes

This section includes the following distresses:

7. Patch/Patch Deterioration
8. Potholes

© Proprietà riservata dell'autore - Digitalizzazione e distribuzione a cura del CENTRO APPUNTI - Corso Luigi Einaudi, 55 - Torino / Pagina 107 di 286

© Proprietà riservata dell'autore - Digitalizzazione e distribuzione a cura del CENTRO APPUNTI - Corso Luigi Einaudi, 55 - Torino / Pagina 109 di 286

FIGURE 23
Distress Type ACP 7—Low Severity Patch

FIGURE 24
Distress Type ACP 7—Moderate Severity Patch

FIGURE 25
Distress Type ACP 7—High Severity Patch

/57

© Proprietà riservata dell'autore - Digitalizzazione e distribuzione a cura del CENTRO APPUNTI - Corso Luigi Einaudi, 55 - Torino / Pagina 109 di 286

© Proprietà riservata dell'autore - Digitalizzazione e distribuzione a cura del CENTRO APPUNTI - Corso Luigi Einaudi, 55 - Torino / Pagina 111 di 286

To eliminate pothides we need to remove a rectangular area of material larger than the pothides, then remove water and other materials and finally put tack coat, cover the layer and compact.

FIGURE 27
Distress Type ACP 8—Low Severity Pothole

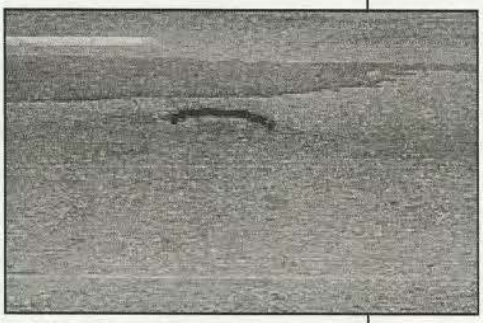

FIGURE 28
Distress Type ACP 8—Moderate Severity Pothole

FIGURE 29
Distress Type ACP 8—Moderate Severity Pothole, Close-up View

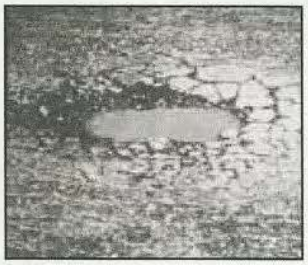

FIGURE 30
Distress Type ACP 8—High Severity Pothole, Close-up View

58

© Proprietà riservata dell'autore - Digitalizzazione e distribuzione a cura del CENTRO APPUNTI - Corso Luigi Einaudi, 55 - Torino / Pagina 111 di 286

© Proprietà riservata dell'autore - Digitalizzazione e distribuzione a cura del CENTRO APPUNTI - Corso Luigi Einaudi, 55 - Torino / Pagina 113 di 286

Rutting give problem in changing direction because of water presence.
Ruts appear on wheel paths. Two cases:
- persistent deformation due to subgrade plastic deformation → bigger ruts;
- persistent deformation due to bituminous layer: Two sub cases:
  - pd with volume variation: vehicle compact pavement → inadequately compacted;
  - pd with constant volume: lateral movement of material due to viscosity which is influenced by high temperature and loads.

9

RUTTING

Description

A rut is a longitudinal surface depression in the wheel path. It may have associated transverse displacement.

↳ caused by vertical deformation

Severity Levels

Not applicable. Severity levels could be defined by categorizing the measurements taken. A record of the measurements taken is much more desirable, because it is more accurate and repeatable than are severity levels.

How to Measure

Specific Pavement Studies (SPS)-3 ONLY. Record maximum rut depth to the nearest millimeter, at 15.25-m intervals for each wheel path, as measured with a 1.2-m straight edge.

All other LTPP sections: Transverse profile is measured with a Dipstick® profiler at 15.25-m intervals.

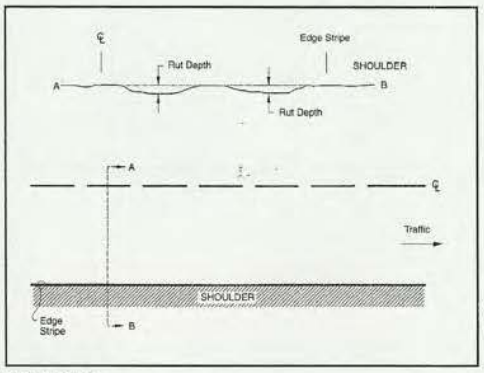

FIGURE 31
Distress Type ACP 9—Rutting

FIGURE 32
Distress Type ACP 9—Rutting

FIGURE 33
Distress Type ACP 9—Standing Water in Ruts

© Proprietà riservata dell'autore - Digitalizzazione e distribuzione a cura del CENTRO APPUNTI - Corso Luigi Einaudi, 55 - Torino / Pagina 113 di 286

© Proprietà riservata dell'autore - Digitalizzazione e distribuzione a cura del CENTRO APPUNTI - Corso Luigi Einaudi, 55 - Torino / Pagina 115 di 286

D

Surface Defects

This section includes the following types of surface defects:

11. Bleeding
12. Polished Aggregate
13. Raveling

/61

© Proprietà riservata dell'autore - Digitalizzazione e distribuzione a cura del CENTRO APPUNTI - Corso Luigi Einaudi, 55 - Torino / Pagina 115 di 286

© Proprietà riservata dell'autore - Digitalizzazione e distribuzione a cura del CENTRO APPUNTI - Corso Luigi Einaudi, 55 - Torino / Pagina 117 di 286

POLISHED AGGREGATE

12

Description

Surface binder worn away to expose coarse aggregate.

→ loss of skid resistence caused by high shear stressed → aggregate lose their microtexture.

Severity Levels

Not applicable. However, the degree of polishing may be reflected in a reduction of surface friction.

How to Measure

Record square meters of affected surface area. Polished aggregate should not be rated on test sections that have received a preventive maintenance treatment that has covered the original pavement surface.

FIGURE 39
Distress Type ACP 12—Polished Aggregate

/62

© Proprietà riservata dell'autore - Digitalizzazione e distribuzione a cura del CENTRO APPUNTI - Corso Luigi Einaudi, 55 - Torino / Pagina 117 di 286

© Proprietà riservata dell'autore - Digitalizzazione e distribuzione a cura del CENTRO APPUNTI - Corso Luigi Einaudi, 55 - Torino / Pagina 119 di 286

E

Miscellaneous Distresses

This section includes the following distresses:

14. Lane-to-Shoulder Dropoff
15. Water Bleeding and Pumping

/63

© Proprietà riservata dell'autore - Digitalizzazione e distribuzione a cura del CENTRO APPUNTI - Corso Luigi Einaudi, 55 - Torino / Pagina 119 di 286

© Proprietà riservata dell'autore - Digitalizzazione e distribuzione a cura del CENTRO APPUNTI - Corso Luigi Einaudi, 55 - Torino / Pagina 121 di 286

WATER BLEEDING AND PUMPING

15

Description

Seeping or ejection of water from beneath the pavement through cracks. In some cases, detectable by deposits of fine material left on the pavement surface, which were eroded (pumped) from the support layers and have stained the surface.

Severity Levels

Not applicable. Severity levels are not used because the amount and degree of water bleeding and pumping changes with varying moisture conditions.

How to Measure

Record the number of occurrences of water bleeding and pumping and the length in meters of affected pavement with a minimum length of 1 m.

Note. The combined length of water bleeding and pumping cannot exceed the length of the test section.

FIGURE 45
Distress Type ACP 15—Water Bleeding and Pumping

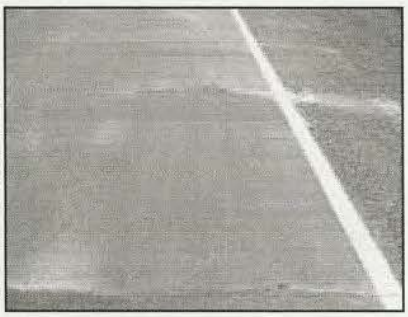

FIGURE 46
Distress Type ACP 15—Fine Material Left on Surface by Water Bleeding and Pumping

/64

© Proprietà riservata dell'autore - Digitalizzazione e distribuzione a cura del CENTRO APPUNTI - Corso Luigi Einaudi, 55 - Torino / Pagina 121 di 286

© Proprietà riservata dell'autore - Digitalizzazione e distribuzione a cura del CENTRO APPUNTI - Corso Luigi Einaudi, 55 - Torino / Pagina 123 di 286

A

Cracking

This section includes the following types of distresses:

1. Corner Breaks
2. Durability Cracking ("D" Cracking)
3. Longitudinal Cracking
4. Transverse Cracking

Figure 47 illustrates the proper measurement of crack width and width of spalling for cracks and joints.

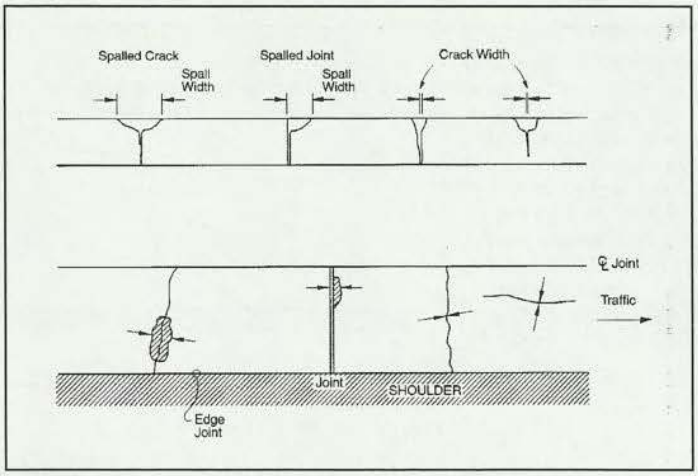

FIGURE 47
Measuring Widths of Spalls and Cracks in Jointed Concrete Pavement

© Proprietà riservata dell'autore - Digitalizzazione e distribuzione a cura del CENTRO APPUNTI - Corso Luigi Einaudi, 55 - Torino / Pagina 123 di 286

© Proprietà riservata dell'autore - Digitalizzazione e distribuzione a cura del CENTRO APPUNTI - Corso Luigi Einaudi, 55 - Torino / Pagina 125 di 286

→ cracks are small, thin and close to each-other
This crack is a function of the properties of concrete (curing condition, mix design)
It will lead to loss of material and could promote other distress

DURABILITY CRACKING ("D" CRACKING)

2

Description

Closely spaced crescent-shaped hairline cracking pattern.

Occurs adjacent to joints, cracks, or free edges; initiating in slab corners. Dark coloring of the cracking pattern and surrounding area.

How to Measure

Record number of slabs with "D" cracking and square meters of area affected at each severity level. The slab and affected area severity rating is based on the highest severity level present for at least 10 percent of the area affected.

Severity Levels

LOW
"D" cracks are tight, with no loose or missing pieces, and no patching is in the affected area.

MODERATE
"D" cracks are well-defined, and some small pieces are loose or have been displaced.

HIGH
"D" cracking has a well-developed pattern, with a significant amount of loose or missing material. Displaced pieces, up to 0.1 m², may have been patched.

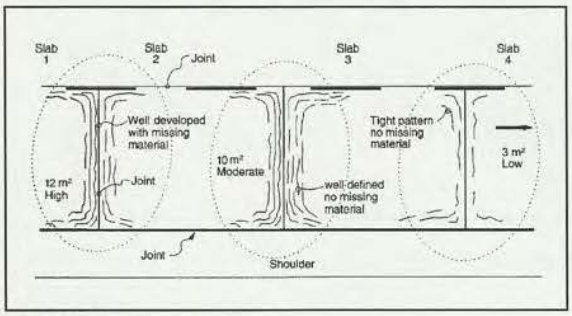

FIGURE 51
Distress Type JCP 2—Durability Cracking ("D" Cracking)

FIGURE 52
Distress Type JCP 2—Moderate Severity "D" Cracking with Well-Defined Pattern

FIGURE 53
Distress Type JCP 2—High Severity "D" Cracking with Loose and Missing Material

© Proprietà riservata dell'autore - Digitalizzazione e distribuzione a cura del CENTRO APPUNTI - Corso Luigi Einaudi, 55 - Torino / Pagina 125 di 286

© Proprietà riservata dell'autore - Digitalizzazione e distribuzione a cura del CENTRO APPUNTI - Corso Luigi Einaudi, 55 - Torino / Pagina 127 di 286

How to Measure

Record length in meters of longitudinal cracking at each severity level. Also record length in meters of longitudinal cracking with sealant in good condition at each severity level.

FIGURE 55
Distress Type JCP 3—Low Severity Longitudinal Cracking

FIGURE 56
Distress Type JCP 3—Moderate Severity Longitudinal Cracking

FIGURE 57
Distress Type JCP 3—High Severity Longitudinal Cracking

© Proprietà riservata dell'autore - Digitalizzazione e distribuzione a cura del CENTRO APPUNTI - Corso Luigi Einaudi, 55 - Torino / Pagina 127 di 286

© Proprietà riservata dell'autore - Digitalizzazione e distribuzione a cura del CENTRO APPUNTI - Corso Luigi Einaudi, 55 - Torino / Pagina 129 di 286

How to Measure

Record number and length of transverse cracks at each severity level. Rate the entire transverse crack at the highest severity level present for at least 10 percent of the total length of the crack. Length recorded, in meters, is the total length of the crack and is assigned to the highest severity level present for at least 10 percent of the total length of the crack.

Also record the length, in meters, of transverse cracking at each severity level with sealant in good condition. The length recorded, in meters, is the total length of the well-sealed crack and is assigned to the severity level of the crack. Record only when the sealant is in good condition for at least 90 percent of the length of the crack.

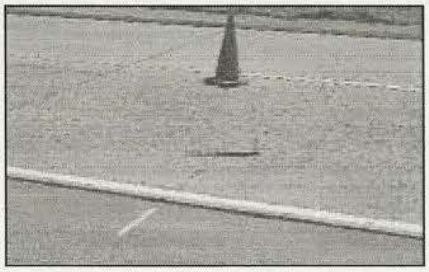

FIGURE 59
Distress Type JCP 4—Moderate Severity Transverse Cracking

FIGURE 60
Distress Type JCP 4—High Severity Transverse Cracking

© Proprietà riservata dell'autore - Digitalizzazione e distribuzione a cura del CENTRO APPUNTI - Corso Luigi Einaudi, 55 - Torino / Pagina 129 di 286

© Proprietà riservata dell'autore - Digitalizzazione e distribuzione a cura del CENTRO APPUNTI - Corso Luigi Einaudi, 55 - Torino / Pagina 131 di 286

Joint seal damage is any condition which enables incompressible materials or water to infiltrate the joint from the surface. In fact joint have to provide slab expansions and if an incompressible material penetrate in the joint it don't allow the precast to move.

5

This is why we need to seal joints with an adequate material which doesn't harden with low temperature but remains elastic.

JOINT SEAL DAMAGE

Is seal necessary to have a long lasting pavement

Description

Joint seal damage is any condition which enables incompressible materials or water to infiltrate the joint from the surface. Typical types of joint seal damage are:

Extrusion, hardening, adhesive failure (bonding), cohesive failure (splitting), or complete loss of sealant.

Intrusion of foreign material in the joint.

Weed growth in the joint.

5a. *TRANSVERSE JOINT SEAL DAMAGE*

Severity Levels

LOW
Joint seal damage as described above exists over less than 10 percent of the joint.

MODERATE
Joint seal damage as described above exists over 10-50 percent of the joint.

HIGH
Joint seal damage as described above exists over more than 50 percent of the joint.

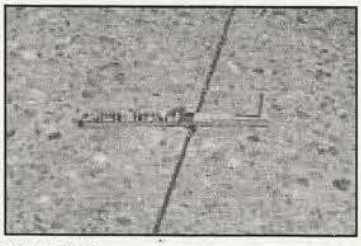

FIGURE 61
Distress Type JCP 5—Low Severity Joint Seal Damage

How to Measure

Indicate whether the transverse joints have been sealed (yes or no). If yes, record number of sealed transverse joints at each severity level. Any joint seal with no apparent damage is considered to be low severity.

5b. *LONGITUDINAL JOINT SEAL DAMAGE*

Severity Levels

None.

How to Measure

Record number of longitudinal joints that are sealed (0, 1, 2). Record total length of sealed longitudinal joints with joint seal damage as described above. Individual occurrences are recorded only when at least 1 m in length.

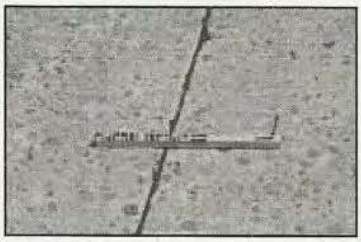

FIGURE 62
Distress Type JCP 5—Moderate Severity Joint Seal Damage

© Proprietà riservata dell'autore - Digitalizzazione e distribuzione a cura del CENTRO APPUNTI - Corso Luigi Einaudi, 55 - Torino / Pagina 131 di 286

© Proprietà riservata dell'autore - Digitalizzazione e distribuzione a cura del CENTRO APPUNTI - Corso Luigi Einaudi, 55 - Torino / Pagina 133 di 286

7

SPALLING OF TRANSVERSE JOINTS

Description

Cracking, breaking, chipping, or fraying of slab edges within 0.3 m from the face of the transverse joint.

Severity Levels

LOW
Spalls < 75 mm wide, measured to the face of the joint, with loss of material, or spalls with no loss of material and no patching.

MODERATE
Spalls 75 mm to 150 mm wide, measured to the face of the joint, with loss of material.

HIGH
Spalls > 150 mm wide, measured to the face of the joint, with loss of material, or broken into two or more pieces, or contains patch material.

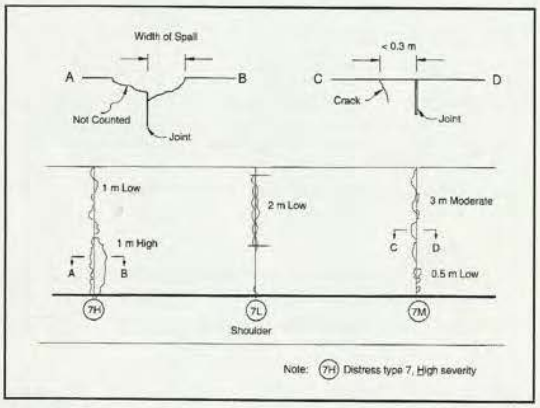

FIGURE 66
Distress Type JCP 7—Spalling of Transverse Joints

How to Measure

Record number of affected transverse joints at each severity level. A joint is affected only if the total length of spalling is 10 percent or more of the length of the joint. Rate the entire transverse joint at the highest severity level present for at least 10 percent of the total length of the spalling.

Record length in meters of the spalled portion of the joint at the assigned severity level for the joint. Spalls that have been repaired by completely removing all broken pieces and replacing them with patching material (rigid or flexible) should be rated as a patch. If the boundaries of the spall are visible, then also rate as a high severity spall. Note: All patches meeting size criteria are rated as patches.

FIGURE 67
Distress Type JCP 7—Moderate Severity Spalling of Transverse Joint, Far View

FIGURE 68
Distress Type JCP 7—Moderate Severity Spalling of Transverse Joint, Close-up View

© Proprietà riservata dell'autore - Digitalizzazione e distribuzione a cura del CENTRO APPUNTI - Corso Luigi Einaudi, 55 - Torino / Pagina 133 di 286

© Proprietà riservata dell'autore - Digitalizzazione e distribuzione a cura del CENTRO APPUNTI - Corso Luigi Einaudi, 55 - Torino / Pagina 135 di 286

8

MAP CRACKING AND SCALING

8a. *MAP CRACKING*

it look like fatigue cracking. series of interconnected cracks but they extend only into upper surface of slab.

non grave, non occorre sostituire le lastre

Description

A series of cracks that extend only into the upper surface of the slab. Larger cracks frequently are oriented in the longitudinal direction of the pavement and are interconnected by finer transverse or random cracks.

Severity Levels

Not applicable.

How to Measure

Record the number of occurrences and the square meters of affected area.

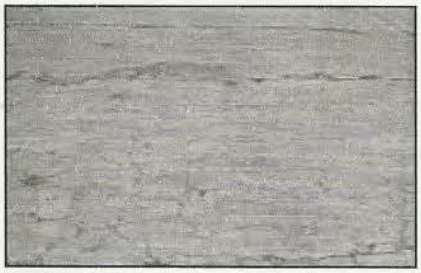

FIGURE 69
Distress Type JCP 8a—Map Cracking

8b. *SCALING*

← It is the evolution of the map cracking. It is the deterioration of the upper concrete slab surface → there is a removal of the material.

Description

Scaling is the deterioration of the upper concrete slab surface, normally 3 mm to 13 mm, and may occur anywhere over the pavement.

Severity Levels

Not applicable.

How to Measure

Record the number of occurrences and the square meters of affected area.

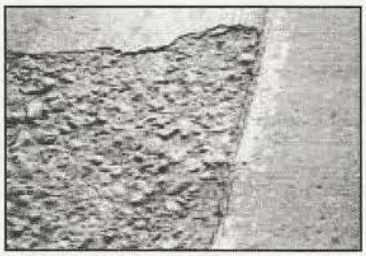

FIGURE 70
Distress Type JCP 8b—Scaling

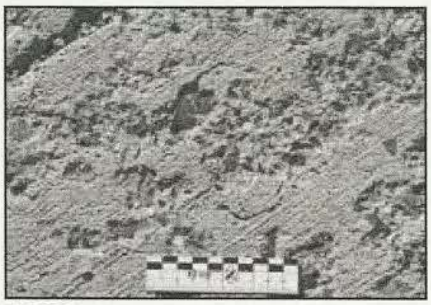

FIGURE 71
Distress Type JCP 8b—Scaling, Close-up View

© Proprietà riservata dell'autore - Digitalizzazione e distribuzione a cura del CENTRO APPUNTI - Corso Luigi Einaudi, 55 - Torino / Pagina 135 di 286

© Proprietà riservata dell'autore - Digitalizzazione e distribuzione a cura del CENTRO APPUNTI - Corso Luigi Einaudi, 55 - Torino / Pagina 137 di 286

10

POPOUTS

Description

Small pieces of pavement broken loose from the surface, normally ranging in diameter from 25 mm to 100 mm, and depth from 13 mm to 50 mm.

Severity Levels

Not applicable. However, severity levels can be defined in relation to the intensity of popouts as measured below.

How to Measure

Not recorded in LTPP surveys.

It isn't a structural problem

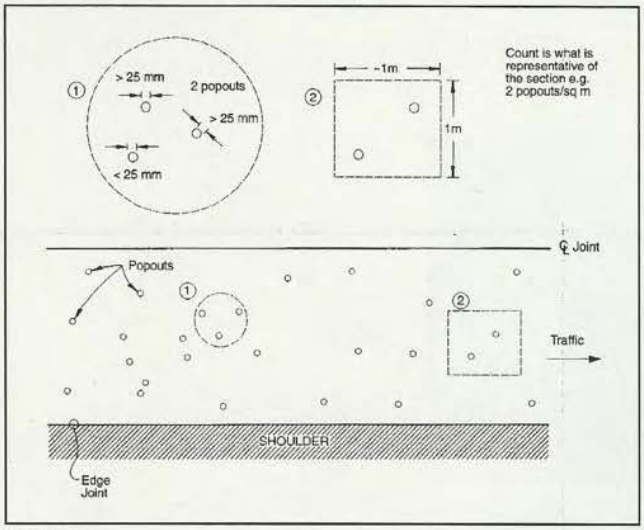

FIGURE 73
Distress Type JCP 10—Popouts

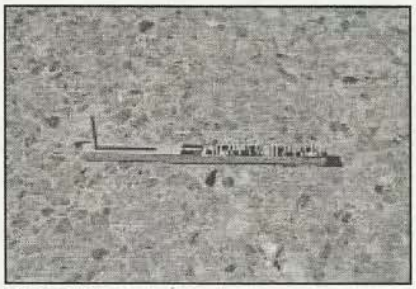

FIGURE 74
Distress Type JCP 10—A Popout

JOINTED PORTLAND CEMENT CONCRETE SURFACES

© Proprietà riservata dell'autore - Digitalizzazione e distribuzione a cura del CENTRO APPUNTI - Corso Luigi Einaudi, 55 - Torino / Pagina 137 di 286

© Proprietà riservata dell'autore - Digitalizzazione e distribuzione a cura del CENTRO APPUNTI - Corso Luigi Einaudi, 55 - Torino / Pagina 139 di 286

11

BLOWUPS

The pavement tries to expand and if the joint has not a sufficient width, the edge of the slabs touch each other and go in compression.

Description

Localized upward movement of the pavement surface at transverse joints or cracks, often accompanied by shattering of the concrete in that area.

Severity Levels

Not applicable. However, severity levels can be defined by the relative effect of a blowup on ride quality and safety.

How to Measure

Record the number of blowups.

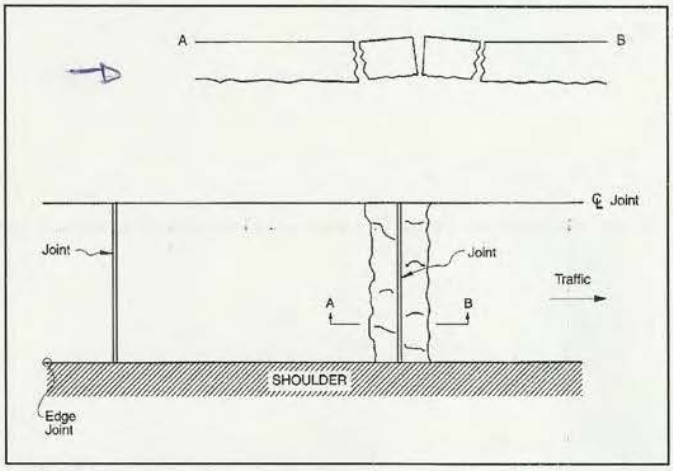

FIGURE 75
Distress Type JCP 11—Blowups

FIGURE 76
Distress Type JCP 11—A Blowup

JOINTED PORTLAND CEMENT CONCRETE SURFACES

There was this problem in Bolzano airport where, due to a certain slope, residues were concentrated in joint and where they try to expand → they broke because of incompressible residues.

© Proprietà riservata dell'autore - Digitalizzazione e distribuzione a cura del CENTRO APPUNTI - Corso Luigi Einaudi, 55 - Torino / Pagina 139 di 286

© Proprietà riservata dell'autore - Digitalizzazione e distribuzione a cura del CENTRO APPUNTI - Corso Luigi Einaudi, 55 - Torino / Pagina 141 di 286

13

LANE-TO-SHOULDER DROPOFF

Description

Difference in elevation between the edge of slab and outside shoulder; typically occurs when the outside shoulder settles.

Severity Levels

Not applicable. Severity levels can be defined by categorizing the measurements taken. A complete record of the measurements taken is much more desirable, however, because it is more accurate and repeatable than are severity levels.

How to Measure

Measure at the longitudinal construction joint between the lane edge and the shoulder.

Record to the nearest millimeter at 15.25-m intervals along the lane-to-shoulder joint.

If the traveled surface is lower than the shoulder, record as a negative (-) value.

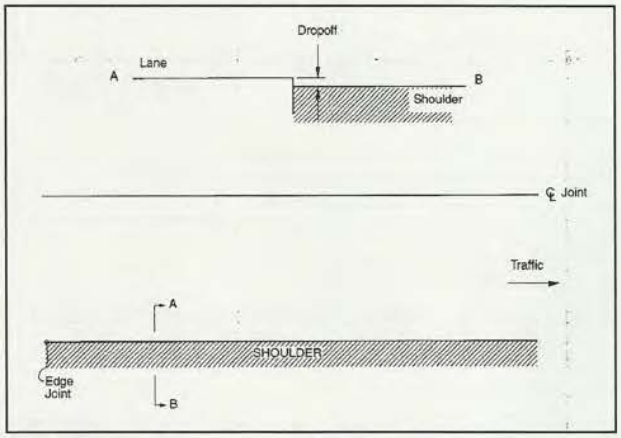

FIGURE 79
Distress Type JCP 13—
Lane-to-Shoulder Dropoff

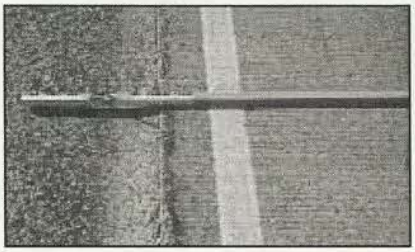

FIGURE 80
Distress Type JCP 13—
Lane-to-Shoulder Dropoff

© Proprietà riservata dell'autore - Digitalizzazione e distribuzione a cura del CENTRO APPUNTI - Corso Luigi Einaudi, 55 - Torino / Pagina 141 di 286

© Proprietà riservata dell'autore - Digitalizzazione e distribuzione a cura del CENTRO APPUNTI - Corso Luigi Einaudi, 55 - Torino / Pagina 143 di 286

15

PATCH/PATCH DETERIORATION

Description

A portion, greater than 0.1 m², or all of the original concrete slab that has been removed and replaced, or additional material applied to the pavement after original construction.

Severity Levels

Is the deterioration depends on the material used

LOW

Patch has low severity distress of any type; and no measurable faulting or settlement; pumping is not evident.

MODERATE

Patch has moderate severity distress of any type; or faulting or settlement up to 6 mm; pumping is not evident.

HIGH

Patch has a high severity distress of any type; or faulting or settlement ≥ 6 mm; pumping may be evident.

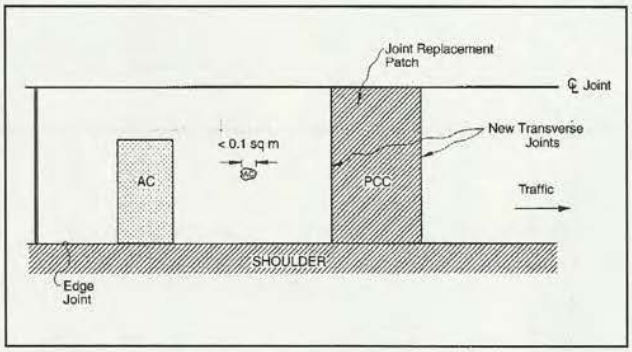

FIGURE 84
Distress Type JCP 15—Patch/Patch Deterioration

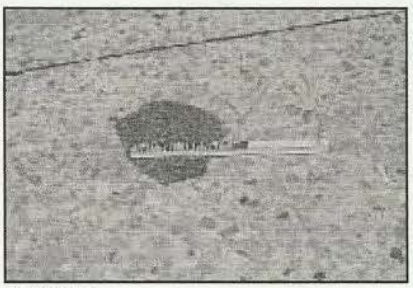

FIGURE 85
Distress Type JCP 15—Small, Low Severity Asphalt Concrete Patch

© Proprietà riservata dell'autore - Digitalizzazione e distribuzione a cura del CENTRO APPUNTI - Corso Luigi Einaudi, 55 - Torino / Pagina 143 di 286

© Proprietà riservata dell'autore - Digitalizzazione e distribuzione a cura del CENTRO APPUNTI - Corso Luigi Einaudi, 55 - Torino / Pagina 145 di 286

16

WATER BLEEDING AND PUMPING

Description

Seeping or ejection of water from beneath the pavement through cracks. In some cases, detectable by deposits of fine material left on the pavement surface, which were eroded (pumped) from the support layers and have stained the surface.

Severity Levels

Not applicable. Severity levels are not used because the amount and degree of water bleeding and pumping changes with varying moisture conditions.

How to Measure

Record the number of occurrences of water bleeding and pumping and the length in meters of affected pavement with a minimum length of 1 m.

Note. The combined length of water bleeding and pumping cannot exceed the length of the test section.

FIGURE 89
Distress Type JCP 16—Water Bleeding and Pumping

© Proprietà riservata dell'autore - Digitalizzazione e distribuzione a cura del CENTRO APPUNTI - Corso Luigi Einaudi, 55 - Torino / Pagina 145 di 286

© Proprietà riservata dell'autore - Digitalizzazione e distribuzione a cura del CENTRO APPUNTI - Corso Luigi Einaudi, 55 - Torino / Pagina 147 di 286

A

Cracking

This section includes the following distresses:

1. Durability Cracking ("D" Cracking)
2. Longitudinal Cracking
3. Transverse Cracking

© Proprietà riservata dell'autore - Digitalizzazione e distribuzione a cura del CENTRO APPUNTI - Corso Luigi Einaudi, 55 - Torino / Pagina 147 di 286

© Proprietà riservata dell'autore - Digitalizzazione e distribuzione a cura del CENTRO APPUNTI - Corso Luigi Einaudi, 55 - Torino / Pagina 149 di 286

LONGITUDINAL CRACKING

Description

Cracks that are predominantly parallel to the pavement centerline.

Severity Levels

LOW
Crack widths < 3 mm, no spalling, and there is no measurable faulting; or well-sealed and with a width that cannot be determined.

MODERATE
Crack widths ≥ 3 mm and < 13 mm; or with spalling < 75 mm; or faulting up to 13 mm.

HIGH
Crack widths ≥ 13 mm; or with spalling ≥ 75 mm; or faulting ≥ 13 mm.

How to Measure

Record length in meters of longitudinal cracking at each severity level. Also record length in meters of longitudinal cracking with sealant in good condition at each severity level.

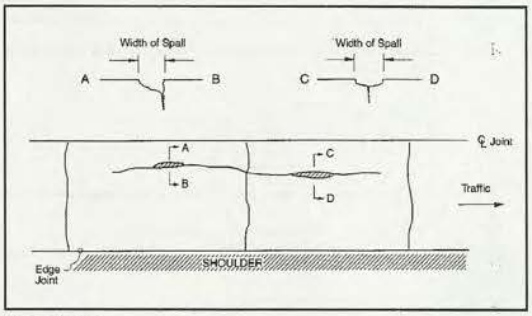

FIGURE 93
Distress Type CRCP 2—Longitudinal Cracking

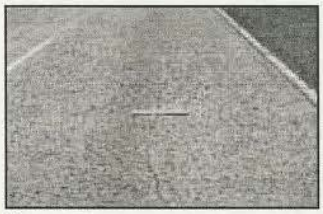

Figure 94
Distress Type CRCP 2—Low Severity Longitudinal Cracking

FIGURE 95
Distress Type CRCP 2—High Severity Longitudinal Cracking

© Proprietà riservata dell'autore - Digitalizzazione e distribuzione a cura del CENTRO APPUNTI - Corso Luigi Einaudi, 55 - Torino / Pagina 149 di 286

© Proprietà riservata dell'autore - Digitalizzazione e distribuzione a cura del CENTRO APPUNTI - Corso Luigi Einaudi, 55 - Torino / Pagina 151 di 286

How to Measure

Record separately the number and length in meters of transverse cracking at each severity level. The sum of all the individual crack lengths shall be recorded. Then record the total number of transverse cracks within the survey section.

Note: Cracks that do not cross midlane, although not counted, should be drawn on the map sheets.

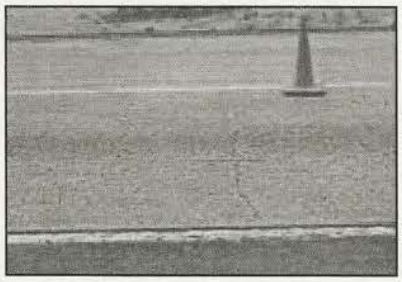

FIGURE 98
Distress Type CRCP 3—Low Severity Transverse Cracking

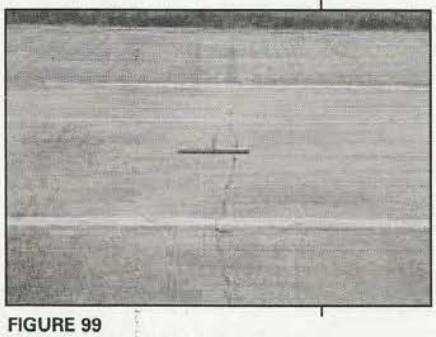

FIGURE 99
Distress Type CRCP 3—Moderate Severity Transverse Cracking

FIGURE 100
Distress Type CRCP 3—High Severity Transverse Cracking

81

© Proprietà riservata dell'autore - Digitalizzazione e distribuzione a cura del CENTRO APPUNTI - Corso Luigi Einaudi, 55 - Torino / Pagina 151 di 286

© Proprietà riservata dell'autore - Digitalizzazione e distribuzione a cura del CENTRO APPUNTI - Corso Luigi Einaudi, 55 - Torino / Pagina 153 di 286

4

MAP CRACKING AND SCALING

4a. *MAP CRACKING*

Description

A series of cracks that extend only into the upper surface of the slab. Larger cracks frequently are oriented in the longitudinal direction of the pavement and are interconnected by finer transverse or random cracks.

Severity Levels

Not applicable.

How to Measure

Record the number of occurrences and the square meters of affected area. When an entire section is affected with map cracking, it should be considered one occurrence.

FIGURE 101
Distress Type CRCP 4a—Map Cracking Attributable to Alkali-Silica Reactivity

4b. *SCALING*

Description

Scaling is the deterioration of the upper concrete slab surface, normally 3 mm to 13 mm, and may occur anywhere over the pavement.

Severity Levels

Not applicable.

How to Measure

Record the number of occurrences and the square meters of affected area.

FIGURE 102
Distress Type CRCP 4b—Scaling

© Proprietà riservata dell'autore - Digitalizzazione e distribuzione a cura del CENTRO APPUNTI - Corso Luigi Einaudi, 55 - Torino / Pagina 153 di 286

© Proprietà riservata dell'autore - Digitalizzazione e distribuzione a cura del CENTRO APPUNTI - Corso Luigi Einaudi, 55 - Torino / Pagina 155 di 286

6

POPOUTS

Description

Small pieces of pavement broken loose from the surface, normally ranging in diameter from 25 mm to 100 mm and depth from 13 mm to 50 mm.

Severity Levels

Not applicable. However, severity levels can be defined in relation to the intensity of popouts as measured below.

How to Measure

Not recorded in LTPP surveys.

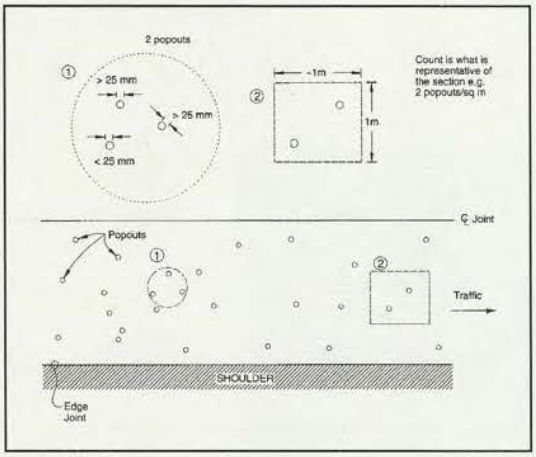

FIGURE 104
Distress Type CRCP 6—Popouts

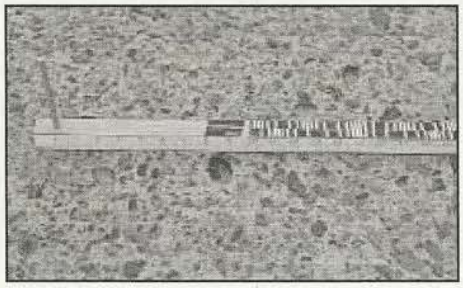

FIGURE 105
Distress Type CRCP 6—Popouts

© Proprietà riservata dell'autore - Digitalizzazione e distribuzione a cura del CENTRO APPUNTI - Corso Luigi Einaudi, 55 - Torino / Pagina 155 di 286

© Proprietà riservata dell'autore - Digitalizzazione e distribuzione a cura del CENTRO APPUNTI - Corso Luigi Einaudi, 55 - Torino / Pagina 157 di 286

7

BLOWUPS

Description

Localized upward movement of the pavement surface at transverse joints or cracks, often accompanied by shattering of the concrete in that area.

Severity Levels

Not applicable. However, severity levels can be defined by the relative effect of a blowup on ride quality and safety.

How to Measure

Record number of blowups.

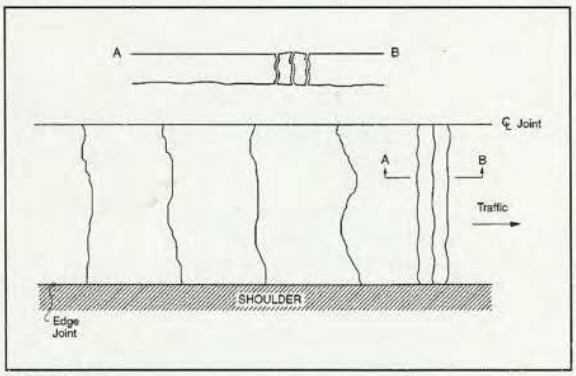

FIGURE 106
Distress Type CRCP 7—Blowups

FIGURE 107
Distress Type CRCP 7—A Blowup

FIGURE 108
Distress Type CRCP 7—Close-up View of a Blowup

FIGURE 109
Distress Type CRCP 7—Exposed Steel in a Blowup

CONTINUOUSLY REINFORCED CONCRETE SURFACES

© Proprietà riservata dell'autore - Digitalizzazione e distribuzione a cura del CENTRO APPUNTI - Corso Luigi Einaudi, 55 - Torino / Pagina 157 di 286

© Proprietà riservata dell'autore - Digitalizzazione e distribuzione a cura del CENTRO APPUNTI - Corso Luigi Einaudi, 55 - Torino / Pagina 159 di 286

9

LANE-TO-SHOULDER DROPOFF

Description

Difference in elevation between the edge of slab and outside shoulder; typically occurs when the outside shoulder settles.

Severity Levels

Not applicable. Severity levels could be defined by categorizing the measurements taken. A complete record of the measurements taken is much more desirable, however, because it is more accurate and repeatable than are severity levels.

How to Measure

Measure at the longitudinal construction joint between the lane edge and the shoulder.

Record in millimeters to the nearest millimeter at 15.25-m intervals along the lane-to-shoulder joint.

If the traveled surface is lower than the shoulder, record as a negative (-) value.

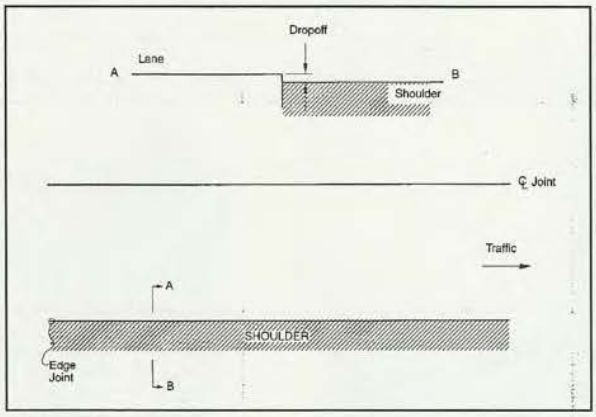

FIGURE 114
Distress Type CRCP 9—Lane-to-Shoulder Dropoff

FIGURE 115
Distress Type CRCP 9—Lane-to-Shoulder Dropoff

© Proprietà riservata dell'autore - Digitalizzazione e distribuzione a cura del CENTRO APPUNTI - Corso Luigi Einaudi, 55 - Torino / Pagina 159 di 286

© Proprietà riservata dell'autore - Digitalizzazione e distribuzione a cura del CENTRO APPUNTI - Corso Luigi Einaudi, 55 - Torino / Pagina 161 di 286

11

PATCH/PATCH DETERIORATION

Description

A portion, greater than 0.1 m², or all of the original concrete slab that has been removed and replaced, or additional material applied to the pavement after original construction.

Severity Levels

LOW
Patch has, at most, low severity distress of any type; and no measurable faulting or settlement; pumping is not evident.

MODERATE
Patch has moderate severity distress of any type; or faulting or settlement up to 6 mm; pumping is not evident.

HIGH
Patch has a high severity distress of any type; or faulting or settlement ≥ 6 mm; pumping may be evident.

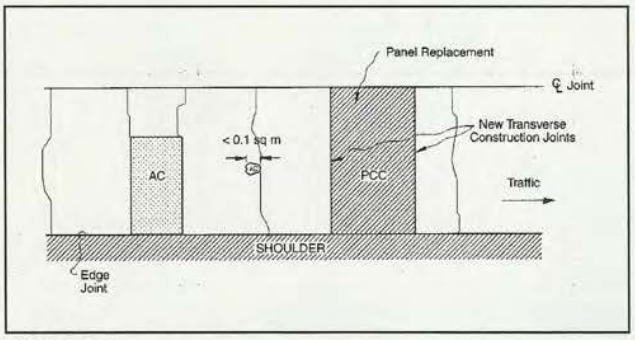

FIGURE 118
Distress Type CRCP 11—Patch/Patch Deterioration

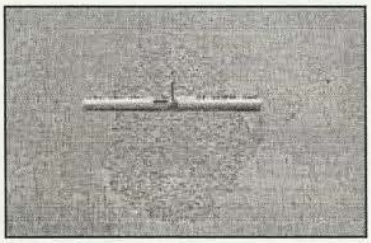

FIGURE 119
Distress Type CRCP 11—Small, Low Severity Asphalt Concrete Patch

© Proprietà riservata dell'autore - Digitalizzazione e distribuzione a cura del CENTRO APPUNTI - Corso Luigi Einaudi, 55 - Torino / Pagina 161 di 286

© Proprietà riservata dell'autore - Digitalizzazione e distribuzione a cura del CENTRO APPUNTI - Corso Luigi Einaudi, 55 - Torino / Pagina 163 di 286

12

PUNCHOUTS → consist in the formation of a longitudinal crack between two transverse cracks.

Description

The area enclosed by two closely spaced (usually < 0.6 m) transverse cracks, a short longitudinal crack, and the edge of the pavement or a longitudinal joint. Also includes "Y" cracks that exhibit spalling, breakup, or faulting.

Severity Levels

LOW

Longitudinal and transverse cracks are tight and may have spalling < 75 mm or faulting < 6 mm with no loss of material and no patching. Does not include "Y" cracks.

MODERATE

Spalling ≥ 75 mm and < 150 mm or faulting ≥ 6 mm and < 13 mm exists.

HIGH

Spalling ≥ 150 mm, or concrete within the punchout is punched down by ≥ 13 mm or is loose and moves under traffic or is broken into two or more pieces or contains patch material.

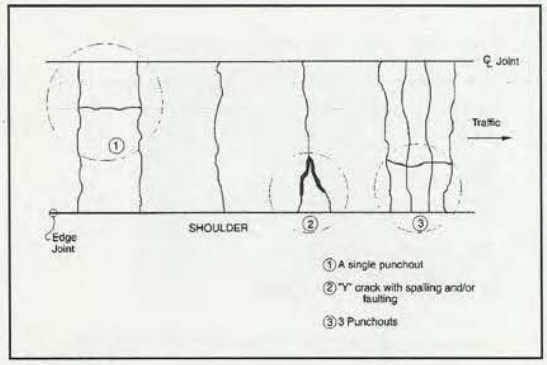

(3) In this part act as a cantilever beam and bends. There will be a longitudinal crack on the top as a result of the excessive tensile strenght

FIGURE 123
Distress Type CRCP 12—Punchouts

FIGURE 124
Distress Type CRCP 12—Low Severity Punchout

© Proprietà riservata dell'autore - Digitalizzazione e distribuzione a cura del CENTRO APPUNTI - Corso Luigi Einaudi, 55 - Torino / Pagina 163 di 286

© Proprietà riservata dell'autore - Digitalizzazione e distribuzione a cura del CENTRO APPUNTI - Corso Luigi Einaudi, 55 - Torino / Pagina 165 di 286

13

SPALLING OF LONGITUDINAL JOINTS

Description

Cracking, breaking, chipping, or fraying of slab edges within 0.3 m of the longitudinal joint.

Severity Levels

LOW
Spalls < 75 mm wide, measured to the face of the joint, with loss of material or spalls with no loss of material and no patching.

MODERATE
Spalls 75 mm to 150 mm wide, measured to the face of the joint, with loss of material.

HIGH
Spalls > 150 mm wide measured to the face of the joint, with loss of material or is broken into two or more pieces or contains patch material.

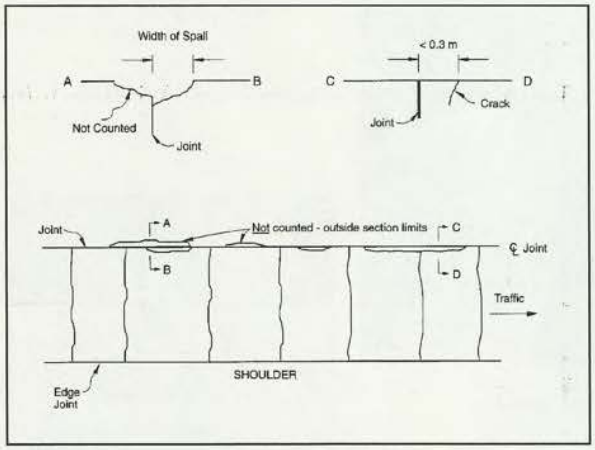

FIGURE 127
Distress Type CRCP 13—Spalling of Longitudinal Joints

© Proprietà riservata dell'autore - Digitalizzazione e distribuzione a cura del CENTRO APPUNTI - Corso Luigi Einaudi, 55 - Torino / Pagina 165 di 286

© Proprietà riservata dell'autore - Digitalizzazione e distribuzione a cura del CENTRO APPUNTI - Corso Luigi Einaudi, 55 - Torino / Pagina 167 di 286

14

WATER BLEEDING AND PUMPING

Description

Seeping or ejection of water from beneath the pavement through cracks or joints. In some cases detectable by deposits of fine material left on the pavement surface, which were eroded (pumped) from the support layers and have stained the surface.

Severity Levels

Not applicable. Severity levels are not used because the amount and degree of water bleeding and pumping changes with varying moisture conditions.

How to Measure

Record the number of occurrences of water bleeding and pumping and the length in meters of affected pavement with a minimum length of 1 m.

Note: The combined quantity of water bleeding and pumping cannot exceed the length of the test section.

FIGURE 131
Distress Type CRCP 14—Water Bleeding and Pumping

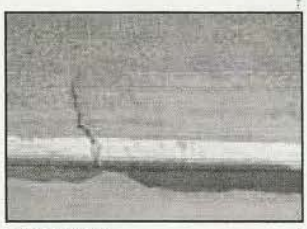

FIGURE 132
Distress Type CRCP 14—Close-up View of Water Bleeding and Pumping

© Proprietà riservata dell'autore - Digitalizzazione e distribuzione a cura del CENTRO APPUNTI - Corso Luigi Einaudi, 55 - Torino / Pagina 167 di 286

© Proprietà riservata dell'autore - Digitalizzazione e distribuzione a cura del CENTRO APPUNTI - Corso Luigi Einaudi, 55 - Torino / Pagina 169 di 286

PAVEMENT DESIGN

Choose the cross section taking into account traffic and performance in time.
Choose the material thicknesses → in the past had very thick granular material but now it tends to do thicker bituminous layers.
Design methods:

- Empirical : it is based on experience. An example is CBR method with related CBR (parameter characterizing soil) with the required thickness;
- Road test : test performed on the pavement built in very controlled conditions. An example is AASHTO design method;
- Mechanistic : analyse influence of stresses, strains and deflection on the pavements. It should be preferred because of generalization, if also this method requires field data (empirical components). An example are SHELL method, AASHTO design method improved;
- Catalogues : very easy to use because they give a lot of information with a little number of input informations. There are a lot of different catalogues and each catalog has been made with one of the three methods before. Italian catalogue is based on AASHTO ROAD TEST.

/91

© Proprietà riservata dell'autore - Digitalizzazione e distribuzione a cura del CENTRO APPUNTI - Corso Luigi Einaudi, 55 - Torino / Pagina 169 di 286

© Proprietà riservata dell'autore - Digitalizzazione e distribuzione a cura del CENTRO APPUNTI - Corso Luigi Einaudi, 55 - Torino / Pagina 171 di 286

where: $\overline{SV}$: average slope variation of the longitudinal profile;

C : area in which there are cracks;

P = area in which there are potholes and patches;

$\overline{RD}$ = average deep of the ruts.

With this relation they link ranking with the most common distresses, obtaining a more objective method.

The equation can't be used to design a pavement it can only be used on an existing pavement.

Evolution in time of the PSI:

$$PSI(t) = PSI_{initial} - A\left(\frac{N}{\rho}\right)^{\beta}$$

where: $A = PSI_{initial} - PSI_{final}$

PSI final is a function of the street importance

PSI initial is usually assumed equal to 4,2;

N = n° of application of standard axle;

$$\rho = 5,93 + 4,36 \log\left(\frac{SN}{2,5}+1\right) - 4,79 \log(L_1+L_2) + 4,33 \log L_2$$

$$\beta = 0,4 + \frac{0,081\,(L_1+L_2)^{3,23}}{\left(\frac{SN}{2,5}+1\right)^{3,19} L_2^{3,23}}$$

L_1 is the weight of the standard axle expressed in 1000 lbs ($L_1 = 18$)

L_2 is the number of axle ($L_2 = 1$)

SN is the structural number

$SN = \Sigma a_i h_i$ h_i = layer thickness

a_i = layer coefficient which depends on layer material

AASHTO values:

bituminous layer	$a_1 = 0,44$
base	$a_2 = 0,14$
foundation	$a_3 = 0,11$

/92

© Proprietà riservata dell'autore - Digitalizzazione e distribuzione a cura del CENTRO APPUNTI - Corso Luigi Einaudi, 55 - Torino / Pagina 171 di 286

© Proprietà riservata dell'autore - Digitalizzazione e distribuzione a cura del CENTRO APPUNTI - Corso Luigi Einaudi, 55 - Torino / Pagina 173 di 286

$D_{axle} = n \, D_{std\ axle}$

$\hookrightarrow n = \left(\frac{w_{axle}}{w_{std\ axle}}\right)^4$ equivalency factor

Through the axles equivalency law we can convert a certain traffic distribution into an equivalent traffic distribution composed of only standard axles.

Standard axle : 18000 pounds = 18 Kips = 8,2 t = 80 kN

How traffic develop in time?

We know the traffic nowadays but how will be to 20 years (design life of pavement).

I need to take into account traffic growth → traffic increase or decrease a % per years.

Prediction of traffic level :

$N_{\substack{\text{vehicle of period} \\ \text{project}}} = F \cdot N_{\substack{\text{nowadays} \\ \text{traffic}}}$

$\hookrightarrow$ growth factor $= \frac{(1+r)^n - 1}{n}$ $\quad n = \text{years}$, $r = \frac{\text{rate}}{100}$

$ESAC = AADT \cdot 365 \cdot TF \cdot G \cdot D_D \cdot D_L \cdot \%HV$

where : AADT = annual average daily traffic which includes both the traffic directions;

TF = total truck factor

D_D = directional factor

D_L = lane distribution factor

%HV = percentage of heavy vehicle

/93

© Proprietà riservata dell'autore - Digitalizzazione e distribuzione a cura del CENTRO APPUNTI - Corso Luigi Einaudi, 55 - Torino / Pagina 173 di 286

© Proprietà riservata dell'autore - Digitalizzazione e distribuzione a cura del CENTRO APPUNTI - Corso Luigi Einaudi, 55 - Torino / Pagina 175 di 286

AASHTO GOIDE FOR DESIGN OF PAVEMENT STRUCTURES

This new method takes into account:

- variability of parameters (reliability);
- behaviour of pavements (expecially thin pavement) is controlled by subgrade → no support factor (empirical approach) but resilient modulus (mechanistic description);
- influence of water: drainage conditions: unbound material should have a very good drainage capability (quick drainage);
- mechanical characteist of materials

RELIABILITY

R is a probability ($N_C \geq N_T$)

N_C = number of applications to reach PSI fin → allowable n° of ESAL

N_T = number of real applications

In calculations this factor is given by:

$S_0 \cdot z_R$ → value of S_0 which correspond to the probability R

S_0 standard deviation of the variable $S_0 = \log N_C - \log N_T$

RESILIENT MODULUS

M_R = resilient modulus: measurement of the elastic response of the subgrade

$M_R = \frac{\sigma}{\varepsilon_r}$ → cycling load
→ recovered deformation

/94

© Proprietà riservata dell'autore - Digitalizzazione e distribuzione a cura del CENTRO APPUNTI - Corso Luigi Einaudi, 55 - Torino / Pagina 175 di 286

© Proprietà riservata dell'autore - Digitalizzazione e distribuzione a cura del CENTRO APPUNTI - Corso Luigi Einaudi, 55 - Torino / Pagina 177 di 286

MECHANICAL CHARACTERISTICS

The layer coefficient a_i were related to the layer stiffness.

- Asphalt concrete mixtures:

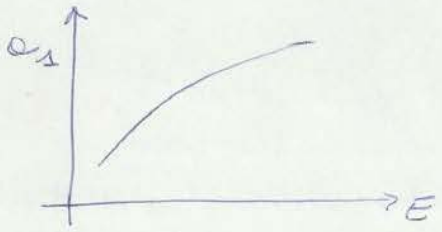

- granular material → cable

a_2, a_3 structural coefficient — CBR — Resilient modulus

/95

© Proprietà riservata dell'autore - Digitalizzazione e distribuzione a cura del CENTRO APPUNTI - Corso Luigi Einaudi, 55 - Torino / Pagina 177 di 286

© Proprietà riservata dell'autore - Digitalizzazione e distribuzione a cura del CENTRO APPUNTI - Corso Luigi Einaudi, 55 - Torino / Pagina 179 di 286

bending beam test

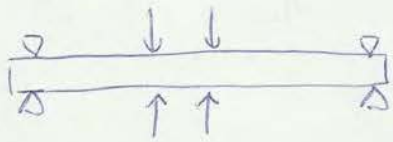

load alternates in sign (sinusoidal load)

beam bends in one direction and then in the other direction alternatively.

Real conditions : oscillation of stresses and strains due to repetitive loadings.

the behaviour can be described with the same law

but we need a function to transfer loading data to the real pavement.

Laboratory test models :

- controlled stress : crack progress really fast due to high local stress;
- controlled strain : maximum magnitude of the imposed strain (constant)

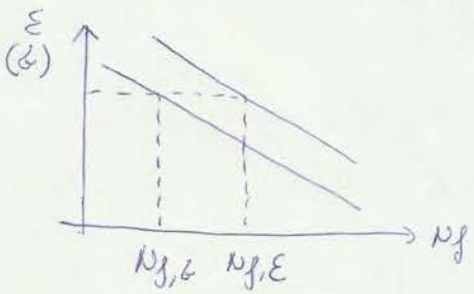

As crack develop, we need to reduce the level of stress to maintain the strain constant.
The mode of loading affects the estimation of number of loadings.

Model :

$$N_f = f_1 \, \varepsilon_t^{-f_2} E^{-f_3}$$

where : N_f = maximum allowable number of load repetitions to prevent fatigue cracking;

ε_t = maximum tensile strain which occur in the bitumen bound layer

E = modulus of the asphalt layer

/96

© Proprietà riservata dell'autore - Digitalizzazione e distribuzione a cura del CENTRO APPUNTI - Corso Luigi Einaudi, 55 - Torino / Pagina 179 di 286

© Proprietà riservata dell'autore - Digitalizzazione e distribuzione a cura del CENTRO APPUNTI - Corso Luigi Einaudi, 55 - Torino / Pagina 181 di 286

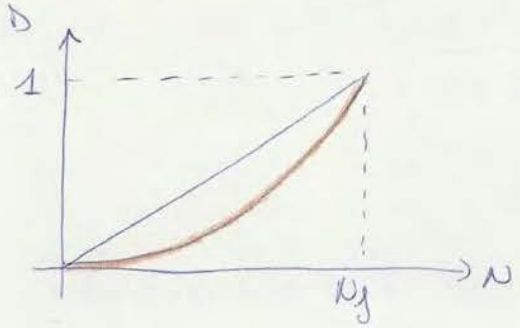

hypothesis of linear cumulation of damage → is not realistic: damage increase in time as pavement becomes weaker

$\begin{cases} N < N_f \rightarrow D < 1 & \text{ok!} \\ N = N_f \rightarrow D = 1 & \sim \text{ok!} \\ N > N_f \rightarrow D > 1 & \text{No!} \end{cases}$

D is really useful to combine together all these effects:
- different loading cases (2 types of trucks → ≠ loading intensity);
- different environmental conditions (hot/cold);
- different lateral positions (lateral wander → important in the case of airports.

EALF : equivalent axle load factor

generic axle x → x kN → N_x : n° applications generic axle
standard axle STD → 80 kN → N_{STD} : n° applications std axle

We can convert N_x in an equivalent number of applications of the std axle to make analysis simple.

$D_{i,x}$ = damage caused by 1 application of x axle $i = 1 \div N_x$

$$D_{1,x} = \frac{1}{f_1 (\varepsilon_{1,x})^{f_2} E^{-f_3}} \quad ; \quad D_{N,x} = \frac{N_x}{f_1 (\varepsilon_{1,x})^{f_2} E^{-f_3}}$$

$$EALF = \frac{D_{1x}}{D_{1STD}} \rightarrow D_{1x} = EALF \cdot D_{1,STD}$$

$$N_x D_{1,x} = EALF \cdot N_x \cdot D_{1,STD}$$

97

© Proprietà riservata dell'autore - Digitalizzazione e distribuzione a cura del CENTRO APPUNTI - Corso Luigi Einaudi, 55 - Torino / Pagina 181 di 286

© Proprietà riservata dell'autore - Digitalizzazione e distribuzione a cura del CENTRO APPUNTI - Corso Luigi Einaudi, 55 - Torino / Pagina 183 di 286

EXAMPLE OF PAVEMENT DESIGN

New motorway in Italy.

- Preliminary design: given cross section (embankments, excavations, tunnel, viaducts, service roads);
- Geographic position: environmental conditions;
- Mobility study: daily traffic;
- Technical specifications:

Requirements: minimum value of deformation modulus (subgrade = 15 MPa, CBR value, density, deformation modulus ≥ 100 MPa granular foundation;
deformation modulus ≥ 150 MPa, elastic dynamic modulus (from back-calculations) → cement stabilized foundation;
bitumen content = 4,5 ÷ 5,5 %; void content ≥ 18 %
or N_{des} = 40 gyrations → % voids = 23 %
Binder course mixture: bitumen content 4 ÷ 7 %
N_{des} = 100 gyrations → % voids = 3 ÷ 8 %
Base course mixture: N_{des} = 100 gyrations,
bitumen content 4-8 % ↳ % voids = 3 ÷ 8 %

Limiting function for fatigue $N_f = f_1 \varepsilon_t^{-f_2} E^{-f_3}$
for rutting $N_c = f_4 \varepsilon_c^{-f_5}$

Traffic:

TGM (AADT) = average daily traffic → provided on a full section of the road.

$$N_{VP} = TGM \cdot 365 \cdot \% V_p \cdot F_R \cdot \frac{(1+r)^n - 1}{r}$$

r = growth rate
n = number of design years

↳ n° total passages of heavy vehicle
↳ % of heavy vehicle
↳ distribution factor referred to the design lane

98

© Proprietà riservata dell'autore - Digitalizzazione e distribuzione a cura del CENTRO APPUNTI - Corso Luigi Einaudi, 55 - Torino / Pagina 183 di 286

© Proprietà riservata dell'autore - Digitalizzazione e distribuzione a cura del CENTRO APPUNTI - Corso Luigi Einaudi, 55 - Torino / Pagina 185 di 286

In the stiffness may decrease as a result of micro cracking due to tensil variations.

Poisson ratio $\nu = 0,25$

- Granular foundation

$$E_{ug} = 0,2 \cdot h^{0,45} \cdot E_S$$

- E_{ug} → unbound granular foundation
- h → thickness of the foundation
- E_S → elastic modulus of the subgrade

This is an indirect way to consider the non linear behaviour of a granular material (2 layer system).

Sensitivity of the model: variable thickness h → given E_S elastic modulus of subgrade soil = 100 MPa → E elastic modulus of foundation = 191 ÷ 313 MPa

I can do the same thing with different value of E_S.

- Bituminous mixture

$E^* = E_{ab} R^*$ → reduced modulus of the mixture

E_{ab} → glassy modulus of the mixture

$$E_{ab} = C \left(\frac{V_a}{V_b}\right) e^{-5,84 \cdot 10^{-2} \cdot (\%V)}$$

V_a = volume occupied by aggregates
V_b = volume occupied by binder
$\%V$ = void content
E_{ab} = depends on its state of compaction ($\%V$) and on the ratio between aggregates and binder

$$\log(R^*) = \log(B^*) - 1,35\left(1 - e^{-0,13\frac{V_a}{V_b}}\right) \cdot \log(B^*) \cdot \left[1 + 0,11 \log(B^*)\right]$$

B^* = reduced modulus of the binder

/99

© Proprietà riservata dell'autore - Digitalizzazione e distribuzione a cura del CENTRO APPUNTI - Corso Luigi Einaudi, 55 - Torino / Pagina 185 di 286

© Proprietà riservata dell'autore - Digitalizzazione e distribuzione a cura del CENTRO APPUNTI - Corso Luigi Einaudi, 55 - Torino / Pagina 187 di 286

Asphalt istitute : limiting condition for fatigue = 20 %
of cracking on the surface

$$N_f = 0,0022\,18 \cdot C \cdot \varepsilon_t^{-3,291} \cdot |E^*|^{-0,854}$$

$C = 10^M$ → function of volumetrics

↑ % V → ↓ N_f fatigue life decreases

↑ V_e → ↑ N_f fatigue life increases

The polymer modified binder provides 30% of increase of fatigue life : $N_f = 1,3 \cdot 0,0022\,18 \cdot C \cdot \varepsilon_t^{-3,291} \cdot |E^*|^{-0,854}$

Asphalt istitute : limiting criterion for rutting
depth of ruts = 1,27 cm

$$N_d = 1,365 \cdot 10^{-9} \varepsilon_c^{-4,477}$$

Interface conditions :

- 1 full adhesion : between two bituminous mixture layers;
- 0 full slip : between two granular layer or one granular layer and one bituminous layer

Maximum damage ratio → at the bottom of layer 3 (base course → the pavement will fail in fatigue.
Finally we obtain the design life = 3,92 years.

© Proprietà riservata dell'autore - Digitalizzazione e distribuzione a cura del CENTRO APPUNTI - Corso Luigi Einaudi, 55 - Torino / Pagina 187 di 286

© Proprietà riservata dell'autore - Digitalizzazione e distribuzione a cura del CENTRO APPUNTI - Corso Luigi Einaudi, 55 - Torino / Pagina 189 di 286

THE SHELL PAVEMENT DESIGN METHOD ON A PERSONAL COMPUTER

by C.P. Valkering*, F.D.R. Stapel* and J Lijzenga*

ABSTRACT

A version of the *Shell Pavement Design Manual* has been developed for use on personal computers. The Manual, based on a rational method for the thickness design of flexible pavements, was published in 1978 in the form of a series of design curves. The separate computer modules of the new version provide for the prediction of material properties and for the calculation of the critical stresses and strains. The method now has greater flexibility in that the user can introduce his specific material properties, traffic or climate without extensive interpolation effort.

INTRODUCTION

In 1963, Shell published a set of design charts for flexible pavements, based on an analytical method with design criteria derived from empirical design methods, results of the AASHO Road Test and laboratory data. In 1978, this system was extended to incorporate all relevant major design parameters and published in the *Shell Pavement Design Manual* (*SPDM* (1)). The method as presented in the SPDM incorporated allowance for the effects of temperature, traffic density, etc. on the pavement, the asphalt mixes being standardised with respect to stiffness and fatigue properties. In 1985, the method was updated in an addendum based on experience over the previous ten years. Though resulting from computer calculations of stresses and strains in pavement structures, the manual is in the form of graphs, charts and tables, so that it can be used by engineers with no access to sophisticated computer aids.

Today, computers, and especially personal computers, have come within the reach of engineers; a PC version of the pavement design method has, therefore, been developed. With computerisation, the system has improved in flexibility: 'standard' conditions (of climate, subgrade/sub-base and asphalt mix properties) can be bypassed if specific information is available.

In the Shell design procedure, the pavement is generally considered as a three-layer system: the subgrade, the base layer(s), and a top layer which represents all bitumen-bound layers. The layers are characterised by Young's modulus of elasticity and Poisson's ratio and thickness. The traffic may be expressed as a standard dual wheel load, and the cumulative number of axles the pavement will have to carry during its service life, is the design life. Stresses and strains in critical positions in the pavement are calculated with the BISAR computer program, with the subgrade strain and the asphalt strain as primary criteria.

We have now developed a program for personal computers which includes all the main elements of the design procedure. The new program consists of several user-friendly modules. These modules, for the prediction of the binder stiffness (Van der Poel nomograph), of the asphalt mix stiffness and of the fatigue strength of the asphalt mix, may be used or overruled if specific data are available or the mix is non-standard. The BISAR program is included as one of the modules and is used in an iterative way to determine the layer thickness, meeting the values set for critical strains.

The prediction of rut formation in the asphalt layers (a very laborious procedure in the SPDM) is also included as a separate option.

In this paper the features of the system are described, with extensive reference to the procedures in the 1978 *SPDM*. The program runs on an IBM (or IBM-compatible) personal computer with a free core memory of 450 kilobytes (DOS 3.x). A fixed disk with a free disk space of at least ten megabytes is required. Use of a mathematical co-processor is not required, but it is recommended.

It is emphasised that this paper is not intended to serve as a computer manual. A manual in which full details of the program are given will be issued separately.

MODULES IN THE PAVEMENT DESIGN PACKAGE

The design package is set up as a collection of distinct, but sequential modules. Some of the modules have already appeared in a package called BANDS ('Bitumen and Asphalt Nomographs Developed by Shell') and BISAR-PC, which were first presented by Koole et al. (2). Each module in the program has a separate, well-defined function in the design procedure as a whole.

The main modules identifiable in the package are:

1. Estimation of asphalt layer thickness for start of calculations.
2. Effect of climate on asphalt layer temperature.
3. Determination of pavement design life in terms of traffic load.
4. Determination of bitumen stiffness.
5. Determination of asphalt mix stiffness.
6. Determination of base and subgrade properties.
7. Definition of a pavement model based on files produced earlier.
8. The BISAR module for calculating strains.
9. Conversion of pavement strains to pavement life.
10. Iterative BISAR calculations to determine pavement structure for required design life.

These modules are now discussed in detail.

Estimation of Asphalt Layer Thickness for Start of Calculations

As this design method is based on an iterative procedure, a start value, or user's estimate for the asphalt layer thickness, is required to begin with. The better the initial guess meets the final design thickness, the fewer iterations are required. Normally, a start thickness will lie between 0.05 m and 0.60 m.

Effect of Climate on Asphalt Mix Temperature

Variations in ambient temperature generally have no significant effect on the moduli of unbound materials but strongly influence the asphalt properties. A procedure has been developed to derive, for design purposes, a 'weighted' mean annual air temperature (w-MAAT) from mean monthly air temperatures (MMAT) for a given location (climate). MMAT values are readily available from, for example, meteorological and tourist publications.

The w-MAAT is related to an effective asphalt temperature, and thus to an effective asphalt modulus. The term 'weighted

* Koninklijke/Shell Laboratorium, Amsterdam

© Proprietà riservata dell'autore - Digitalizzazione e distribuzione a cura del CENTRO APPUNTI - Corso Luigi Einaudi, 55 - Torino / Pagina 189 di 286

© Proprietà riservata dell'autore - Digitalizzazione e distribuzione a cura del CENTRO APPUNTI - Corso Luigi Einaudi, 55 - Torino / Pagina 191 di 286

A computer simulation of the nomograph developed by Van der Poel (3), is used for the prediction of the bitumen stiffness modulus under relevant loading conditions. The following data are required as input:

- The temperature of the bitumen (= temperature of the mix, T_{mix}). (This value was derived in an earlier design step).
- The T_{800pen} value of the bitumen (the temperature at which the penetration value is 800 (0.1 mm)). For conventional bitumens this temperature is approximately the softening point.
- The penetration index, PI, which is a measure of the temperature susceptibility.
- The loading time (normally 0.02 s, which is considered to be representative for moving traffic).
- When the penetration index is not known, the user can optionally specify a penetration value with a corresponding temperature. In this case, the program will calculate the PI. Alternatively, the binder rheology may be derived from two penetration values obtained at two temperatures. The output of this procedure is the bitumen stiffness (S_{bit}) at the temperature and loading time required for the thickness design.

With non-standard binders where the Van der Poel nomograph is not valid, the user can introduce an alternative relationship between T_{mix} and S_{bit} for the loading time of interest.

Determination of Asphalt Mix Stiffness

In the course of time, there has been a continuous effort to develop methods for the prediction of the mechanical properties of asphalt mixes from the properties and relative volumes of the constituent materials. The method used by the default computer routine is based on the work reported by Bonnaure et al. Twelve asphalt mixes, vastly different in composition bu standard mixes for road applications in various countries, studied to quantify the influence of the volumetric composi of the mix in mineral aggregate, binder and voids on the stiffness. The relationships thus obtained formed the basis o S_{mix} determination. The following input is required:

- The bitumen stiffness (S_{bit}). (This value has b determined in an earlier step).
- The percentage by volume of the binder (V_{bit}).
- The percentage by volume of the mineral aggregate ($V_$

The relations were used to construct a nomograph visuali the relation between S_{bit} and S_{mix} as a function of V_{bit} and (see Figure 3).

Determination of Base and Subgrade Properties

The design system incorporates the dynamic modulus o subgrade as one of the principal design parameters.

Since most subgrades show stress-dependent behaviour subgrade modulus should preferably be determined in situ f dynamic deflection measurements with loads representativ road traffic, and further also at a moisture content which the is likely to have in service under the road struct Alternatively, laboratory tests such as repeated-load tri-a tests can be used to estimate the moduli of the unbound lay

When such data are not available, the California Bea Ratio (CBR), the Hveem Resistance value, plate bea deflections or soil classifications may be used with enginee judgement to select a value for the subgrade modulus base the relations shown in Figure 4 (Chart E of the *SPDM* (1))

FIGURE 3: NOMOGRAPH FOR MIX STIFFNESS

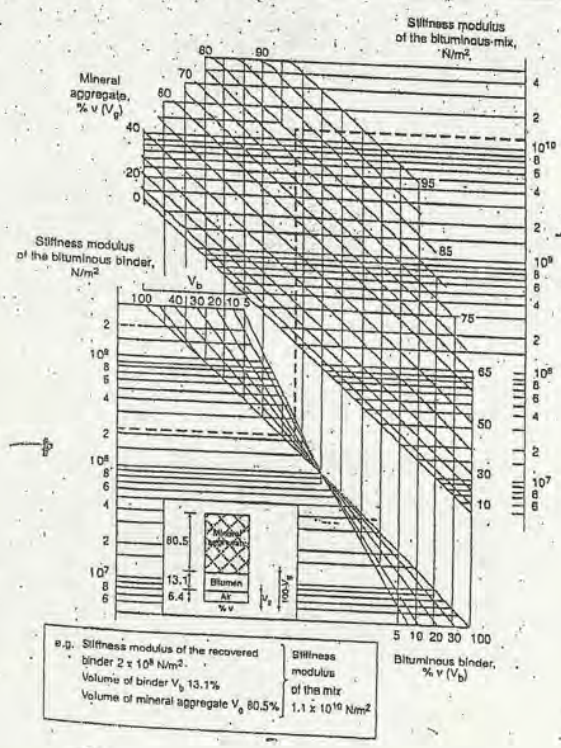

FIGURE 4 : ESTIMATION OF DYNAMIC MODULUS SUBGRADE OR OF UNBOUND BASE MATERIALS

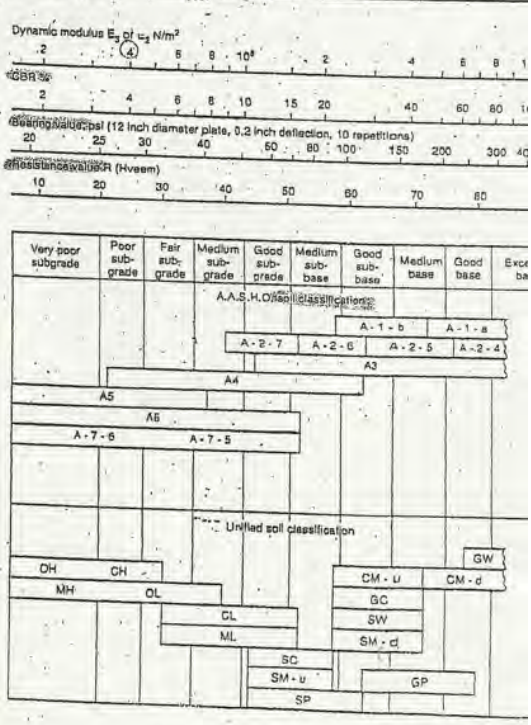

© Proprietà riservata dell'autore - Digitalizzazione e distribuzione a cura del CENTRO APPUNTI - Corso Luigi Einaudi, 55 - Torino / Pagina 191 di 286

© Proprietà riservata dell'autore - Digitalizzazione e distribuzione a cura del CENTRO APPUNTI - Corso Luigi Einaudi, 55 - Torino / Pagina 193 di 286

Asphalt Strains

Several nomographs have been developed for the prediction of the fatigue performance of asphalt mixes based on the composition of the mix, the properties of the binder and the loading conditions. The systems differ in complexity, i.e. in the number of parameters to characterise the mix and the binder, the test conditions (constant stress and/or strain) and in the type and number of mixes covered in the experimental data which were used to devise the method.

The default method used here is a computerised version of a relatively simple nomograph presented in the *SPDM* and is reproduced in this paper as Figure 6. The nomograph was developed using fatigue data obtained in constant strain tests on 13 different mixes which were representative of basecourse and wearing course mixes in various countries.

FIGURE 6: FATIGUE NOMOGRAPH

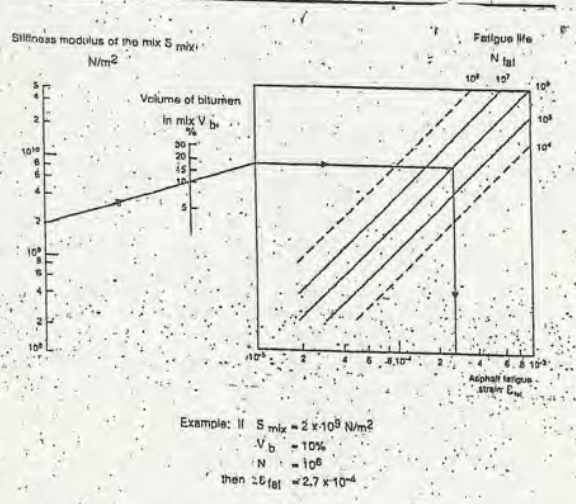

The nomograph was developed in the following steps.

In general, the fatigue data for a specific mix can be presented in the form:

$$\log (N_{fat}) = \log k - n \times \log (\varepsilon_{fat}) \qquad (Eq.\ 1)$$

where

N_{fat} is the number of applications of the strain ε_{fat} to failure and k and n are mix-dependent constants. Although the value of n may vary between mixes and with temperature, a value of 5 was assumed for all mixes. The fatigue strain is dependent on temperature and this has been expressed through the mix stiffness:

$$\log (\varepsilon_{fat}) = -0.36 \times \log (S_{mix}) + \text{constant} \qquad (Eq.\ 2)$$

The fatigue strain is known to be greatly dependent on the bitumen content V_{bit} of the mix and the relationship:

$$\varepsilon_{fat}\ (N=10^6) = (17.4 \times V_{bit} + 22) \times 10^{-6} \qquad (Eq.\ 3)$$

has been derived from the available data at a mix stiffness level of 5×10^9 N/m²

Combination of the above relationships yields:

$$\varepsilon_{fat} = (0.856 \times V_{bit} + 1.08) \times S_{mix}^{-0.36} \times N_{fat}^{-0.2} \qquad (Eq.\ 4)$$

and the nomograph shown in Figure 6.

The accuracy of the procedure is illustrated in Figure 7, which gives a plot of predicted fatigue strain versus actual strain for fatigue lives of 10^5, 10^6 up to 10^7 load applications. This verification included only test data with bitumen stiffness exceeding 10^7 N/m². The figure shows satisfactory agreement between measured and predicted strain levels.

The *SPDM* further mentions the energy approach as a way to describe the fatigue data (6). This approach is not included in the computer program.

FIGURE 7: COMPARISON BETWEEN PREDICTED AND MEASURED FATIGUE STRAINS

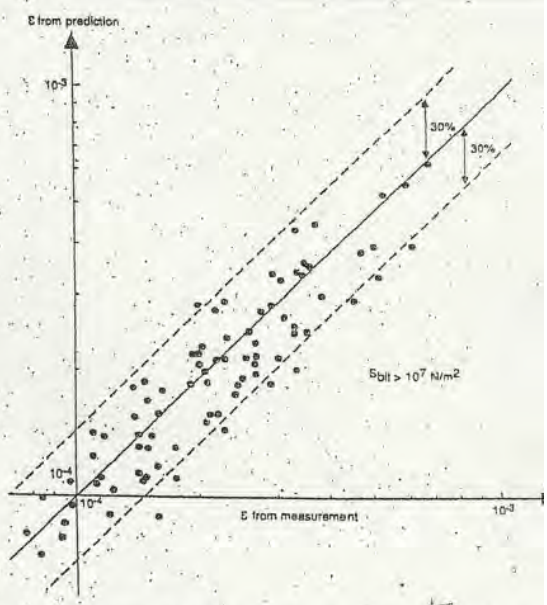

The aspects of lateral distribution of the traffic and t healing of the asphalt pavement are dealt with by the progra by introducing a factor of 10 increase in the mix life in the actu pavement. This factor, which was also included in the desi charts of the *SPDM* (1), reflects the result of healing facto measured in laboratory experiments together with the effects lateral traffic distribution on a standard pavement.

In summary, this module requires the bitumen content, mix stiffness and the asphalt strain level as input to calculate asphalt fatigue life.

Subgrade Strains

The relation between the number of strain repetitions caused by the standard design load and the permissi compressive strain in the subgrade (ε_{subgr}), has been obtai by analysis with the BISAR program of a representat selection of test sections in the AASHO Road Test (7). W thicker asphalt layers, rutting may be the result of deformat within the asphalt layer: this is considered as a sepa mechanism and is discussed in the next section.

The tensile (horizontal) asphalt strain is introduced a criterion for cracking of the asphalt layer.

The selection of, for instance, the vertical subgrade strain been made on the assumption that a fraction of this deforma will be permanent. The introduction of this deformation 'strength' criterion for unbound materials may be questio and the alternatives such as the energy of deformation or sh strain may be considered as more appropriate. In a large num of AASHO structures it has been verified that the maxim vertical subgrade strain, the maximum deformation energy, maximum energy of distortion and the maximum sh deformation closely correlate. This correlation is indepen of the type of base - granular or bitumen-bound - and whe the wheel loading is dual or tandem. As an exampl correlation is shown in Figure 8. This means that energie shear may be used as a criterion as long as the permissible le are calculated from the actual structures.

The permissible compressive strain in the subgrade function of the number of dual wheel load applicat

© Proprietà riservata dell'autore - Digitalizzazione e distribuzione a cura del CENTRO APPUNTI - Corso Luigi Einaudi, 55 - Torino / Pagina 193 di 286

© Proprietà riservata dell'autore - Digitalizzazione e distribuzione a cura del CENTRO APPUNTI - Corso Luigi Einaudi, 55 - Torino / Pagina 195 di 286

With the following procedure the yearly effective viscosity is derived:

MMAT values for the twelve months are converted to monthly effective temperatures T_{meff} for the layer $h_{1\text{-}1}$ using Figure 9 (Chart T). From readings in Van der Poel's nomograph at very long loading times, $VISC_{meff\ 1\text{-}1}$ values are derived corresponding to these temperatures. The effective viscosity for the year, $VISC_{yeff\ 1\text{-}1}$ is then derived from the sum of the twelve reciprocal values of $VISC_{meff\ 1\text{-}1}$. In Van der Poel's nomograph, $MAAT_{eff}$ corresponding to the $VISC_{yeff\ 1\text{-}1}$ value is determined; this effective temperature is required for the determination in Figure 9 of the $VISC_{yeff}$ for the other sub-layers.

FIGURE 9: CHARACTERISTIC RELATIONSHIP BETWEEN T_{MEFF} AND MMAT OR T_{YEFF} AND $MAAT_{EFF}$ FOR DIFFERENT ASPHALT LAYERS

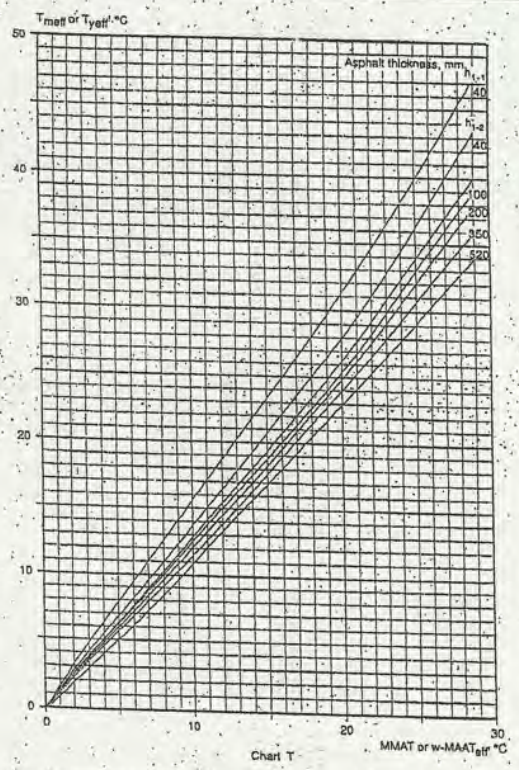

Chart T

Mix Characteristics

The permanent deformation is particularly a phenomenon at higher service temperatures and within the model a cumulative, long, loading time under traffic is obtained. This means that stiffnesses of the mixes (S_{mix}) at values of the stiffness of the bitumen (S_{bit}) below 10^2 to 10^3 N/m^2 will be required.

The relation between S_{bit} and S_{mix} is obtained in static creep tests on the mixes. Typical creep curves are given in Figure 10. The level and slope of these curves are characteristic values for the resistance of the mix to permanent deformation.

Traffic

The total number of commercial axles is converted to an equivalent number W of standard single design wheels, each with a contact stress of 6 x 10^5 N/m^2 per track during the design life.

FIGURE 10: TYPICAL LOW STIFFNES CHARACTERISTICS OF MIXES

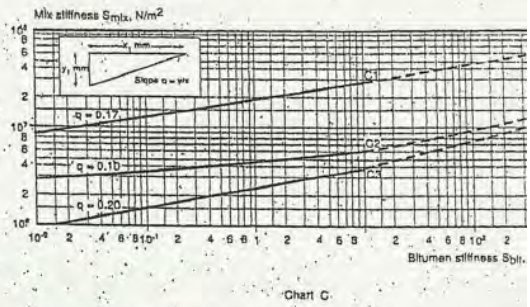

Chart C

The traffic conversion is dependent on the creep curve thus mix-dependent. A weight factor A is obtained in Figur from the slope q of the creep curve. The procedure is suitable for the usual, relatively long design periods with cumulative loading times where a linear log S_{mix} / log relationship is found.

FIGURE 11: CHARACTERISTIC RELATIONS BETWEEN WHEEL LOAD CONVERSION FACT AND SLOPE OF LOW STIFFNESS CURVE

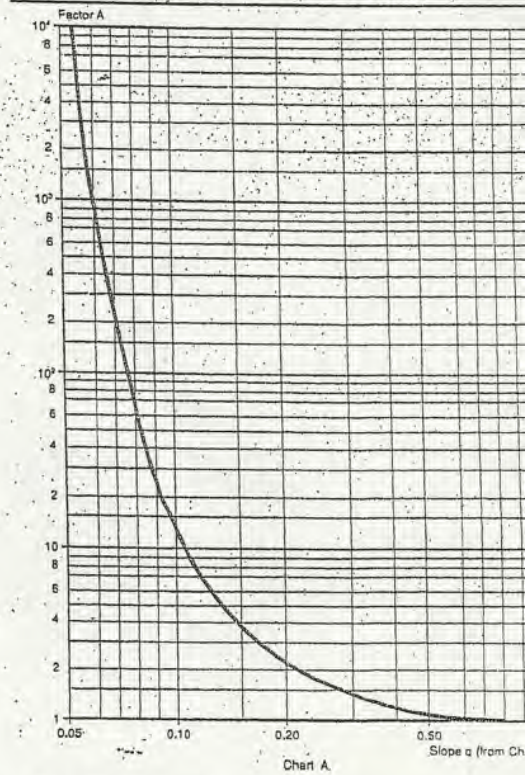

Chart A

Mix Stiffness

For the service temperatures and binder viscosities respective sub-layers, the effective stiffness of each asphalt sub-layers ($S_{mix\ 1\text{-}i}$) needs to be determined.

These $S_{mix\ 1\text{-}i}$ values are those which correspond to the curves and are thus the reciprocal values of the perm

© Proprietà riservata dell'autore - Digitalizzazione e distribuzione a cura del CENTRO APPUNTI - Corso Luigi Einaudi, 55 - Torino / Pagina 195 di 286

© Proprietà riservata dell'autore - Digitalizzazione e distribuzione a cura del CENTRO APPUNTI - Corso Luigi Einaudi, 55 - Torino / Pagina 197 di 286

VESYS METHOD

It is an alternative to shell method.

Vesys method takes into account viscoelastic properties of the material, but it is simply because requires a limited number of laboratory tests.

Hypothesis 1 : $\varepsilon_p(N) = \mu \varepsilon N^{-\alpha}$

↳ ε is the resilient strain measured in laboratory after 200 repetitions of loading

$$\varepsilon_p = \int_0^N \varepsilon_p(N)\, dN = \mu\varepsilon \frac{N^{(1-\alpha)}}{1-\alpha}$$

μ, α parameters of the material function of loading and temperature.

In logarithmic form:

$$\log(\varepsilon_p) = \log\left(\frac{\varepsilon\mu}{1-\alpha}\right) + (1-\alpha)\log N$$

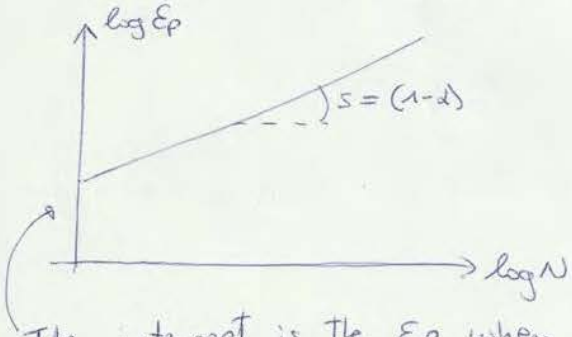

linear relationship between ε_p and N, with $(1-\alpha)$ slope

The intercept is the ε_p when $N=1$ → $\frac{\varepsilon\mu}{1-\alpha}$

This theory is for one mixture but we have a multi-layer system and so we need to extend it.

Hypothesis 2 : $\varepsilon = \varepsilon_p(N) + \varepsilon_e(N)$

total strain ↵ ↳ reversible deformation

$$\varepsilon_e(N) = \varepsilon - \varepsilon_p(N)$$
$$= \varepsilon\left(1 - \mu N^{-\alpha}\right)$$

106

© Proprietà riservata dell'autore - Digitalizzazione e distribuzione a cura del CENTRO APPUNTI - Corso Luigi Einaudi, 55 - Torino / Pagina 197 di 286

© Proprietà riservata dell'autore - Digitalizzazione e distribuzione a cura del CENTRO APPUNTI - Corso Luigi Einaudi, 55 - Torino / Pagina 199 di 286

Steps of the method:

- calculate $E_r(N)$. It change for different value of N, so for each of this value you need to calculate $E_r(N)$;
- This should be done for each layer because each layer has a different value of μ and ε;
- Using $E_r(N)$ we can calculate the deflection $w_r(N)$;
- Calcule $1 - \frac{w_r(N)}{w}$ for each value of N;
- Plotting these values on a bi-logarithmic graph;
- Fitting the line, knowing the equation of the line you obtain μ_{syst} and α_{syst};
- It is possible to calculate percent deformation:

  $w_p(N) = \mu_{syst} w N^{-\alpha_{syst}}$ → rut depth

Problem of the method is the temperature dependency:

- superposition of effect obtained at different temperatures;
- use reference temperature

Extra factors: wandering
loading level

The real situation is very complicated!

© Proprietà riservata dell'autore - Digitalizzazione e distribuzione a cura del CENTRO APPUNTI - Corso Luigi Einaudi, 55 - Torino / Pagina 199 di 286

© Proprietà riservata dell'autore - Digitalizzazione e distribuzione a cura del CENTRO APPUNTI - Corso Luigi Einaudi, 55 - Torino / Pagina 201 di 286

Appendix #1

Boussinesq's equations for a point load. (Ullidtz and Forlag, 1998)

Normal stresses

$$\sigma_z = \frac{3P}{2\pi R^2}\cos^3\theta$$

$$\sigma_r = \frac{P}{2\pi R^2}\left[3\cos\theta\sin^2\theta - \frac{1-2\nu}{1+\cos\theta}\right]$$

$$\sigma_t = \frac{(1-2\nu)P}{2\pi R^2}\left[-\cos\theta + \frac{1}{1+\cos\theta}\right]$$

Shear stresses

$$\tau_{rz} = \frac{3P}{2\pi R^2}\cos^2\theta\sin\theta$$

$$\tau_{rt} = \tau_{tz} = 0$$

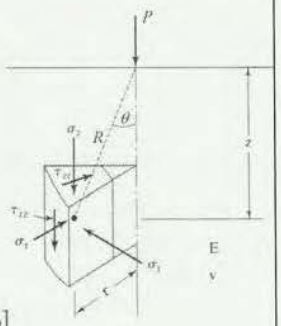

Normal strains

$$\varepsilon_z = \frac{(1+\nu)P}{2\pi R^2 E}\left[3\cos^3\theta - 2\nu\cos\theta\right]$$

$$\varepsilon_r = \frac{(1+\nu)P}{2\pi R^2 E}\left[-3\cos^3\theta + (3-2\nu)\cos\theta - \frac{1-2\nu}{1+\cos\theta}\right]$$

$$\varepsilon_t = \frac{(1+\nu)P}{2\pi R^2 E}\left[-\cos\theta + \frac{1-2\nu}{1+\cos\theta}\right]$$

Displacements

$$d_z = \frac{(1+\nu)P}{2\pi RE}\left[2(1-\nu) + \cos^2\theta\right]$$

$$d_r = \frac{(1+\nu)P}{2\pi RE}\left[\cos\theta\sin\theta - \frac{(1-2\nu)\sin\theta}{1+\cos\theta}\right]$$

$$d_t = 0$$

Boussinesq's equations for a circular uniformly distributed load. (Ullidtz and Forlag, 1998)

$$\sigma_z = \sigma_o\left(1 - \frac{1}{\left(\sqrt{1+\left(\frac{a}{z}\right)^2}\right)^3}\right)$$

$$\sigma_r = \sigma_t = \sigma_o\left[\frac{1+2\nu}{2} - \frac{1+\nu}{\sqrt{1+\left(\frac{a}{z}\right)^2}} + \frac{1}{2\left(\sqrt{1+\left(\frac{a}{z}\right)^2}\right)^3}\right]$$

$$\varepsilon_z = \frac{(1+\nu)\sigma_o}{E}\left[\frac{\frac{z}{a}}{\left(\sqrt{1+\left(\frac{z}{a}\right)^2}\right)^3} - (1-2\nu)\left(\frac{\frac{z}{a}}{\sqrt{1+\left(\frac{z}{a}\right)^2}} - 1\right)\right]$$

$$\varepsilon_r = \frac{(1+\nu)\sigma_o}{2E}\left[\frac{-\frac{z}{a}}{\left(\sqrt{1+\left(\frac{z}{a}\right)^2}\right)^3} - (1-2\nu)\left(\frac{\frac{z}{a}}{\sqrt{1+\left(\frac{z}{a}\right)^2}} - 1\right)\right]$$

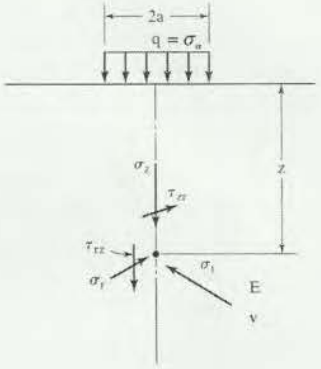

$$d_z = \frac{(1+\nu)\sigma_o a}{E}\left[\frac{1}{\sqrt{1+\left(\frac{z}{a}\right)^2}} + (1-2\nu)\left(\sqrt{1+\left(\frac{z}{a}\right)^2} - \frac{z}{a}\right)\right]$$

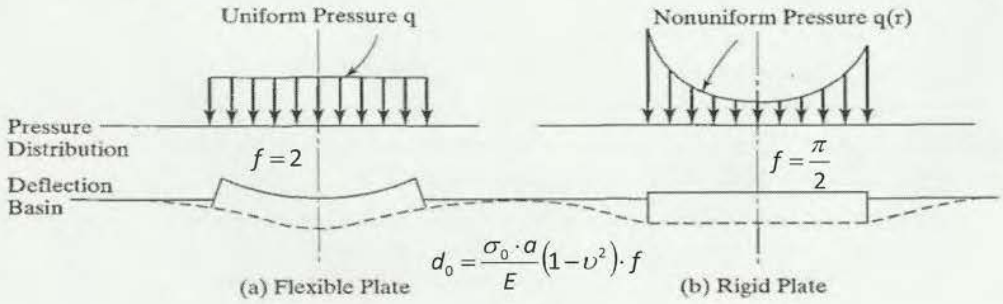

$$d_0 = \frac{\sigma_0 \cdot a}{E}\left(1-\upsilon^2\right)\cdot f$$

© Proprietà riservata dell'autore - Digitalizzazione e distribuzione a cura del CENTRO APPUNTI - Corso Luigi Einaudi, 55 - Torino / Pagina 201 di 286

© Proprietà riservata dell'autore - Digitalizzazione e distribuzione a cura del CENTRO APPUNTI - Corso Luigi Einaudi, 55 - Torino / Pagina 203 di 286

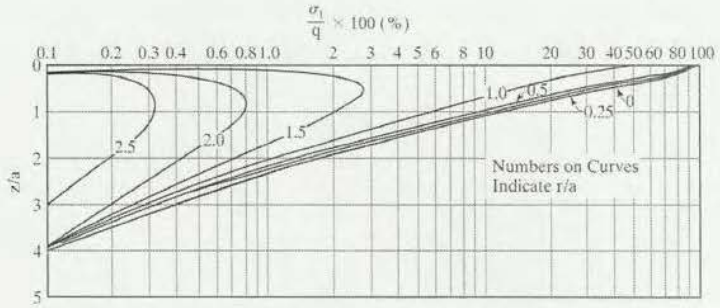

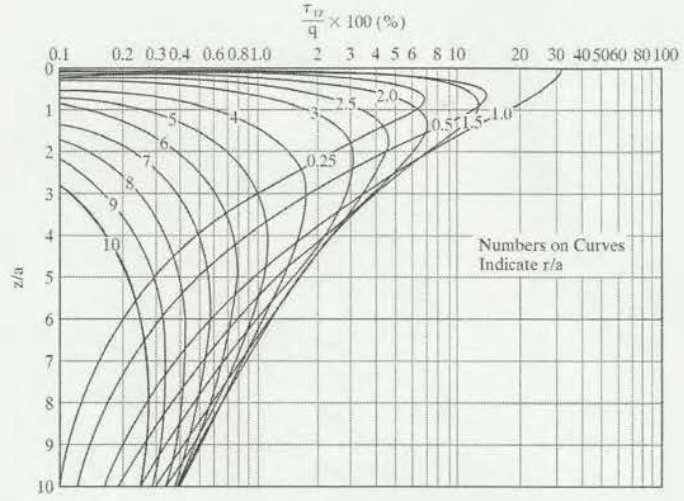

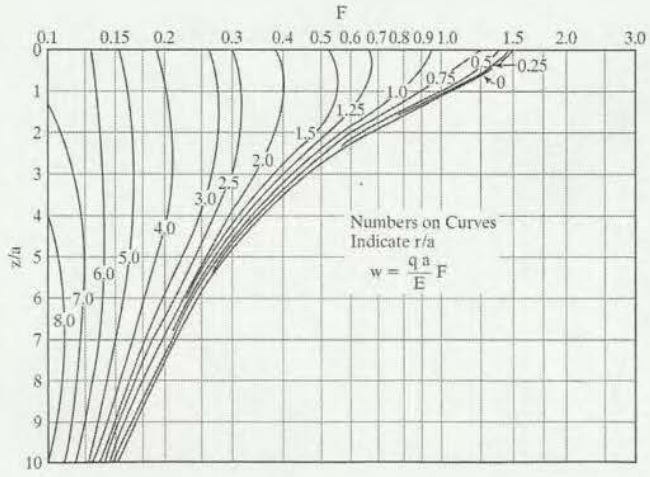

© Proprietà riservata dell'autore - Digitalizzazione e distribuzione a cura del CENTRO APPUNTI - Corso Luigi Einaudi, 55 - Torino / Pagina 203 di 286

© Proprietà riservata dell'autore - Digitalizzazione e distribuzione a cura del CENTRO APPUNTI - Corso Luigi Einaudi, 55 - Torino / Pagina 205 di 286

Appendix #3

Stress factors for Three-Layer System (Huang, 2004)

$$k_1 = \frac{E_1}{E_2} \qquad k_2 = \frac{E_2}{E_3}$$

$$A = \frac{a}{h_2} \qquad H = \frac{h_1}{h_2}$$

$$\sigma_{z1} = q\,(ZZ1)$$

$$\sigma_{z2} = q\,(ZZ2)$$

$$\sigma_{z1} - \sigma_{r1} = q\,(ZZ1 - RR1)$$

$$\sigma_{z2} - \sigma_{r2} = q\,(ZZ2 - RR2)$$

$$\epsilon_z = \frac{1}{E}(\sigma_z - \sigma_r)$$

$$\epsilon_r = \frac{1}{2E}(\sigma_r - \sigma_z)$$

$$\sigma_{z1} - \sigma'_{r1} = \frac{\sigma_{z1} - \sigma_{r1}}{k_1}$$

$$\sigma_{z2} - \sigma'_{r2} = \frac{\sigma_{z2} - \sigma_{r2}}{k_2}$$

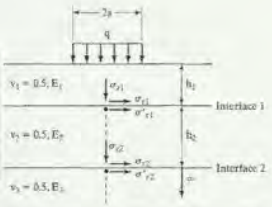

			$k_1 = 2$				$k_1 = 20$				$k_1 = 200$			
H	k_2	A	ZZ1	ZZ2	(ZZ1 − RR1)	(ZZ2 − RR2)	ZZ1	ZZ2	(ZZ1 − RR1)	(ZZ2 − RR2)	ZZ1	ZZ2	(ZZ1 − RR1)	(ZZ2 − RR2)
		0.1	0.42950	0.00896	0.70622	0.01716	0.14529	0.00810	1.81178	0.01542	0.03481	0.00549	3.02259	0.00969
		0.2	0.78424	0.03493	0.97956	0.06647	0.38799	0.03170	3.76886	0.06003	0.11491	0.02167	8.02452	0.03812
	2	0.4	0.98044	0.12667	0.70970	0.23531	0.78651	0.11650	5.16717	0.21640	0.33218	0.08229	17.64175	0.14286
		0.8	0.99434	0.36932	0.22319	0.63003	1.02218	0.34941	3.43631	0.60493	0.72695	0.27307	27.27701	0.45208
		1.6	0.99364	0.72113	−0.19982	0.97707	0.99060	0.69014	1.15211	0.97146	1.00203	0.63916	23.38638	0.90861
		3.2	0.99922	0.96148	−0.28916	0.84030	0.99893	0.93487	−0.06894	0.88358	1.00828	0.92560	11.87014	0.91469
0.125														
		0.1	0.43022	0.00228	0.69332	0.03467	0.14447	0.00182	1.80664	0.02985	0.03336	0.00128	3.17763	0.01980
		0.2	0.78414	0.00899	0.92086	0.13541	0.38469	0.00716	3.74573	0.11697	0.10928	0.00509	8.66097	0.07827
	20	0.4	0.97493	0.03392	0.46583	0.49523	0.77394	0.02710	5.05489	0.43263	0.31094	0.01972	20.12259	0.29587
		0.8	0.97806	0.11350	−0.66535	1.49612	0.98610	0.09061	2.92533	1.33736	0.65934	0.07045	36.29943	1.01694
		1.6	0.96921	0.31263	−2.82859	3.28512	0.93712	0.24528	−1.27093	2.99215	0.87931	0.20963	49.40857	2.64313
		3.2	0.98591	0.68433	−5.27906	5.05952	0.96330	0.55490	−7.35384	5.06489	0.93309	0.49938	57.84369	4.89895
		0.1	0.15524	0.00710	0.28362	0.01353	0.04381	0.00530	0.63215	0.00962	0.00909	0.00259	0.96553	0.00407
		0.2	0.42809	0.02783	0.70225	0.05278	0.14282	0.02091	1.83766	0.03781	0.03269	0.01027	3.10763	0.01611
	2	0.4	0.77939	0.10306	0.96634	0.19178	0.37882	0.07933	3.86779	0.14159	0.10684	0.04000	8.37852	0.06221
		0.8	0.96703	0.31771	0.66885	0.55211	0.75904	0.26278	5.50796	0.44710	0.30477	0.14513	18.95534	0.21860
		1.6	0.98156	0.66753	0.17331	0.95080	0.98743	0.61673	4.24281	0.90115	0.66786	0.42940	31.18909	0.58553
		3.2	0.99840	0.93798	−0.05691	0.89390	1.00064	0.91258	1.97494	0.93254	0.98447	0.84545	28.98500	0.89191
0.25														
		0.1	0.15436	0.00179	0.25780	0.02728	0.04236	0.00123	0.65003	0.01930	0.00776	0.00065	1.08738	0.00861
		0.2	0.42462	0.00706	0.67115	0.10710	0.13708	0.00488	1.90693	0.07623	0.02741	0.00257	3.59448	0.03421
	20	0.4	0.76647	0.02697	0.84462	0.39919	0.35716	0.01888	4.13976	0.29072	0.08634	0.01014	10.30923	0.13365
		0.8	0.92757	0.09285	0.21951	1.26565	0.68947	0.06741	6.48948	0.98565	0.23137	0.03844	26.41442	0.49135
		1.6	0.91393	0.26454	−1.22411	2.94860	0.85490	0.20115	6.95639	2.55231	0.46835	0.13148	57.46409	1.53833
		3.2	0.95243	0.60754	−3.04320	4.89878	0.90325	0.48647	6.05854	4.76234	0.71083	0.37342	99.29034	3.60964
		0.1	0.04330	0.00465	0.08250	0.00878	0.01122	0.00259	0.17997	0.00440	0.00215	0.00094	0.26620	0.00128
		0.2	0.15325	0.01836	0.28318	0.03454	0.04172	0.01028	0.64779	0.01744	0.00826	0.00373	0.98772	0.00509
	2	0.4	0.42077	0.06974	0.70119	0.12934	0.13480	0.03998	1.89817	0.06722	0.02946	0.01474	3.19580	0.01996
		0.8	0.75683	0.23256	0.96681	0.41187	0.35175	0.14419	4.09592	0.23476	0.09508	0.05622	8.71973	0.07434
		1.6	0.93447	0.56298	0.70726	0.85930	0.70221	0.42106	6.22002	0.62046	0.27135	0.19358	20.15765	0.23838
		3.2	0.98801	0.85655	0.33878	0.96353	0.97420	0.82256	5.41828	0.93831	0.62399	0.52912	34.25229	0.54931
0.5														
		0.1	0.04193	0.00117	0.08044	0.01778	0.00990	0.00063	0.19872	0.00911	0.00149	0.00023	0.31847	0.00257
		0.2	0.14808	0.00464	0.27574	0.07027	0.03648	0.00251	0.72264	0.03620	0.00564	0.00094	1.19598	0.01025
	20	0.4	0.40386	0.01799	0.67174	0.26817	0.11448	0.00988	2.19520	0.14116	0.01911	0.00372	1.02732	0.04047
		0.8	0.69098	0.06476	0.86191	0.91168	0.27934	0.03731	5.24726	0.51585	0.05574	0.01453	12.00885	0.15452
		1.6	0.79338	0.19803	0.39588	2.38377	0.50790	0.12654	10.30212	1.59341	0.13946	0.05399	32.77028	0.53836
		3.2	0.85940	0.49238	−0.41078	4.47022	0.70903	0.35807	16.38520	3.69109	0.30247	0.18091	77.62943	1.56409
		0.1	0.01083	0.00241	0.02179	0.00453	0.00263	0.00100	0.04751	0.00160	0.00049	0.00029	0.06883	0.00035
		0.2	0.04176	0.00958	0.08337	0.01797	0.01029	0.00347	0.18481	0.00637	0.00195	0.00116	0.26966	0.00138
	2	0.4	0.14665	0.03724	0.28491	0.06934	0.03810	0.01565	0.66727	0.02498	0.00746	0.00460	1.00131	0.00545
		0.8	0.39942	0.13401	0.71341	0.24250	0.12173	0.05938	1.97428	0.09268	0.02647	0.01797	3.24971	0.02092
		1.6	0.71032	0.38690	1.02680	0.63631	0.31575	0.20098	4.37407	0.29253	0.08556	0.06671	8.92442	0.07335
		3.2	0.92112	0.75805	0.90482	0.97509	0.66041	0.53398	6.97695	0.65446	0.25186	0.22047	20.83387	0.21288
1														
		0.1	0.00963	0.00061	0.02249	0.00920	0.00193	0.00024	0.05737	0.00322	0.00027	0.00007	0.08469	0.00062
		0.2	0.03697	0.00241	0.08618	0.03654	0.00751	0.00098	0.22418	0.01283	0.00104	0.00028	0.33312	0.00248
	20	0.4	0.12805	0.00950	0.29640	0.14241	0.02713	0.00387	0.82430	0.05063	0.00384	0.00110	1.25495	0.00985
		0.8	0.33263	0.03578	0.76292	0.51815	0.08027	0.01507	2.59672	0.19267	0.01236	0.00436	4.26100	0.03825
		1.6	0.52721	0.12007	1.25168	1.56503	0.17961	0.05549	6.77014	0.66326	0.03379	0.01683	12.91809	0.13989
		3.2	0.65530	0.33669	1.70723	3.51128	0.34355	0.18344	15.23252	1.88634	0.08859	0.06167	36.04291	0.45544
		0.1	0.00250	0.00100	0.00555	0.00188	0.00059	0.00033	0.01219	0.00051	0.00011	0.00008	0.01737	0.00009
		0.2	0.00991	0.00397	0.02199	0.00750	0.00235	0.00130	0.04843	0.00203	0.00045	0.00033	0.06913	0.00036
	2	0.4	0.03832	0.01569	0.08465	0.02950	0.00922	0.00518	0.18857	0.00803	0.00179	0.00131	0.27103	0.00142
		0.8	0.13516	0.05974	0.29365	0.11080	0.03412	0.02023	0.68382	0.03093	0.00685	0.00520	1.00808	0.00553
		1.6	0.36644	0.20145	0.75087	0.35515	0.10918	0.07444	2.04134	0.10864	0.02441	0.02003	3.27590	0.02043
		3.2	0.67384	0.51156	1.17294	0.77434	0.29183	0.23852	4.60426	0.30709	0.08061	0.07248	9.02195	0.06638
2														
		0.1	0.00181	0.00025	0.00652	0.00378	0.00033	0.00008	0.01568	0.00094	0.00005	0.00002	0.02160	0.00014
		0.2	0.00716	0.00099	0.02586	0.01507	0.00130	0.00031	0.06236	0.00374	0.00018	0.00007	0.08604	0.00058
	20	0.4	0.02746	0.00394	0.10017	0.05958	0.00503	0.00123	0.24425	0.01486	0.00071	0.00030	0.33866	0.00229
		0.8	0.09396	0.01535	0.35641	0.22795	0.01782	0.00485	0.90594	0.05789	0.00261	0.00119	1.27835	0.00901
		1.6	0.23065	0.05599	1.00785	0.78347	0.05012	0.01862	2.91994	0.21190	0.00819	0.00467	4.35311	0.03390
		3.2	0.37001	0.17843	2.16033	2.13215	0.11331	0.06728	7.95104	0.67732	0.02341	0.01784	13.26873	0.11666

Sign convention: positive in compression and negative in tension.

© Proprietà riservata dell'autore - Digitalizzazione e distribuzione a cura del CENTRO APPUNTI - Corso Luigi Einaudi, 55 - Torino / Pagina 205 di 286

© Proprietà riservata dell'autore - Digitalizzazione e distribuzione a cura del CENTRO APPUNTI - Corso Luigi Einaudi, 55 - Torino / Pagina 207 di 286

σ_z is indipendent from E, ν stresses → in general are indipendent from E.

chart approach:

enter with $\frac{z}{a}$, $\frac{r}{a}$ → obtain $\frac{\sigma_z}{q} \cdot 100$; $\frac{\sigma_r}{q}$; $\frac{\sigma_t}{q}$

So you can evaluate deformations:

$$\varepsilon_z = \frac{1}{E}\left(\sigma_z - \nu\left(\sigma_r + \sigma_t\right)\right)$$

$$\varepsilon_r = \frac{1}{E}\left(\sigma_r - \nu\left(\sigma_t + \sigma_z\right)\right)$$

$$\varepsilon_t = \frac{1}{E}\left(\sigma_t - \nu\left(\sigma_z + \sigma_r\right)\right)$$

Repeate all the question using $\nu = 0,35$.
Pay attention that chart are built only for $\nu = 0,5$ so you cannot use!

Example #2

Inverse problem: we know the response of the pavement in terms of deflection and we are interested in finding E.

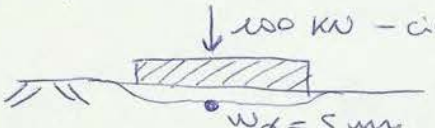

$E = ?$
$\nu = 0,5$

Rigid plate → same displacement for all the plate.

$$w_\phi = \frac{\sigma_0 \cdot a}{E} \underbrace{\left(1-\nu^2\right) f}_{f'}$$

→ rigid plate $f = \frac{\pi}{2}$

→ flexible plate $f = 2$

obtaining E, modulus of subgrade.

© Proprietà riservata dell'autore - Digitalizzazione e distribuzione a cura del CENTRO APPUNTI - Corso Luigi Einaudi, 55 - Torino / Pagina 207 di 286

© Proprietà riservata dell'autore - Digitalizzazione e distribuzione a cura del CENTRO APPUNTI - Corso Luigi Einaudi, 55 - Torino / Pagina 209 di 286

Example #3

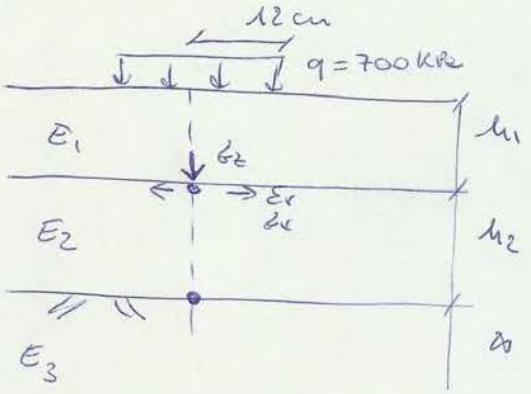

3 layer-system

$\nu = 0,5$ for all layers

Assumptions:

- each layer is homogeneus, isotropic, linear elastic and characterized by E, ν
- h_i = cost
- continuity conditions: at the interface point we have the same vertical stress, the same horizontal strain, the same w_z and w_r.
  σ_r is different in the two layers 

Jones table

$K_1 = \frac{E_1}{E_2}$; $K_2 = \frac{E_2}{E_3}$; $A = \frac{a}{h_1}$; $H = \frac{h_1}{h_2}$

Stress factors ZZ1, ZZ2, RR1, RR2
(1 = first interface)

$\sigma_{z1} = q \cdot ZZ1$

$\sigma_{z1} - \sigma_{r1} = q\,(ZZ1 - RR1)$

ε determinate using hooke's law ($\sigma_r = \sigma_t$)

$$\frac{\sigma_{z1} - \sigma_{r1}}{2E_1} = \frac{\sigma_{z1} - \sigma'_{r1}}{2E_2}$$

© Proprietà riservata dell'autore - Digitalizzazione e distribuzione a cura del CENTRO APPUNTI - Corso Luigi Einaudi, 55 - Torino / Pagina 209 di 286

© Proprietà riservata dell'autore - Digitalizzazione e distribuzione a cura del CENTRO APPUNTI - Corso Luigi Einaudi, 55 - Torino / Pagina 211 di 286

ex 1

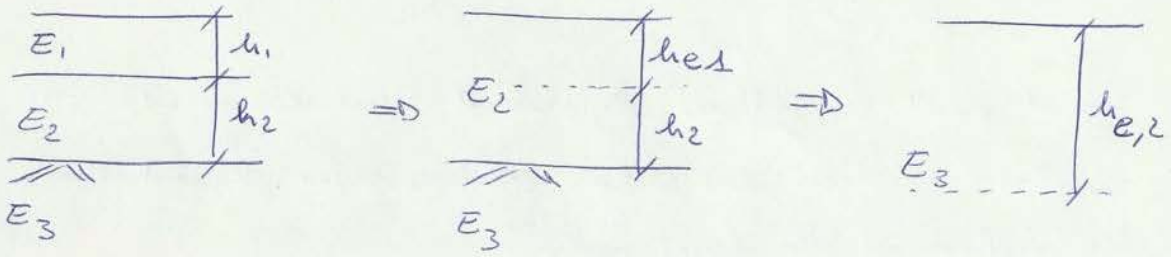

$$h_{e1} = \beta \cdot h_1 \sqrt[3]{\frac{E_1}{E_2}}$$

$$h_{e2} = (h_{e1} + h_2) \sqrt[3]{\frac{E_2}{E_3}}$$

© Proprietà riservata dell'autore - Digitalizzazione e distribuzione a cura del CENTRO APPUNTI - Corso Luigi Einaudi, 55 - Torino / Pagina 211 di 286

© Proprietà riservata dell'autore - Digitalizzazione e distribuzione a cura del CENTRO APPUNTI - Corso Luigi Einaudi, 55 - Torino / Pagina 213 di 286

2.1 Given a coefficient of friction of 1.5, determine stress due to friction in longitudinal and transverse reinforcement.

2.2 Given a coefficient of friction of 1.5, determine stress due to friction in tie bars and in distributed reinforcement in the case of a two-lane highway.

2.3 Determine maximum bearing stress between dowel and concrete when two 40 kN loads are applied in correspondence of dowels A and B (Figure 1).

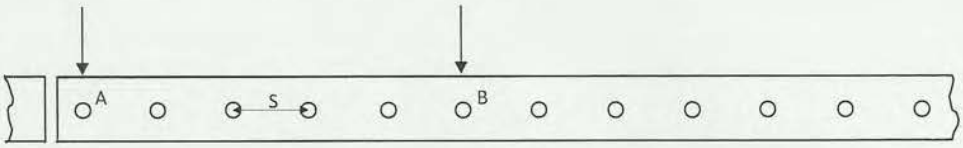

Figure 1.

Appendix #1

Corner Loading

$$\sigma_c = \frac{3P}{h^2}\left[1 - \left(\frac{a\sqrt{2}}{\ell}\right)^{0.6}\right]$$

$$\Delta_c = \frac{P}{k\ell^2}\left[1.1 - 0.88\left(\frac{a\sqrt{2}}{\ell}\right)\right]$$

Interior Loading

$$\sigma_i = \frac{3(1+\nu)P}{2\pi h^2}\left(\ln\frac{\ell}{b} + 0.6159\right)$$

$b = a$ when $a \geq 1.724h$

$b = \sqrt{1.6a^2 + h^2} - 0.675h$ when $a < 1.724h$

$$\Delta_i = \frac{P}{8k\ell^2}\left\{1 + \frac{1}{2\pi}\left[\ln\left(\frac{a}{2\ell}\right) - 0.673\right]\left(\frac{a}{\ell}\right)^2\right\}$$

Edge Loading

$$\underset{\text{(circle)}}{\sigma_e} = \frac{3(1+\nu)P}{\pi(3+\nu)h^2}\left[\ln\left(\frac{Eh^3}{100ka^4}\right) + 1.84 - \frac{4\nu}{3} + \frac{1-\nu}{2} + \frac{1.18(1+2\nu)a}{\ell}\right]$$

$$\underset{\text{(semicircle)}}{\sigma_e} = \frac{3(1+\nu)P}{\pi(3+\nu)h^2}\left[\ln\left(\frac{Eh^3}{100ka^4}\right) + 3.84 - \frac{4\nu}{3} + \frac{(1+2\nu)a}{2\ell}\right]$$

$$\underset{\text{(circle)}}{\Delta_e} = \frac{\sqrt{2 + 1.2\nu}P}{\sqrt{Eh^3k}}\left[1 - \frac{(0.76 + 0.4\nu)a}{\ell}\right]$$

$$\underset{\text{(semicircle)}}{\Delta_e} = \frac{\sqrt{2 + 1.2\nu}P}{\sqrt{Eh^3k}}\left[1 - \frac{(0.323 + 0.17\nu)a}{\ell}\right]$$

© Proprietà riservata dell'autore - Digitalizzazione e distribuzione a cura del CENTRO APPUNTI - Corso Luigi Einaudi, 55 - Torino / Pagina 213 di 286

© Proprietà riservata dell'autore - Digitalizzazione e distribuzione a cura del CENTRO APPUNTI - Corso Luigi Einaudi, 55 - Torino / Pagina 215 di 286

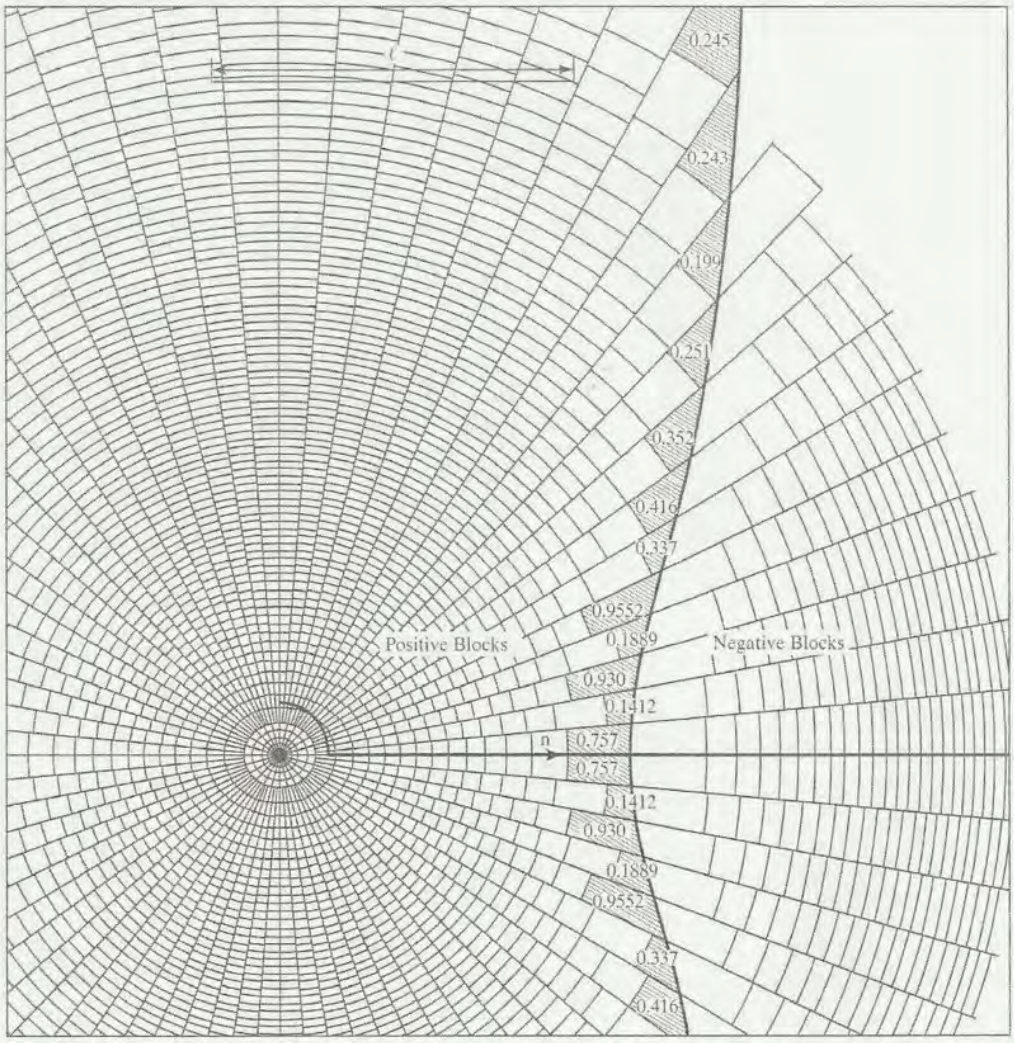

FIGURE 4.14

Influence chart for moment due to interior loading. (After Pickett and Ray (1951).)

© Proprietà riservata dell'autore - Digitalizzazione e distribuzione a cura del CENTRO APPUNTI - Corso Luigi Einaudi, 55 - Torino / Pagina 215 di 286

© Proprietà riservata dell'autore - Digitalizzazione e distribuzione a cura del CENTRO APPUNTI - Corso Luigi Einaudi, 55 - Torino / Pagina 217 di 286

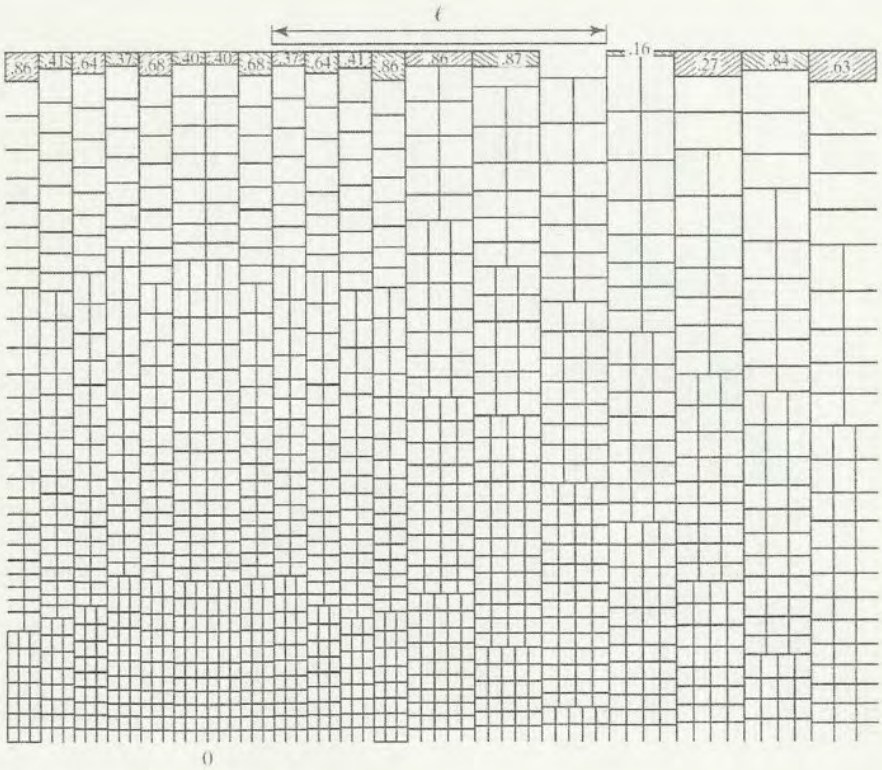

FIGURE 4.16

Influence chart for deflection due to edge loading. (After Pickett and Ray (1951).)

APPENDIX #3

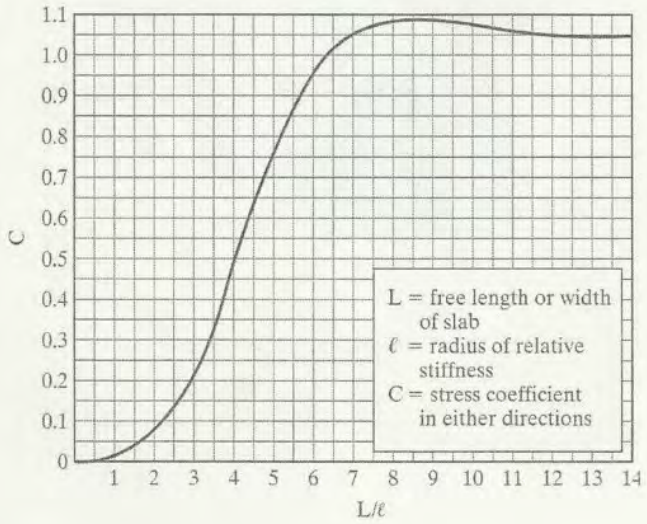

FIGURE 4.4

Stress correction factor for finite slab. (After Bradbury (1938).)

© Proprietà riservata dell'autore - Digitalizzazione e distribuzione a cura del CENTRO APPUNTI - Corso Luigi Einaudi, 55 - Torino / Pagina 217 di 286

© Proprietà riservata dell'autore - Digitalizzazione e distribuzione a cura del CENTRO APPUNTI - Corso Luigi Einaudi, 55 - Torino / Pagina 219 di 286

deflection: $\Delta = \frac{0{,}0005\, q l^4 \nu}{D}$

↳ modulus of rigidity

$$D = \frac{E h^3}{12(1-\nu^2)}$$

1.2) Temperature differential

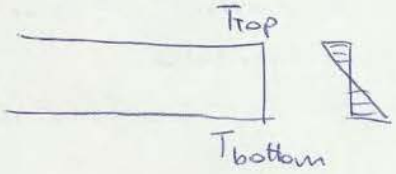

$\Delta T = 10°C$

The slabs tends to cool but this moment is prevented.

Case of infinite slab – Bradbury

$$\sigma_x = \frac{E \alpha \Delta T}{2(1-\nu^2)} (C_x + \nu C_y)$$

$$\sigma_y = \frac{E \alpha \Delta T}{2(1-\nu^2)} (C_y + \nu C_x)$$

C_x, C_y are coefficient factor determined by using Bradbury's chart: $C_x \rightarrow$ I have to use l_x/l

$C_y \rightarrow$ I have to use l_y/l

$C_x = C_y = 1$ infinite slab

case of edge: no confinment effect to concrete: $\nu = 0$

Eisenmann approach: $\rightarrow l_{crit}$

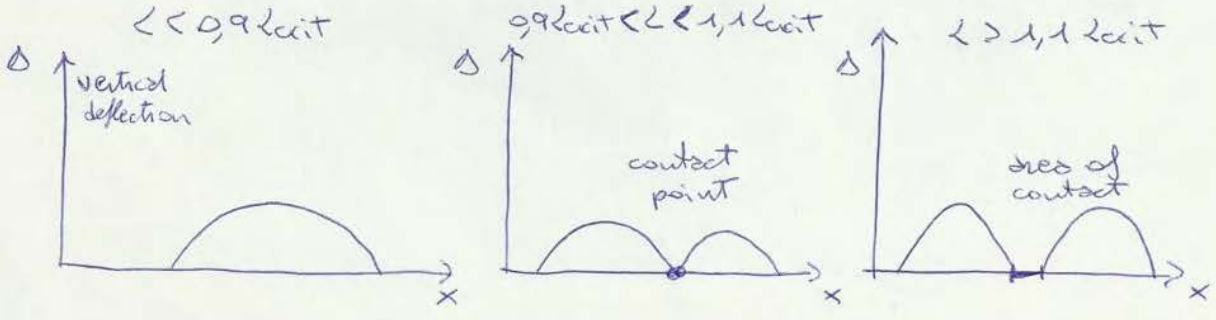

© Proprietà riservata dell'autore - Digitalizzazione e distribuzione a cura del CENTRO APPUNTI - Corso Luigi Einaudi, 55 - Torino / Pagina 219 di 286

© Proprietà riservata dell'autore - Digitalizzazione e distribuzione a cura del CENTRO APPUNTI - Corso Luigi Einaudi, 55 - Torino / Pagina 221 di 286

1.3) Equilibrium between frictional stresses and tensile stresses

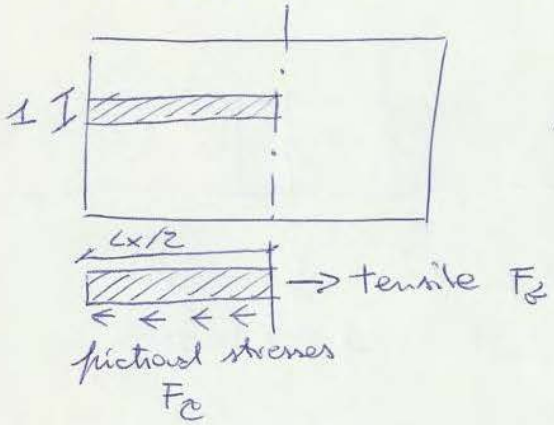

1 = u = unit width

Equilibrium of the two:

$F_e = \delta \cdot h \cdot 1$ — unit width

$F_c = F_e \cdot \gamma \cdot \left(h \cdot \frac{Lx}{2} \cdot 1 \right)$

γ = friction coefficient

volume

Repeate in the other direction

Example #2

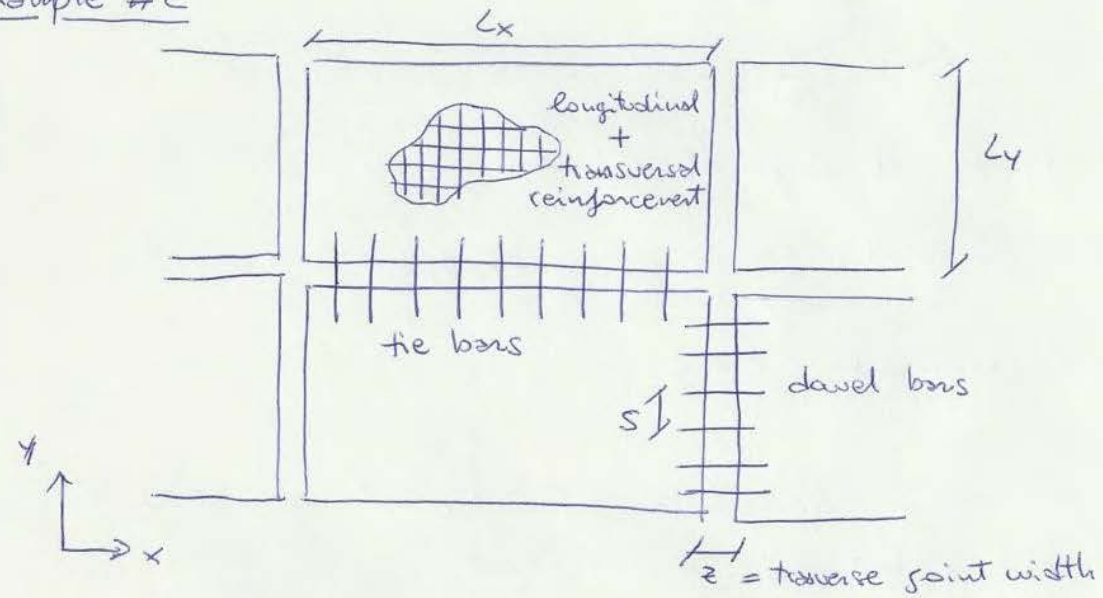

A_x = sectional area of x direction

A_y = " " y "

} interior distribution steel

E_d = modulus of elasticity of dowels

© Proprietà riservata dell'autore - Digitalizzazione e distribuzione a cura del CENTRO APPUNTI - Corso Luigi Einaudi, 55 - Torino / Pagina 221 di 286

© Proprietà riservata dell'autore - Digitalizzazione e distribuzione a cura del CENTRO APPUNTI - Corso Luigi Einaudi, 55 - Torino / Pagina 223 di 286

if four-lane highway

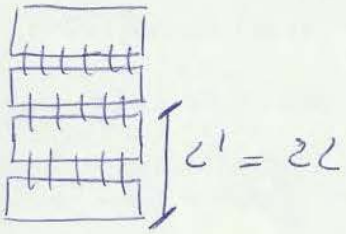

2.3

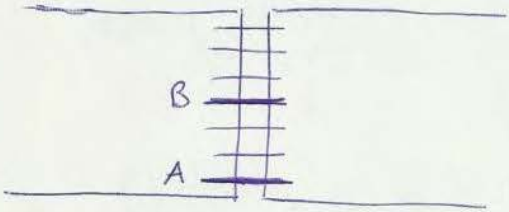

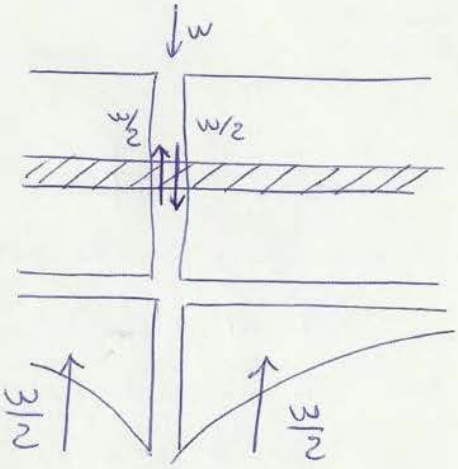

First load:

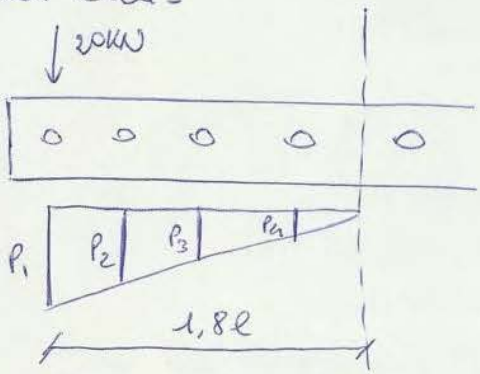

$1,8\ell$ maximum negative bending moment and shear = 0

How much of this load (w/2) is carried by every dowel?

$$\frac{w}{2} = P_1 + P_2 + P_3 + P_4$$

Second load:

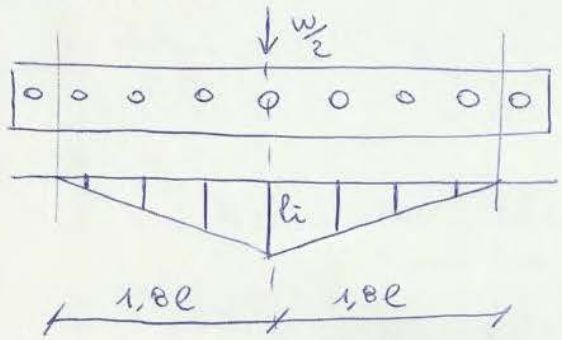

$$\Sigma P_i = \frac{w}{2}$$

Now I can compare the effects of the two loadings and find which element has the maximum load

Then you can use Tymoshenko theory

© Proprietà riservata dell'autore - Digitalizzazione e distribuzione a cura del CENTRO APPUNTI - Corso Luigi Einaudi, 55 - Torino / Pagina 223 di 286

© Proprietà riservata dell'autore - Digitalizzazione e distribuzione a cura del CENTRO APPUNTI - Corso Luigi Einaudi, 55 - Torino / Pagina 225 di 286

Politecnico di Torino – Corso di Laurea Magistrale in Ingegneria Civile

Pavement and Track Engineering - 02IODMX

A.A. 2014/15

PRACTICAL APPLICATION #3 – 10/11/2014

Example #1 RAILWAY TRACK (Rails)

The following loading and structure data are given:

Table 1.

P_{axle}	[kN]	176.6
V_{max}	[km/h]	110
R_{curve}	[m]	600
h	[cm]	15
s	[m]	1.5
R_w	[m]	0.625
y_G	[m]	1.29
A_{rail}	[mm^2]	7686
α_{rail}	[$°C^{-1}$]	1.2E-05
E_{rail}	[GPa]	210
I_{rail}	[cm^4]	3055
v_{rail}	[-]	0.3
c_{rail}	[m]	0.15
u	[MPa]	25

1.1 Determine vertical forces (with respect to the rolling plane) by using the Eisenmann and the ORE approaches in the following conditions:

- Level of reliability equal to 99.7% (t = 3);
- Track in standard conditions (ϕ = 0.2);
- Braking conditions (DAF_{ORE} = 1.11)

1.2 Determine lateral forces (with respect to the rolling plane) by taking into account:

- non-uniform distribution of the load among the connected axles (β = 1.1);
- abnormal movements.

1.3 Given a temperature increase with respect to the temperature of placement of 40°C, determine longitudinal forces by taking into account the effects of abnormal movements, breakings, crashes ($\Delta N = 15\%N$).

1.4 Determine deflection and bending moment in the longitudinal axis according to both Zimmermann (γ = 0) and Pasternak (γ =3) solutions.

1.5 According to the Zimmermann solution, use Talbot's formulae to determine :

- maximum deflection in the rail;
- maximum bending moment in the rail.

© Proprietà riservata dell'autore - Digitalizzazione e distribuzione a cura del CENTRO APPUNTI - Corso Luigi Einaudi, 55 - Torino / Pagina 225 di 286

© Proprietà riservata dell'autore - Digitalizzazione e distribuzione a cura del CENTRO APPUNTI - Corso Luigi Einaudi, 55 - Torino / Pagina 227 di 286

PRACTICAL APPLICATION #3

Example #1

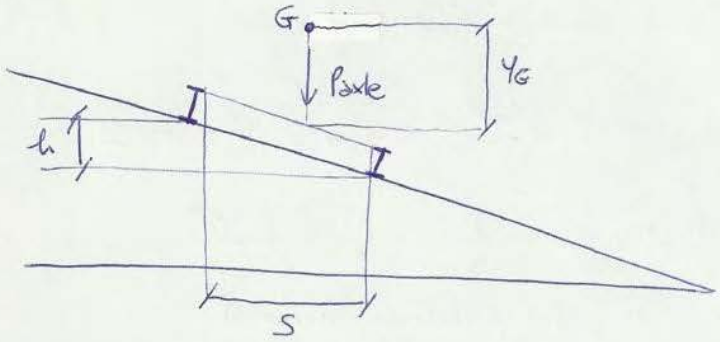

S = distance between two contact point (wheel – rail)

h = superelevation

R_w = wheel radius

y_G = distance between baricentre of the load and rolling plane

A_{rail} = section area of rail

α_{rail} = termal espansion coefficient

E_{rail} = young modulus of rail

I_{rail} = inertial moment of rail

u = modulus of track elasticity

ν = poisson ratio of rail

C_{rail} = width of rail

V_{max} because we consider dynamic condition

1.1)

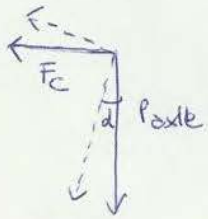

F_C = centrifugal force

$$F_C = \frac{V^2}{R} \cdot \frac{P_{axle}}{g}$$

© Proprietà riservata dell'autore - Digitalizzazione e distribuzione a cura del CENTRO APPUNTI - Corso Luigi Einaudi, 55 - Torino / Pagina 227 di 286

© Proprietà riservata dell'autore - Digitalizzazione e distribuzione a cura del CENTRO APPUNTI - Corso Luigi Einaudi, 55 - Torino / Pagina 229 di 286

1.4)

Zimmermann:

$$y_z(x) = \frac{P_{ed}}{\sqrt[4]{64\, E_{sd} \cdot I_{sail}\, u^3}}\, e^{\lambda x}(\cos\lambda x + \sin\lambda x)$$

x = longitudinal axis

λ = damping factor $\quad \lambda = \sqrt[4]{\dfrac{u}{4 E_{sail} I_{sail}}}$

Pasternak:

$$y_p(x) = \frac{P_{ed}}{8 E_{sd} I_{sail}\, a\, b\, \beta^2}\, e^{-bx}(a\cos ax + b\sin ax)$$

a, b factor of Pasternak model

$$a = \frac{1}{2}\sqrt{4\beta^2 - \gamma} \qquad \text{where } \beta = \lambda$$

$$b = \frac{1}{2}\sqrt{4\beta^2 + \gamma}$$

$\gamma = \dfrac{GA}{EA}$ = relative stiffness between shear stiffness (GA) and bending stiffness (EA) of the sail.

if $\gamma = 0$ is the identical expression of Ziemmermann, where there are not shear forces.

$$M_z(x) = \frac{P_{ed}}{4\lambda}\, e^{-\lambda x}(\cos\lambda x - \sin\lambda x)$$

$$M_p(x) = \frac{P_{ed}}{4ab}\, e^{-bx}(a\cos ax - b\sin ax)$$

1.5) Talbot

$$y_{max} = 0{,}391\, \frac{P_{ed}}{u\, x_1}$$

x_1 is the distance for the application of point load where bending moment and curvature are equal to 0!

© Proprietà riservata dell'autore - Digitalizzazione e distribuzione a cura del CENTRO APPUNTI - Corso Luigi Einaudi, 55 - Torino / Pagina 229 di 286

© Proprietà riservata dell'autore - Digitalizzazione e distribuzione a cura del CENTRO APPUNTI - Corso Luigi Einaudi, 55 - Torino / Pagina 231 di 286

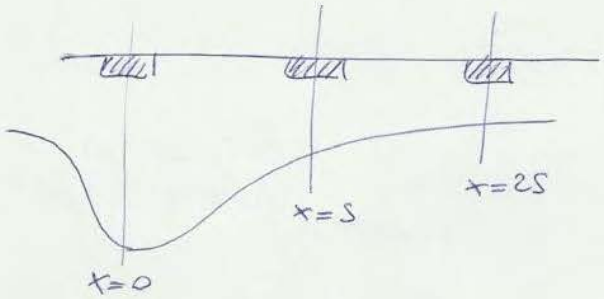

1.7) Bending moment on ties

- Rigid body with full support

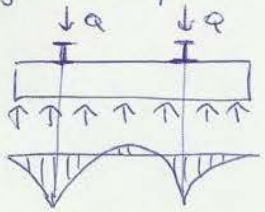

continuous pressure under area of ties

M_{rail}, M_{centre}

- Rigid body with end support

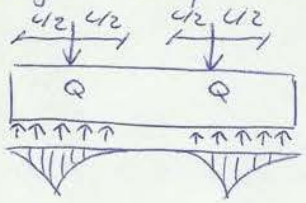

central point of the ties is not reacted, only the two part c_2 where Q are reacted.

$M_{rail}, M_{centre} = \phi$

- ORE empirical method

evaluation of the maximum resting load:

$$Q_{max} = \varphi \frac{P_{axle}}{2} B \cdot \chi$$

φ = dynamic amplification factor (empirical method) function of speed $f(v)$ → $v = 100$ km/h → $\varphi = 1{,}375$

B = average value of load applied of the ratio between the load on the sleeper and that of the wheel ($\frac{P_{axle}}{2}$)

χ = geometrical amplification factor

© Proprietà riservata dell'autore - Digitalizzazione e distribuzione a cura del CENTRO APPUNTI - Corso Luigi Einaudi, 55 - Torino / Pagina 231 di 286

© Proprietà riservata dell'autore - Digitalizzazione e distribuzione a cura del CENTRO APPUNTI - Corso Luigi Einaudi, 55 - Torino / Pagina 233 di 286

Politecnico di Torino – Corso di Laurea Magistrale in Ingegneria Civile

Pavement and Track Engineering - 02IODMX

A.A. 2014/15

PRACTICAL APPLICATION #4 - 20/11/2014

Example #1 ACCUMULATED ESAL ON THE DESIGN LANE

A six-lane two-way highway has an average annual daily traffic (AADT) in both direction of 11000 during the first year of traffic. Traffic composition and axle loads are reported in **Table 1**. It is assumed that they will remain constant over the analysis period of 30 years. Traffic volumes for all vehicle types is expected to increase at a rate of 2.5 percent per year. The pavement has a terminal serviceability index (p_t) of 2.5 and a structural number (SN) of 5. The directional distribution factor (D_D) is 0.5 and the percent of traffic on the design lane (D_L) is 65 percent. Determine the design ESAL and the traffic versus time relationship.

Table 1.

Vehicle Types	Percentage (%)	Axle loads Distribution (kips)
Passenger cars	50	total weight < 7
2-axle single-unit trucks	25	↓2 ↓5
3-axle single-unit trucks	10	↓9 ↓18 ↓18
5-axle multiple-unit trucks	15	↓9 ↓23 ↓18 ↓18 ↓18

Example #2 EFFECTIVE ROADBED RESILIENT MODULUS

Figure 2.4 shows the 12 monthly subgrade resilient moduli (M_r) estimated by means of a laboratory relationship between resilient modulus and moisture content of soil beneath the pavement. Determine the effective roadbed resilient modulus (M_R).

Example #3 LAYER THICKNESSES

Calculate the required layer thicknesses for a new flexible pavement consisting of an asphalt concrete surface, a crushed-stone base, and a granular subbase. The subbase has a resilient modulus (E_3) of 20 ksi, resilient modulus of the base (E_2) is 40 ksi, and resilient modulus of asphalt concrete (E_1) is 400 ksi. It is estimated that water drains out of the pavement within a period of one day and the pavement structure will be exposed to moisture levels approaching saturation for 20 percent of the time. As cumulative ESAL in the design lane, consider the traffic versus time relationship developed in example #1 and a performance period of 15 years. As effective roadbed soil consider the result obtained in example #2. Assume a reliability level of 95 percent and an overall standard deviation of 0.45. The initial serviceability index (p_i) is 4.2 and the terminal serviceability index (p_t) is 2.5.

/18

© Proprietà riservata dell'autore - Digitalizzazione e distribuzione a cura del CENTRO APPUNTI - Corso Luigi Einaudi, 55 - Torino / Pagina 233 di 286

© Proprietà riservata dell'autore - Digitalizzazione e distribuzione a cura del CENTRO APPUNTI - Corso Luigi Einaudi, 55 - Torino / Pagina 235 di 286

NOMOGRAPH SOLVES:

$$\log_{10} W_{18} = Z_R * S_o + 9.36 * \log_{10}(SN+1) - 0.20 + \frac{\log_{10}\left[\frac{\Delta PSI}{4.2 - 1.5}\right]}{0.40 + \frac{1094}{(SN+1)^{5.19}}} + 2.32 * \log_{10} M_R - 8.07$$

Table 2.2. Suggested Levels of Reliability for Various Functional Classifications

Functional Classification	Recommended Level of Reliability	
	Urban	Rural
Interstate and Other Freeways	85–99.9	80–99.9
Principal Arterials	80–99	75–95
Collectors	80–95	75–95
Local	50–80	50–80

NOTE: Results based on a survey of the AASHTO Pavement Design Task Force.

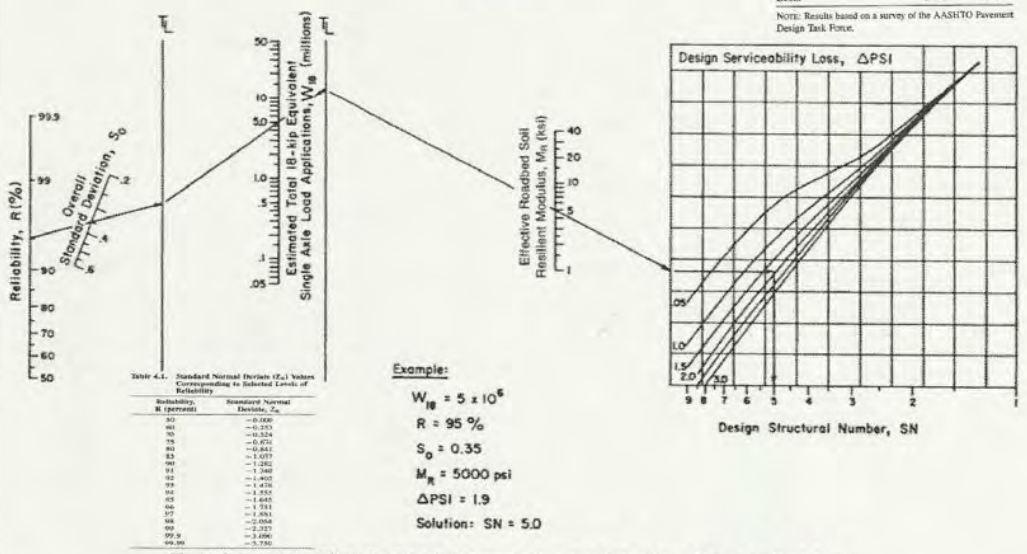

Table 4.1. Standard Normal Deviate (Z_R) Values Corresponding to Selected Levels of Reliability

Reliability, R (percent)	Standard Normal Deviate, Z_R
50	−0.000
60	−0.253
70	−0.524
75	−0.674
80	−0.841
85	−1.037
90	−1.282
91	−1.340
92	−1.405
93	−1.476
94	−1.555
95	−1.645
96	−1.751
97	−1.881
98	−2.054
99	−2.327
99.9	−3.090
99.99	−3.750

Figure 3.1. Design Chart for Flexible Pavements Based on Using Mean Values for Each Input

Month	Roadbed Soil Modulus, M_R (psi)	Relative Damage, u_f
Jan.	20,000	
Feb.	20,000	
Mar.	2,500	
Apr.	4,000	
May	4,000	
June	7,000	
July	7,000	
Aug.	7,000	
Sept.	7,000	
Oct.	7,000	
Nov.	4,000	
Dec.	20,000	
Summation: Σu_f =		

Average: $\bar{u}_f = \frac{\Sigma u_f}{n}$ = _____ =

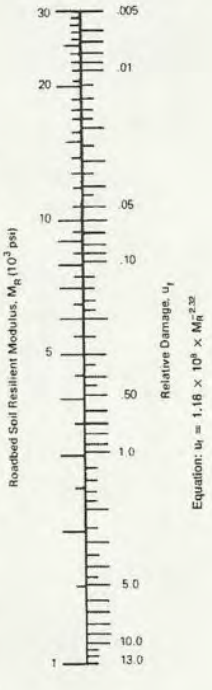

Effective Roadbed Soil Resilient Modulus, M_R (psi) = _____ (corresponds to $\bar{u}_f$)

Figure 2.4. Chart for Estimating Effective Roadbed Soil Resilient Modulus for Flexible Pavements Designed Using the Serviceability Criteria

Table 4.1. Suggested Seasons Length (Months) for the Six U.S. Climatic Regions

U.S. Climatic Region	Season (Roadbed Soil Moisture Condition)			
	Winter (Roadbed Frozen)	Spring-Thaw (Roadbed Saturated)	Spring/Fall (Roadbed Wet)	Summer (Roadbed Dry)
I	0.0*	0.0	7.5	4.5
II	1.0	0.5	7.0	3.5
III	2.5	1.5	4.0	4.0
IV	0.0	0.0	4.0	8.0
V	1.0	0.5	3.0	7.5
VI	3.0	1.5	3.0	4.5

*Number of months for the season.

Table 4.2. Suggested Seasonal Roadbed Soil Resilient Moduli, M_R (psi), as a Function of the Relative Quality of the Roadbed Material

Relative Quality of Roadbed Soil	Season (Roadbed Soil Moisture Condition)			
	Winter (Roadbed Frozen)	Spring-Thaw (Roadbed Saturated)	Spring/Fall (Roadbed Wet)	Summer (Roadbed Dry)
Very good	20,000*	2,500	8,000	20,000
Good	20,000	2,000	6,000	10,000
Fair	20,000	2,000	4,500	6,500
Poor	20,000	1,500	3,300	4,900
Very poor	20,000	1,500	2,500	4,000

*Values shown are Resilient Modulus in psi.

Table 4.3. Effective Roadbed Soil Resilient Modulus Values, M_R (psi), That May be Used in the Design of Flexible Pavements for Low-Volume Roads. Suggested values depend on the U.S. climatic region and the relative quality of the roadbed soil.

U.S. Climatic Region	Relative Quality of Roadbed Soil				
	Very Poor	Poor	Fair	Good	Very Good
I	2,800*	3,700	5,000	6,800	9,500
II	2,700	3,400	4,500	5,500	7,300
III	2,700	3,000	4,000	4,400	5,700
IV	3,200	4,100	5,600	7,900	11,700
V	3,100	3,700	5,000	6,000	8,200
VI	2,800	3,100	4,100	4,500	5,700

*Effective Resilient Modulus in psi.

REGION	CHARACTERISTICS
I	Wet, no freeze
II	Wet, freeze–thaw cycling
III	Wet, hard-freeze, spring thaw
IV	Dry, no freeze
V	Dry, freeze–thaw cycling
VI	Dry, hard freeze, spring thaw

Figure 4.1. The Six Climatic Regions in the United States (12)

19

© Proprietà riservata dell'autore - Digitalizzazione e distribuzione a cura del CENTRO APPUNTI - Corso Luigi Einaudi, 55 - Torino / Pagina 235 di 286

© Proprietà riservata dell'autore - Digitalizzazione e distribuzione a cura del CENTRO APPUNTI - Corso Luigi Einaudi, 55 - Torino / Pagina 237 di 286

PRACTICAL APPLICATION #4

1993 last version of AASHTO method

it is based on W_{18} => allowable number of ESAC (standard axle) that cause a reduction of the level of serviceability ΔPSI

it is a function of: z_R = standard normal deviate

S_0 = standard deviation

S_N = structural number (describes the performance of the pavement)

M_R = resilient modulus

Design procedure:

- Pavement performance
- Reliability
- traffic loads
- effective roadbed resilient modulus
- structural number:
  - material of construction;
  - drainage;
  - layer thicknesses
- environmental effects

In detail:

PAVEMENT PERFORMANCE

divided in two different type:

- structural performance: effect of traffic loads (crack, rutting..)
- functional performance: comfort, riding

PSI is the index to associate [0 ÷ 5]

P_0 = initial or original (4,2 if flexible pavement)

P_T = terminal value: minimum value of PSI index at the end of the evaluation time [2,5 ÷ 3]

function:
- pavement type
- construction quality

/20

© Proprietà riservata dell'autore - Digitalizzazione e distribuzione a cura del CENTRO APPUNTI - Corso Luigi Einaudi, 55 - Torino / Pagina 237 di 286